The University Of Sheffield.

The role of nitroreductases, nitrilases and nitrile hydratase in breakdown of aromatic compounds in *Rhodopseudomonas palustris*

BY

Reem M Farsi

A thesis submitted in part fulfillment for the degree of Doctor of Philosophy

Department of Molecular Biology and Biotechnology,
University of Sheffield

December 2016

Abstract

Aromatic compounds are among the most persistent and prevalent toxic pollutants in the environment. Biotransformation and bioremediation processes can convert these compounds into non-toxic compounds and valuable products. The purple phototrophic bacterium *Rhodopseudomonas palustris* (*R. palustris*) has the ability to degrade a wide range of aromatic compounds and the identification of several nitroreductases, nitrilases and a nitrile hydratase (NHase) in the genome sequence indicates an ability to degrade nitroaromatic and nitrile compounds respectively. The candidate nitroreductases RPA1711 and RPA4285 were recombinantly produced in *E. coli* and the purified proteins were assayed for their ability to reduce the nitro-groups of ligands to amino groups by UV-Spectrophotometry. Michaelis-Menten constants (Km) for RPA1711 of 0.21 mM and 0.13 mM were obtained for 2,4-Dinitrotoluene (2,4-DNT) and 2,6-Dinitrotoluene (2,6-DNT) respectively, while RPA4285 had higher Km values with 2,4-DNT of 0.76 mM and with 2,6-DNT of 0.41 mM. On the other hand, nitriles were utilised by nitrilases and a nitrile hydratase and both aromatic and aliphatic nitriles were degraded. The RPA0599, RPA1563 and RPA4166 nitrilases were purified and their activities were determined by the release of ammonia using the continuous coupled assay, phenol-hypochlorite, *o*-phthalaldehyde (OPA) methods. 4-cyanopyridine was a preferred substrate. Furthermore, a NHase of two subunits RPA2805-2806 and NHase with activator (P14K) RPA2805-2806-RPA2807 was also purified and characterised. Benzonitrile was a preferred substrate for the NHase. Exploring the ability of *R. palustris* to degrade nitroaromatic and nitrile pollutants might help improve bioremediation biotechnology.

Acknowledgments

First and foremost, I would like to express my sincere gratitude to my supervisor Prof. Dave Kelly for his patience, motivation, and for his valuable guidance. His continuous guidance has helped me throughout my course and I am very grateful to have such advisor. My sincere thanks also go to Dr. Svetlana Sedelnikova, Dr.Neil Bramall, Dr. Simon Thorpe and Mrs. Andrea Hounslow for their help and technical support. Also, I would like to thank everyone in F1, it has been a amazing four years to work with each and every one of you.

The best part of my PhD study was making friends with such incredible people, I would especially like to thank Dr. Abrar Akbar. Thanks for your help and patience through my PhD study and my life. Sometimes I think that you are a fairy in disguise. Thanks for everything. I cannot imagine my life during the past four years without someone special like you.

A special warm thanks to my family, words cannot express how grateful I am to my Mom and Dad who continuously supported me in every possible way. And a special thanks to my sister and my brothers (especially Nasser) for supporting me with unconditional love. I would also like to thank my beloved husband, Yasser for all of the sacrifices that you have made. Thank you for supporting me for everything, and especially I cannot thank you enough for encouragement throughout my PhD study, without you I couldn't have survived thus far. To my beloved twins Mohammed and Mamoun and my beautiful princesses Dana and Tuleen, I would like to express my thanks for being such good children and for doing their best to understand a mother who had to be confined to her study for such a long time always cheering me up.

Finally, I would like to thank my sponsor King Abdulaziz University for funding my PhD research.

R.F
2016

Abbreviations

A	Absorbance
A_{340}	Absorbance at 340nm
APS	Ammonium persulphate
bp	Base pair
CO_2	Carbon dioxide
CoA	Coenzyme A
D_2O	Deuterium oxide
dH_2O	Distilled water
DMSO	Dimethyl sulfoxide
DNA	deoxyribonucleic acid
DTT	Dithiothreitol
EDTA	ethylenediamine tetra-acetic acid
FAD	Flavin adenine dinucleotide
FMN	Flavin mono nucleotide
g	Gram
GC	Gas chromatography
GDH	Glutamate Dehydrogenase
H_2O	Water
HPLC	High performance liquid chromatography
hr	Hour
IPTG	Isopropyl β-D-1-thiogalactopyranoside
kb	Kilobase
kDa	kiloDalton
k_m	Michaelis constant
KPB	Potassium phosphate buffer
L	Litre
LB	Luria-Bertani
M	Molar
min	Minute
mg	Milligram
mm	Millimetre
mM	Millimolar
mol	Mole
MW	Molecular weight
NAD	Nicotinamide adenine dinucleotide (oxidised form)
NADH	Nicotinamide adenine dinucleotide (reduced form)
NAD(P)	Nicotinamide adenine dinucleotide (phosphate) (oxidised form)
NAD(P)H	Nicotinamide adenine dinucleotide (phosphate) (reduced form)
nm	Nanometer
NMR	Nuclear magnetic resonance
O.D.	Optical density

OPA	*o*-Phthalaldehyde
^{o}C	Degrees Celsius
PAGE	polyacrylmide gel electrophoresis
PCR	polymerase chain reaction
pH	hydrogen potential
PYE	peptone-yeast extract
RCV	Rhodobacter capsulatus vitamins
rpm	Revolutions per minute
s	Seconds
SDS	Sodium dodecyl sulphate
TCA	Trichloroacetic acid
TEMED	N,N,N',N'-tetramethyl- ethane-1,2-diamine
Tm	Melting temperature
TSP	Trimethyl-silyl propionate
UV	Ultra-violet
v/v	Concentration, volume/volume
V_{max}	Maximal velocity
w/v	Concentration, weight/volume
WT	Wild-type
xg	Multiplied by gravitational force
µg	Micrograms
µl	Microlitre
µM	Micromolar

Table of contents

CHAPTER 1

INTRODUCTION

1 Introduction

1.1 Aromatic compounds

Aromatic compounds are considered the most widespread class of organic compounds in nature after carbohydrates. These compounds are divided into three main types: substituted aromatics; heterocyclic aromatic compounds; and polycyclic aromatic hydrocarbons or PAHs. The PAH-group aromatics each have a minimum of 2 fused aromatic rings which may form a cluster, linear or angular pattern (Seo et al., 2009). Plant life generates large amounts of PAHs in the form of secondary products which are soluble, including flavonoids and phenols, as well as lignin, a polymer. PAHs are also widely found in substances present in the environment as pollution, including benzene, toluene, ethylbenzene and xylene (BTEX), present in petrol and other oil derivatives (Fuchs et al., 2011). Thus, besides their natural occurrence, PAHs are also considered among the most persistent and prevalent pollutants in the environment, resulting from anthropogenic activities, and most of these substances are of high toxicity (Seo et al., 2009). An example of this is seen in phenol-producing industries. In addition to phenol, acetophenone, α-methylstyrene, benzoic acid, dimethyl phenyl carbinol, methanol and isopropylbenzene can be found in the effluent from such anthropogenic activities, all of which are toxic (Alexievab et al., 2008). These toxic compounds may significantly influence both the health of humans and the ecosystem. Therefore, the degradation and detoxification of growing quantities of such substances from contaminated sites is an interesting target for biotechnological research. Thus, it is important to study the consequences of these compounds in nature, including their biodegradation (Hongwei et al., 2006). Furthermore, aromatic compounds might be used as feedstocks for the bioproduction of a number of substances in the industrial, agricultural, pharmaceutical,

health and food sectors, which possibile stresses the study of aromatic bioconversion processes (Díaz et al., 2013).

All aromatic compounds have pleasant odours – they are "aromatic", and they are based on benzene, C_6H_6, which has a ring of six carbon atoms. Each of the six bonds linking carbon to carbon is of identical length, being shorter than single bonds but longer than double bonds. Further, these bonds show a greater than normal strength when considering other conjugated structures, and are better described as representing electron density which are no longer localized but are held jointly by each of the ring's atoms (Figure1.1) (Jim, 2000, Seo et al., 2009). Aromatic compounds may have a side-chain or a functional group attached directly to the ring (Figure 1.2).

1.1.1 Biodegradation of aromatic compounds

Biodegradation is a workable technique of bioremediation for organic pollutants. The degradation of aromatic compounds by ring cleavage is an important biochemical step in nature's 'carbon cycle' and is performed by different kinds of microorganism. Bioremediation applies the metabolic adaptability of microorganisms in degrading hazardous contaminants to mineralize the pollutants to primary metabolites such as carbon dioxide and water, or to transform pollutants from organic to harmless metabolites (Seo et al., 2009). Moreover, such techniques can hydrolyse the toxic aromatic compound to its corresponding products (Kabaivanova et al., 2008).

Feasible remediation techniques need highly adapted microorganisms, to use pollutants in a reasonable period of time (Seo et al., 2009).

Plants are the major source of aromatic compounds, and the complex aromatic polymer lignin comprises about a quarter of the land-based biomass on Earth, and the recycling of this and other plant-derived aromatic compounds is vital for maintaining the Earth's carbon cycle (Peng et al., 1999, Diaz et al., 2001).

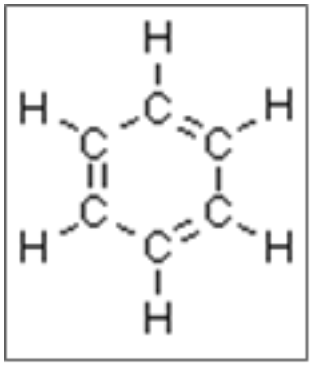

Figure 1.1 Aromatic ring with six carbon atoms each one attached hydrogen.

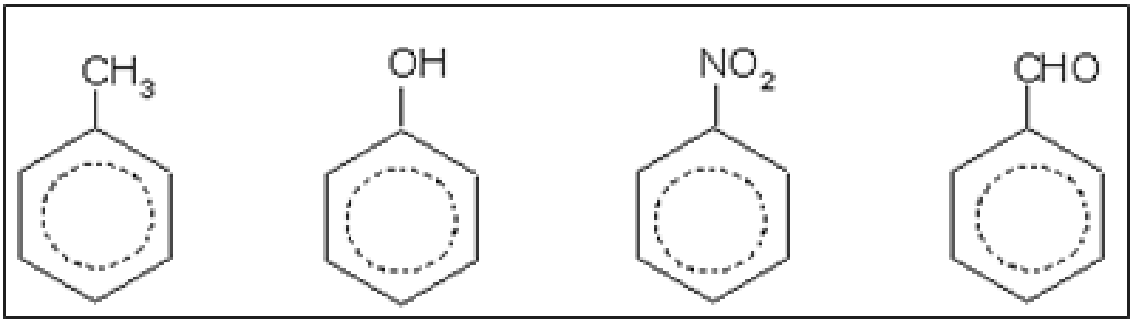

Figure 1.2 Aromatic ring with different functional group. (a) Toluene, (b) Phenol, (c) Nitrobenzene and (d) Benzaldehyde.

However, plants lack the pathways of degradation, and cannot recycle carbon from these substances. Also, animals have a weak ability to metabolize aromatic substances, except for aromatic amino acids and a small number of other compounds (Fuchs et al., 2011).

In the last two decades, the use of white-rot fungi in pollutant biodegradation has received great attention. Canala-Echvarria (2010) reports that white-rot fungi, and particularly Chilean *Anthracophyllum discolor* Sp4, have shown the ability to degrade complex aromatic molecules such as PAHs. This fungus, which was isolated from decayed wood in the rainforest of southern Chile, has the ability to degrade chlorophenols and azodyes, due to producing ligninolytic enzymes, and especially manganese peroxidase (MnP)(Canala-Echvarria, 2010). Hence, aerobic and anaerobic bacteria and aerobic fungi dominate the degradation of aromatic substances. However, aerobic fungi and bacteria perform the process of lignin degradation slowly, and the incomplete transformation of lignin into humus is central to soil fertility. Thus, microorganisms assume a major role in the recycling of carbon from the aromatic ring. It is suggested that fungi act centrally in biodegrading lignin, through the production of a range of enzymes external to the cell, including manganese and lignin peroxidase (MnP and LIP) and laccase, which can form radicals within lignin, leading its bonds to become unstable and allowing the macromolecules to break down (Song, 2009). In Semple et al.'s (1999) study, it was demonstrated that eukaryotic algae can act on frequent aromatic pollutants of waste and natural waters to biotransform and biodegrade those pollutants (Semple et al., 1999). In addition, photosynthetic microalgae *Parachlorella kessleri* are able to utilize BTEX as a carbon source (Takáčová et al., 2015). While the central role of fungi in biodegrading lignin has been discussed above, the action of bacterial agents in biodegrading lignin is thought to be less significant, based on their possible inability to

first depolymerise lignin. Rather, bacterial microbes use monomers which are derivatives of fungal biodegradation (Song, 2009).

A number of previously isolated bacterial species rely solely on the most basic polycyclic aromatic hydrocarbon, aromatic naphthalene, for their energy and carbon. These bacteria include species from *Burkholderia, Alcaligenes, Pseudomonas, Mycobacteria, Polaromonas, Ralstonia, Rhodococcus, Streptomyces* and *Sphingomonas* (Seo et al., 2009). It is noteworthy that degradation of aromatic substrates has been reported for few species of archaea (Fuchs et al., 2011).

1.1.1.1 Aerobic degradation of aromatic compounds

The aerobic degradation of aromatic compounds normally requires one molecule of oxygen in the cleavage of the aromatic ring (Fuchs et al., 2011). Aerobically, bacteria generally achieve activation and cleavage of aromatic rings and by one of two methods, as dictated by how much oxygen is available (Díaz et al., 2013), with each approach depending on an oxygenase, and resulting in cleaving the aromatic ring. Oxygenases facilitate the insertion of hydroxyl groups in the aromatic ring, utilising molecular oxygen (Carmona et al., 2009, Butler and Mason, 1997, Zhang and Anderson, 2012). The majority of aerobic pathways classically described show a convergence into catecholic substrates, and these may then be subjected to intradiol or ortho-cleavage, as in type 1, or to extradiol or meta-cleavage, as in type 2. Substrates including *cis,cis* -muconate undergo ortho-cleavage and go into the β-ketoadipyl-CoA pathway, creating either acetyl-CoA or succinyl-CoA, as shown in Figure 1.3 (Díaz et al., 2013). Compounds undergoing meta-cleavage on the other hand, including for example hydroxymuconate-semialdehyde, may pass through a range of pathways, generating acetyl-CoA or pyruvate, as seen in Figure 1.3 (Díaz et al., 2013). Thus, once the aromatic ring has been cleaved,

products take a range of metabolic pathways, generating useful byproducts or energy for the cell (Sugimoto et al., 1999). Oxygenases introduce phenolic hydroxyl groups in aerobic catabolism for aromatic ring activation. This contrasts with anaerobic pathways, where reduction of the aromatic ring takes place, with removal of phenolic hydroxyl groups which causes alicyclic compounds to be formed (Carmona et al., 2009)

A second aerobic pathway for cleaving the aromatic compound ring depends on the use of oxygenases, and is categorized as an aerobic hybrid type of pathway due to possessing some characteristics which are similar to those of anaerobic pathways (Díaz et al., 2013). The aerobic hybrid pathway uses CoA ligase to activate the ring to CoA thioesters, with hydrolytic cleavage of the ring taking place. The resultant CoA thioesters, which are not aromatic use reactions similar to β-oxidation metabolically, generating β-ketoadipyl-CoA, as shown in Figure 1.3 (Fuchs et al., 2011).

A number of aerobic bacteria from across various genera, including *Rhodopseudomonas palustris* and *Mycobacterium* sp. can achieve degradation of compounds containing one aromatic ring (Zhang and Anderson, 2012, Harwood and Gibson, 1988).

1.1.1.2 Anaerobic degradation of aromatic compounds

Some anaerobic bacteria have the ability to degrade aromatic compounds with various aromatic structures. Anaerobic degradation of aromatic compounds as a process is very slow and all oxygen dependent reactions are replaced by reduction reactions (Benner et al., 1984). Almost all aromatic compounds would be converted to be degradation of phenol is considered one of the best models to understand anaerobic nzoyl-CoA as a central intermediate by many side reactions and pathways. Anaerobic degradation where phenol is converted to 4-hydroxybenzoate (via phenylphosphate) then

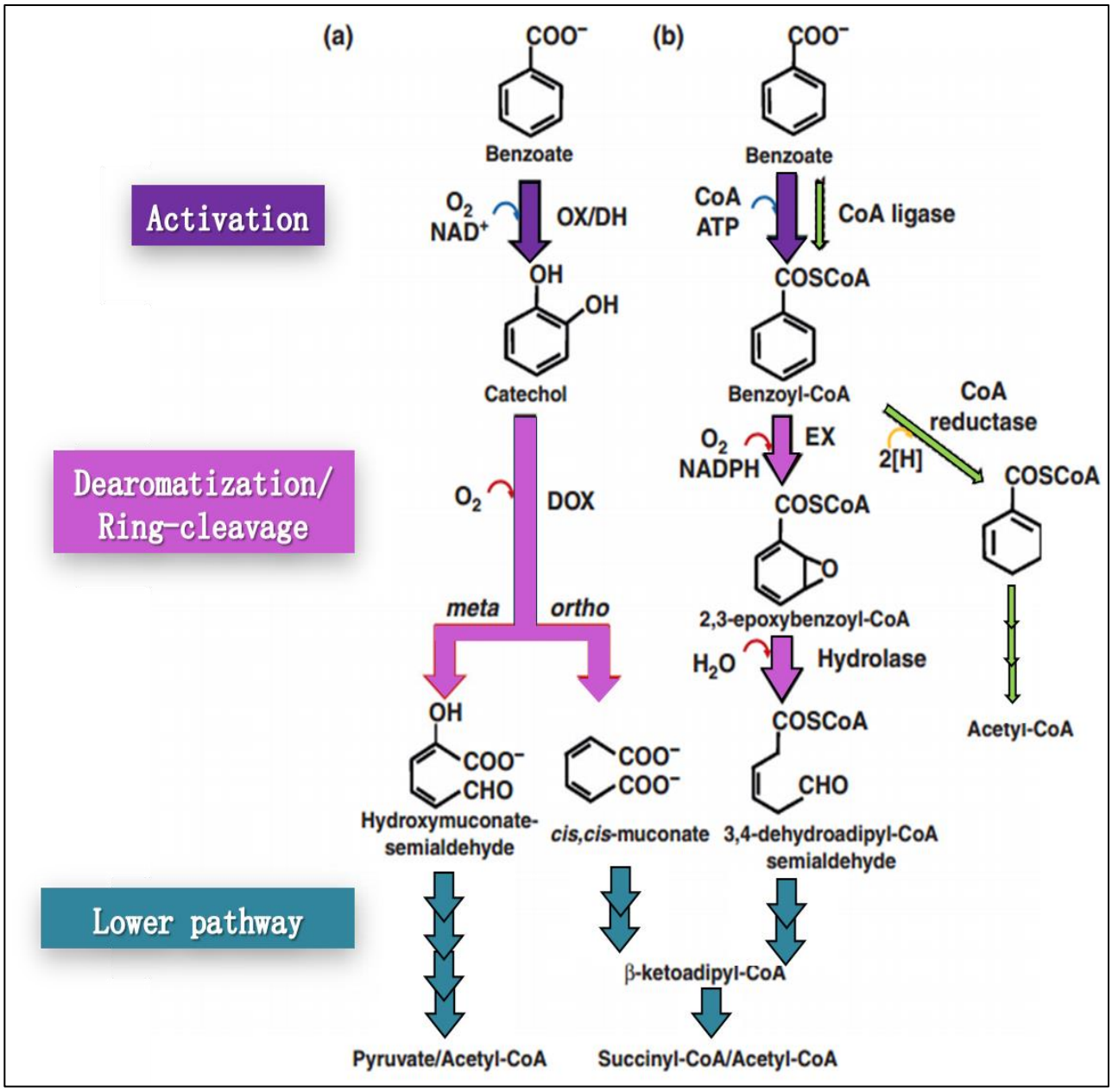

Figure 1.3: Aerobic degradation pathway for benzoate. (a) Classical aerobic degradation pathway. b) Hybrid degradation pathway, aerobic and anaerobic pathways have activation (puple), dearomatizaton/ring cleavage (pink) and additional reduction in lower pathways producing the central metabolites (blue). Ortho cleavage ring catechol while benzoyl-CoA in the hybrid pathway usually producing β-ketoadipyl-CoA intermediate. whereas in the anaerobic pathway (green) aromatic ring reduction occurs forming acetyl-CoA due to β-oxidation reactions. Figure was modified from (Díaz et al., 2013).

a benzoyl-CoA ligase adds a CoA group to produce the central intermediate benzoyl-CoA (Fuchs, 2008). The formation of a CoA thioester would lower the redox potential of electron transfer and "activates" the compound for further reactions (Gall et al., 2013).Then a reduction reaction occurs with the help of benzoyl-CoA reductase which would produce cyclohex-1-ene-1-carbonyl-CoA at the end (Koch et al., 1993) . This compound would enter ring cleavage pathway and β-oxidation pathway. In the ring cleavage pathway the cyclohex-1-ene-1-carbonyl-CoA compound is reduced to acyclic pimelyl-CoA that would be converted to 3-hydroxypimeyl-CoA to enter the β-oxidation pathway (Figure1.4) (Pelletier and Harwood, 2000). In the β-oxidation pathway three molecules of acetyl-CoA and one molecule of CO_2 are produced using, for example, enzymes encoded in the *pimFABCDE* gene cluster in *R. palustris* (Figure1.4) (Harrison and Harwood, 2005).

1.1.2 Nitroaromatic compounds and the enzyme nitroreductase

1.1.2.1 Nitroaromatic compounds

Nitroaromatic compounds are organic molecules which contain one or more nitro groups (NO_2-) attached to a benzene ring; for example, nitrobenzene, nitrophenols, nitrotoluenes etc. (Figure 1.5). They are found naturally comparatively seldomly but they are among the most significant environmental contaminants associated with human activities, because they are one of the largest groups of industrial chemicals to be used recently (Ju and Parales, 2010). They are mainly produced from incomplete combustion of petroleum and natural gases. These compounds are routinely used in the industrial manufacturing of explosives, pesticides, dyes and pharmaceuticals as intermediates and products (Ju and Parales, 2010, Marvin-Sikkema and de Bont, 1994, Misal et al., 2015). Emissions of the compounds as waste products from industry damages both human health

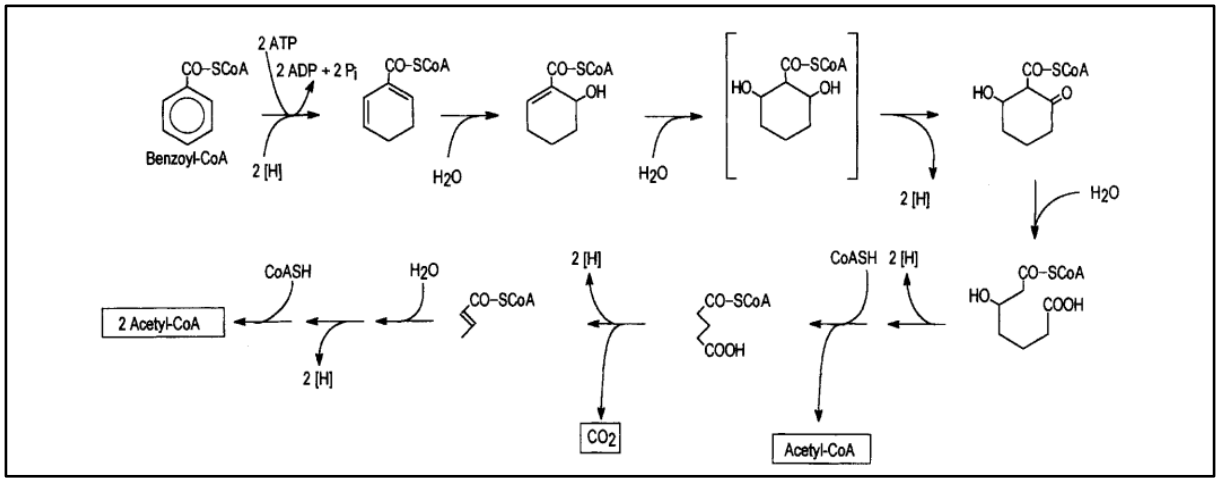

Figure1.4:Benzoyl-CoA anaerobic degradation pathway. Benzoyl-CoA transformation to acetyl-CoA and CO2 (Heider and Fuchs, 1997)(Heider & Fuchs 1997).

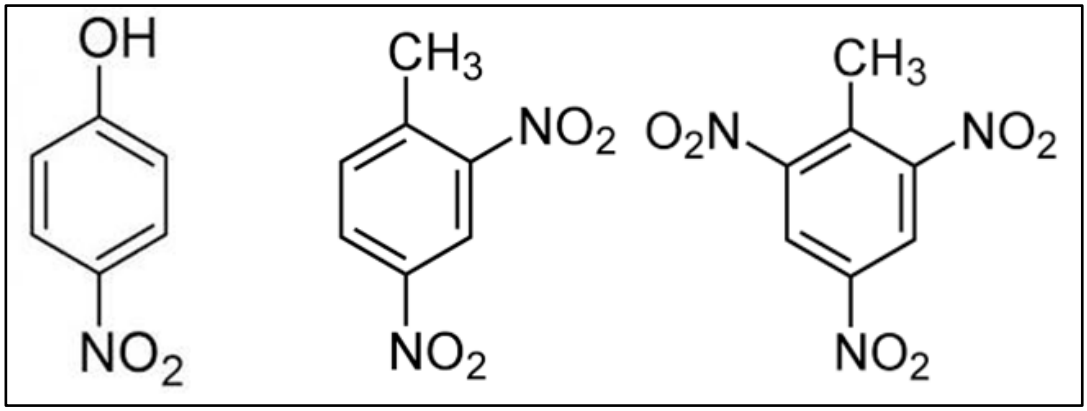

(a) **(b)** **(c)**

Figure 1.5: Shows benzene ring binding one or more nitro group.(a) 4-Nitrophenol. (b) 2,4-Dinitrotoluene. (c) 2,4,6-Trinitrotoluene (TNT).

and the health of the surrounding environment (Misal et al., 2015). Naturally-occurring nitroaromatic compounds generally come from various bacteria, plants and fungal organisms (Singh et al., 2015) and they are mostly antibiotics (Spain, 1995). Those organisms capable of forming nitroaromatic compounds, such as from the *Streptomyces* genera, create a broad range of antibiotic substances, such as chloramphenicol (chloromycetin) (Singh et al., 2015, Ehrlich et al., 1948) azomycin (Osato et al., 1955), dioxapyrrolomycin (Charan et al., 2006, Ehrlich et al., 1948). In addition, some nitroaromatics, such as nitrotoluene, nitrobenzene, nitrobenzoate and nitrophenols, are common for use in synthesizing nitrogenous organic aromatic compounds for industrial and other uses (Misal et al., 2015). For example, the pesticides parathion and bifenox are synthesized from nitrophenols (Fletcher et al., 1950). Further, for production of the painkiller and fever-reducer acetaminophen, more commonly called paracetamol, a single stage reductive acetamidation process for p-nitrophenol is used in production(Singh et al., 2015). Moreover, Picric acid and 2,4,6-trinitrotoluene (TNT) came to be synthesized in large quantities in the two world wars. It is possible to fuse 2 TNT molecules via hexanitrostilbene production in which methyl groups are oxidatively coupled (Ju and Parales, 2010). It is then possible for microbial agents in the ecosystem to transform the compounds into compounds which are not toxic (Misal et al., 2015).

A number of the compounds discussed above are identified as demonstrating carcinogenicity, mutagenicity or toxicity (De Oliveira et al., 2010b) which may explain the rapid evolution of analogous pathways of degradation (Kivisaar, 2011, Ju and Parales, 2010). Chemical and physical treatment creates intermediates which also show toxicity, proving costly as well as damaging to the environment (Singh et al., 2015). Therefore, treating such compounds biologically may offer benefits, since affordable methods can be developed and a large number of compounds can be biodegraded (Cho et al., 2008).

Most nitroaromatics need to undergo enzymatic reduction within organisms to exert their therapeutic and/or cytotoxic effects. The nitroreductase proteins form a group of enzymes that have a central role in the reduction of nitro groups on nitrocompounds (De Oliveira et al., 2010b).

1.1.2.2 Nitroreductases

Nitroreductases are a superfamily of flavoprotein enzymes which can reduce the nitro group ($-NO_2$) to their corresponding nitroso (-NO), hydroxylamine (-NHOH) and, in some cases amine ($-NH_2$) This family can be classified into two subgroups: nitroreductases and flavin reductases (Parkinson et al., 2000), Nitroreductase enzymes characteristically appear as a homodimeric protein associated with a prosthetic group; flavin mononucleotide (FMN) or flavin adenine dinucleotide (FAD) (Roldan et al., 2008). Further, they tend to prefer one of the two groups. Reductive action relies upon the use of nicotinamide adenine dinucleotide phosphate (NADPH) or nicotinamide adenine dinucleotide (NADH) as a source of electrons for nitroaromatic reduction (Little 2015, De Oliveira et al., 2010b, Roldan et al., 2008).

Nitroreductases have been grouped into two categories based on their ability to reduce nitro groups in the presence or absence of oxygen: the oxygen-insensitive (Type I) and the oxygen-sensitive (Type II) enzymes (Little 2015). Type I nitroreductases can be divided into two main groups, due to their similarity with *Escherichia coli* nitroreductases. NfsA (group A) are the major oxygen-insensitive nitroreductases using NADPH as an electron source, whereas NfsB (group B) are minor oxygen-insensitive enzymes which can use either NADH or NADPH as an electron donor (Bryant et al., 1981, de Oliveira et al., 2010a, Race et al., 2005, Whiteway et al., 1998, Song et al., 2015) . Nitroreductase has potential uses in bioremediation and chemotherapy (Haynes et

al., 2002). Recently, nitroreductases have come under increasing research attention within two spheres. First, in the field of environmental engineering, nitroreductases play a major part in the mediation of toxicity from nitroaromatics as well as showing possibilities for biocatalysis and bioremedial uses. Secondly, in medicine, there are possibilities in prodrug activation within chemotherapy (Roldan et al., 2008, De Oliveira et al., 2010b), as well as links between nitroreductases and antibiotic vulnerability (De Oliveira et al., 2010b). For example, chlorinated nitroaromatic antibiotic chloramphenicol (CAP) toxicity can be effectively mitigated by anaerobic transformation of nitroaromatics to aromatic amines, with the latter being less toxic and considerably easier to mineralize than the former (Liang et al., 2013).

1.1.2.2.1 Nitroreductase mechanism

Type I Nitroreductases (oxygen-insensitive) reduce nitro groups through the addition of two electrons following a Ping-Pong, bi-bi kinetic mechanism where the cycling of the FMN group between the oxidized and reduced states is dependent on NADH or NADPH as reducing agents (Little 2015, Roldan et al., 2008, De Oliveira et al., 2010b).

The first step is when a reduced NAD(P)H reacts with the active site of the nitroreductase and reduces the associated flavin co-factor. Subsequently, the flavin co-factor can then transfer the two electrons to reduce a nitroaromatic substrate to nitroso, hydroxylamino and amino derivatives (De Oliveira et al., 2010b, Little 2015, Roldan et al., 2008, Yang et al., 2012) (Figure 1.6). Nevertheless, the hydroxylamino derivative might be the final product of the reaction and usually the nitroso intermediate is not detected because the second two-electron reaction has a much faster rate than the first two electron transfers (De Oliveira et al., 2010b).

In contrast, nitroreductases of type II (oxygen-sensitive) transfer a single electron from nitroreductase to the nitro group to form an unstable anion free radical intermediate which rapidly reacts with oxygen forming superoxide, in a “futile redox cycle”, which regenerates the nitro group substrate (Peterson et al., 1979, Roldan et al., 2008, Little 2015, De Oliveira et al., 2010b) (Figure 1.6). Therefore, nitroreductase type II can mediate the reduction of nitroaromatic compounds by transferring only two electrons anaerobically in a futile cycle which uses reducing power, generating superoxide anions, and does not yield reduced nitroaromatic substrate (De Oliveira et al., 2010b, Roldan et al., 2008). Two nitro radical anions under anaerobic conditions can undergo a disproportionation reaction forming one molecule of nitroaromatic and a nitroso compound. It has been suggested that this mechanism may produce nitroso compounds in biological schemes (Patterson and Wyllie, 2014).

1.1.3 Nitriles and their hydrolysis enzymes

1.1.3.1 Organic cyanides (nitriles)

Cyanides are chemical compounds containing the cyano group (-CN) and are widespread in nature as inorganic cyanide (H-CN) and as organic cyanides or nitriles (R-CN) (Matam, 2013). About 84% of the inorganic cyanide that is produced in industry is used in producing organic cyanides (nitriles) (Eisler, 1991, Bhalla et al., 2012).

Nitriles are a group of extremely poisonous organic compounds containing the cyano group (Fang et al., 2015) , they are mainly present in the nature as cyanoglycosides which are produced by animals and plants by releasing hydrogen cyanide, which is responsible for forming the toxic cyanoglycosides (Kaul et al., 2007, Ramteke et al., 2013).

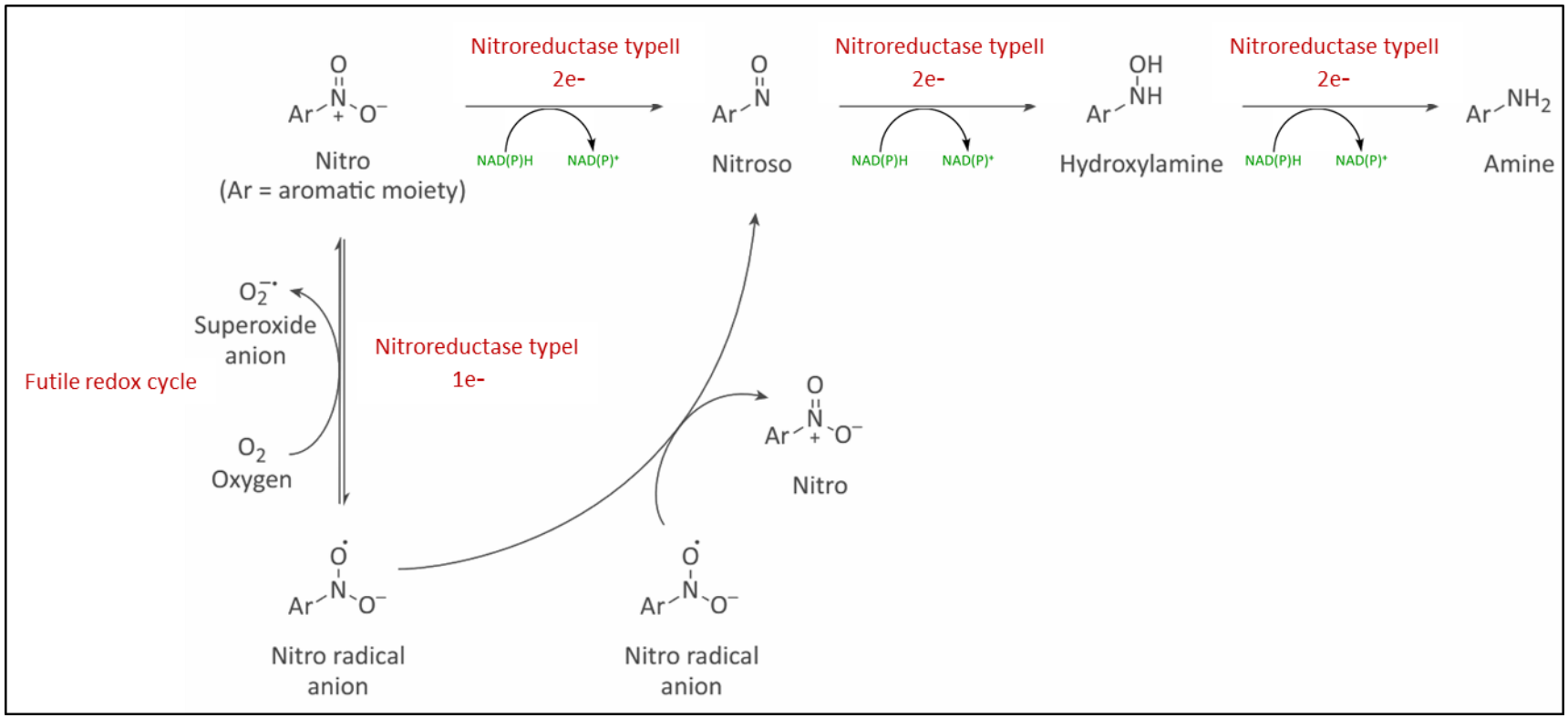

Figure 1.6: Nitroreductase Type I and Type II and their mechanism of action, using a typical nitroaromatic compound. Type I nitroreductases transfer two electrons from NAD(P)H, forming nitroso then hydroxylamino as intermediates, as well as ultimately the amino group. Type II nitroreductases transfer one electron to the nitro group, and forming nitro anion radical , this radical aerobically forming a superoxide anion and cause a futile redox cycle, and the nitro group is regenerated . Figure was modified from Patterson and Wyllie (2014).

In addition, nitriles are formed widely in industrial synthesis of solvents, plastics, cosmetics, rubbers, pharmaceuticals, agricultural and chemical industries (Fang et al., 2015, Agarwal et al., 2012) and are also used in fossil fuel processing (Ramteke et al., 2013).

Creating carboxylic acids by converting nitriles is significant for synthetics, as nitriles produce a range of these acids, with simple access to nitrile educts (Matam, 2013). Nitrile compounds can be degraded chemically or biologically. The chemical procedure for detoxification of nitriles is expensive and requires hazardous chemicals such as sodium hypochlorite. Furthermore these methods can lead to production of many unwanted by-products as well as inorganic waste (Agarwal et al., 2012). In contrast, a microbial procedure has been considered an effective way to remove highly toxic nitriles and the most acceptable method because of its lower cost than chemical methods and the fact that it is characterized as environmentally friendly (Fang et al., 2015, Kaul et al., 2007).

In general, microbial degradation of nitriles follows the hydrolytic pathway, which comprises two enzymatic pathways to convert nitriles, either directly through one step to the corresponding carboxylic acid and ammonia using nitrilase (EC 3.5.5.1) or through converting the nitriles to amides as an intermediate using nitrile hydratase (NHase, EC 4.2.1.84) and afterward converting this to carboxylic acids and ammonia using amidase (EC 3.5.1.4) (Fang et al., 2015, Agarwal et al., 2012) (Figure 1.7).

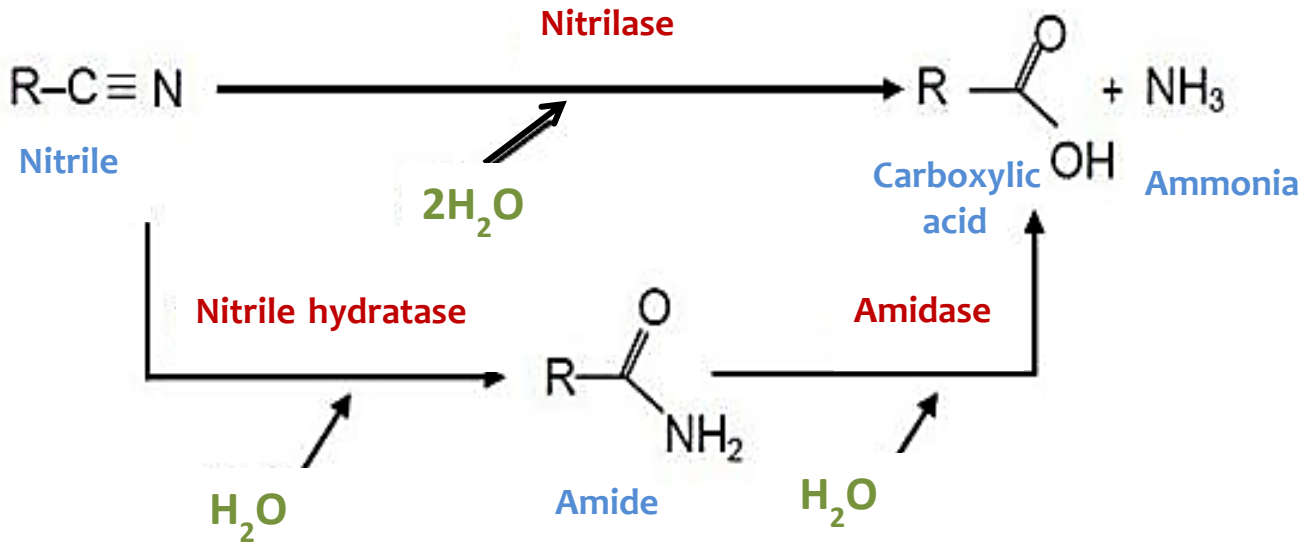

Figure 1.7: Enzymatic pathway to convert Nitriles to carboxylic acid and ammonia.
Figure was modified from (Rao et al., 2010)

All of the members in the superfamily contain a conserved catalytic triad Cys-Glu-Lys at the active site, and a significant similarity in α-β-β-α architecture (Pace and Brenner, 2001) (Table 1.1). In seven branches of this superfamily, the nitrilase is fused to another

1.1.3.2 Nitrile hydrolyzing enzymes

1.1.3.2.1 The nitrilase superfamily

Originally, carbon-nitrogen (C-N) hydrolyzing enzymes included nitrilases, cyanide hydratase, aliphatic amidase and β-ureidopropionase (Ramteke et al., 2013, Bork and Koonin, 1994). These enzymes have been categorized into 13 distinct branches based on amino acid sequence similarities as the nitrilase superfamily (Pace and Brenner, 2001). Only one branch is observed to have true nitrilase activity, which uses only nitriles, and the nitrilase enzyme belongs to this branch along with cyanide hydratase and cyanide dihydratase (Agarwal et al., 2012, Pace and Brenner, 2001). However, nitrile hydratases (NHases), which also hydrolyze nitriles, are not included in any branch in this superfamily (Singh et al., 2006). However, most of the remaining 12 branches display amidase activity with differing specificity. Enzymes of branches 2, 3, 4 and 5 consist of aliphatic amidases, amino-terminal amidase, biotinidase, and β -ureidopropionase respectively. Carbamylase belongs to branch 6, which is specific for the decarbamylation of D-amino acids (Thuku et al., 2007, Agarwal et al., 2012). Branches 7 and 8 comprise prokaryotic and eukaryotic NAD^+ synthetase respectively (Agarwal et al., 2012, Bellinzoni et al., 2005). Enzymes of branch 9 are apolipoprotein N-acyltransferases and catalyze reverse amidase (condensation) reactions (Agarwal et al., 2012). Enzymes of branch 10 are characterized as having a fusion protein construction at the atomic level, NitFhit, and this domain of nitrilase fuses to the nucleotide-binding Fhit protein

Table1. 1: Thirteen branches of the nitrilase superfamily. Seven branches denote domains found in only some members of the nitrilase superfamily. The conserved consensus sequences on either side of catalytic triad (EKC) residue are illustrated for all branches. Shading of residues denotes the following: pink, residue is conserved in all branches; green, residue is conserved in nine or more branches, while blue, residue is conserved in six to eight of the branches. Upper case letters indicate 90% or greater consensus levels within a branch, while lower case letters are 50% or greater. Table was modified from Pace and Brenner (2001) and Mascré Nel (2009).

			Conserved signature sequence surrounding Catalytic triad residues																													
			GLU						LYS								CYS															
	Branches	Additional domains																														
1	Nitrilase		f	P	E	A	F		h	R	K	I	.	P	T		I	.	C	W	E	N	.	.	p
2	Aliphatic amidase		F	P	E	Y	S		Y	R	K	I	P	W	c		i	I	C	d	D	G	n	y	P
3	Amino-terminal amidas	-unknown domain	F	P	E	.	.		Y	r	K	.	F	L	.		.	I	C	M	D	.	.	P	Y
4	Biotinidase	full/partial nitrilase domain) and -carboxyl domain	F	P	E	D	.		Y	r	K	.	h	L	y		F	t	C	F	D	i	I	f	y
5	β-ureidopropionase		.	Q	E	A	W		.	R	K	N	H	I	P		N		C	Y	G	R	H	H	P
6	Carbamylase		F	P	E	L	A		Y	R	K	I	H	L	P		f	I	C	N	D	R	R	W	P
7	Prokaryote NAD^+ synthetase	-NAD^+ synthetase domain	f	P	E	L	.		.	.	K	.	.	L	P		.	I	C	E	D	.	w	.	P
8	Euokaryote NAD^+ synthetase	-NAD^+synthetase domain	G	P	E	L	E		R	p	K	M	.	I	a		E	I	C	E	E	L	w	.	P
9	Apolipoprotein N-acyltransferase	Hydrophobic domain- and -dolichol phosphate mannose synthetase domain	W	P	E	.	a		.	.	K	.	.	I	V		.	i	C	y	E	.	.	f	.
10	Nit and NitFhit	-Fhit domain	L	P	E	.	f		y	r	K	.	H	I	F		.	i	C	Y	D	.	R	f	p
11	Nit11		.	q	E	L	f		Y	R	K	.	H	I	P		.	i	C	W	D	q	w	f	p
12	Nit12	-N-terminal acetyltransferase	F	P	E	I	F		Q	y	K	I	H	i	T		q	I	C	Y	D	I	E	F	P
13	Nonfused		I	P	E	.	.		y	r	K	.	h	L	f		.	i	C	y	D	.	r	F	P

(Mascré Nel, 2009, Pace and Brenner, 2001). Enzymes of branches 11, 12 and 13 consist of NB11, NB12 and nonfused outliers, respectively (Agarwal et al., 2012, Singh et al., 2006).

domain: for instance, the prokaryotic *Mycobacterium tuberculosis* has NAD+ synthetase, which is associated with the N-terminal amidase domain to utilize released ammonia from the nitrogen source glutamine for NAD+ synthesis (Mascré Nel, 2009, Bellinzoni et al., 2005, Agarwal et al., 2012) (Table1.1).

1.1.3.2.1.1 Nitrilase

Nitrilase has been known of as an enzyme which metabolizes nitriles for almost four decades, being the first of this type of enzyme to be identified. In plant species, Nitrilase converts indole-3-acetonitrile into the auxin indole-3-acetic acid. In recent years, enzymes which hydrolyse nitriles, and nitrilases in particular, have been recognized as presenting possibilities for use in biotechnology. This interest has resulted in a number of fungal and bacterial organisms with nitrile-hydrolising ability being isolated (O'Reilly and Turner, 2003, Kaul et al., 2007).

A number of the isolated nitrilase-active microbes show nitrile-metabolizing capacity for a range of nitriles, including naturally-occurring and synthetic types. For example, the bacteria *Pseudomonas* sp., *Rhodococcus* sp., *Bacillus* sp. show this ability, as well as the fungi *Fusarium* sp. and *Penicillium* sp. In particular, the substrate specificities of the enzymes vary broadly. Therefore, these enzymes are classified into 3 different types based on their substrate specificities, namely aromatic nitrilases, aliphatic nitrilases and arylacetonitrilase (Figure 1.8) (Kaul et al., 2007).

Generally, nitrilases exist as inactive dimers that, after activation, subsequently form a large homo-oligomer with a differing number of subunits. The monomer form of nitrilase exists in a 4-layered αββα fold that associates to form an 8

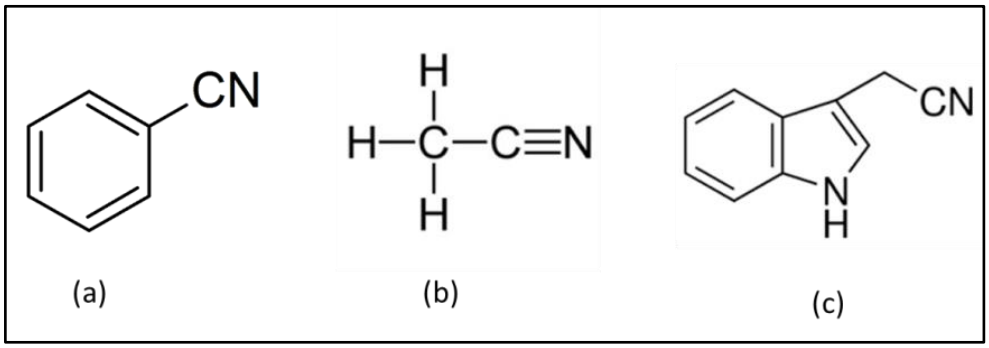

Figure 1.8 :Types of different nitrile substrate. (a) Aromatic nitrile (benzonitrile). (b) Aliphatic nitrile (acetonitrile). (c) Arylacetonitrile (3-Indoleacetonitrile).

layered αββα-αββα dimeric form: therefore, the oligomeric form is an active enzyme (Andrade et al., 2007; Agarwal et al., 2012). These enzymes do not contain any metal cofactor or prosthetic groups for their activity. They are presumed to contain cysteine residues at or near the active site, which is necessary for the catalytic activity of the enzyme (Ramteke et al., 2013). The reaction mechanism is suggested to involve a nucleophilic attack of the carbon atom of the cyano group by a sulfhydryl group of a cysteine residue (Ramteke et al., 2013), yielding ammonia with the first H_2O addition, followed by production of acid and a regenerated enzyme with the second H_2O (Singh et al., 2006) .

1.1.3.2.1.2 Nitrile hydratase (NHase)

Nitrile hydratase (NHase) was formally identified two decades ago following the first identification of nitrilases (Robinson and Hook, 1964). NHase is an important enzyme in the enzymatic pathway that catalyzes the hydration of nitriles to corresponding valuable amides, which are further catalyzed to the corresponding carboxylic acid by amidases (Kaul et al., 2007, Banerjee et al., 2002). The action of enzymes on acrylonitrile to generate acrylamide with use of nitrile-hydrating entire *Rhodococcus* sp. N-774, *Rhodococcus rhodochrous* J1 and *Pseudomonas chlororaphis* B23 cells, starting in 1985, was the first large-scale process employed industrially which relied on biocatalysts to convert nitriles (Yamada and Kobayashi, 1996).

These enzymes consist of two types of subunits, α and β complexed, in varying numbers. They are metalloenzymes; more than one third of all proteins are known to be metalloproteins, and metal ions have many roles in proteins, for example as catalytic centres, in oxygen reduction, electron transfer, gene regulation and in the folding and stabilization of the protein (Xia et al., 2016, Waldron et al., 2009). Based on the presence of metal ions, NHases may fall into 2 major categories; non-heme Fe

(III) ion (ferric NHases) or non-corrin Co (III) ion (cobalt NHases) (Kaul et al., 2007, Yamada and Kobayashi, 1996, Banerjee et al., 2002). These metal ions are located at the active site of the α subunit (Xia et al., 2016, Black et al., 2010). All of the NHases characterized showed a significantly homologous amino acid sequence, C**X**LCSC, which forms the active metal binding site. In Cobalt NHase, **X** is usually threonine (T) in the active centre, while in ferric NHases, it is usually serine (S) (Banerjee et al., 2002, Precigou et al., 2001).

X-ray crystallography of both cobalt and ferric NHases and structural analysis show that both enzymes have the same geometry at the active site. In all known NHases, the metal ion enzyme ligands at the active site in the α-subunit consist of three conserved amino acids sequence residues (αCys^{109}, cysteine-sulfinic acid (αCys-SO_2H) and cysteine-sulfenic acid (αCys-SOH). Moreover, the β-subunit provides the stability for the protein structure of the active centre via hydrogen bonding with two conserved sequences (βArg^{56} and βArg^{141}) (Piersma et al., 2000, Kaul et al., 2007).

1.1.3.2.1.3 The NHase activator protein

Characterization of metalloproteins has been in progress for many years, but in more recent times attention has been drawn for the first time to the mechanisms through which biological metallocentres are constructed. An appropriate "activator protein" mediates the transfer to NHases of metal ions (Liu et al., 2012, Xia et al., 2016).

The activators for Fe-NHases have been revealed to act as metallochaperones, which are metal-binding proteins considered to transfer the appropriate metal ion or metal-containing molecules to a target protein (Lu et al., 2003, Xia et al., 2016). On the other hand, cobalt is incorporated into the majority of Co-NHases via activator proteins filling the role of "self-subunit swapping chaperones" (Zhou et al., 2008, Zhou et al., 2010, Xia et al., 2016) "Self-subunit

swapping" is one of the post-translational maturation processes of the Co-NHase family (Zhou et al., 2010, Liu et al., 2012). Activator proteins are present in a complex form alongside the NHase α-subunit, with this subunit being required to swap between the NHase α-subunit, which does not contain cobalt, and the α-subunit in the complex, which contains cobalt, in order for cobalt to be incorporated into NHase (Liu et al., 2012, Xia et al., 2016, Zhou et al., 2008). Therefore, activator proteins are important for NHase maturation (Liu et al., 2013).

Highly purified NHase is used widely in the industrial production of acrylamide and nicotinamide (Kobayashi and Shimizu, 1998). Nevertheless, most NHases with high activity lose stability in industrial manufacturing (Liu et al., 2008). Thus, a more stable NHase with high activity and high tolerance is required for industrial applications. Subunit gene fusion can enhance protein stability. For this NHase, fusion of *Monosiga brevicollis* NHase α-subunits and NHase β-subunits, which are frequently separated, occurs within a peptide. It is proposed that this fused NHase may present advantages, including greater activity levels, greater stability and/or novel specificities of substrates. Thus, gene-fusing approaches have the potential to enhance or expand NHase applications (Xia et al., 2016).

1.2 *Rhodopseudomonas palustris* (*R. palustris*)

In this project, the enzymes discussed above were studied in the versatile phototroph *Rhodopseudomonas palustris*, which has been found to contain several genes encoding nitroreductases, nitrilases and a single nitrile hydratase gene cluster. *R. palustris* a Gram-negative rod shaped bacterium (Figure 1.9) that reproduces by budding. *R. palustris* is found in a plethora of environments, including pond water, soil and manufacturing waste. It can thrive widely in the environment as a result of its highly flexible metabolism. It is classified as a member of the Rhodospirillaceae, or

Figure 1.9 purple phototrophic bacterium ***Rhodopseudomonas palustris***

purple non sulphur bacteria: a family of the anoxygenic phototrophic purple bacteria. *R. palustris,* typical of the Rhodospirillaceae in having a diverse carbon and energy metabolism, being able to grow aerobically in the dark chemotrophically, or anaerobically in the light phototrophically, using either organic compounds (heterotrophy) or CO_2 (autotrophy) as a carbon source. Photoheterotrophic or chemoheterotrophic growth of *R. palustris* is supported by a number of organic substrates, including sugar, organic acids and fatty acids (Larimer et al., 2004). Therefore, *R. palustris* has the capability to survive in changeable conditions, while the optimum temperature for growth is 30°C (Wong et al., 2014, Harwood and Gibson, 1988). Furthermore, the microbe can fix nitrogen into ammonia for growth, as well as generating gaseous hydrogen through a nitrogenase side reaction (Simpson & Burris 1984). It has the ability to grow on a variety of aromatic compounds as a sole carbon source, meaning that it has potential for use in bioremediation (Dutton and Evans, 1969).

R. palustris is distinctive among the photosynthetic bacteria with respect to its ability to utilize a wide range of aromatic compounds as a sole carbon source, both under aerobic and anaerobic conditions. It has long been established that anaerobic breakdown of such compounds by *R. palustris* is carried out through the anaerobic benzoyl-CoA pathway (Salmon et al., 2013). *R. palustris* has the ability to metabolise many aromatic compounds derived from plants and lignin, such as p-coumaric acid, benzoic acid, p-hydroxybenzaldehyde, vanillin, 4-hydroxyacetophenone, acetovanillone, as well as aromatic amides from ammonia fibre expansion (AFEX) (Austin et al., 2015). *R. palustris* is capable of growth with the aliphatic amide acrylamide under photoheterotrophic conditions (Wampler and Ensign, 2005). Meanwhile, some other members of the Rhodospirillaceae have been reported to have the capacity to degrade or transform aromatic compounds. *Rhodobacter capsulatus* strain E1F1 is capable of photoassimilating nitrates and possesses a nitrophenol

reductase that photoreduces 2,4 –dinitrophenol and 2-amino-4-nitrophenol (Blasco and Castillo, 1993). *Rhodospirillum fulvum* grows anaerobically on benzoate as a carbon source (Pfennig et al., 1965).

Aims of the project:

The overall aim of the study was to explore the possibility of using nitroreductases , nitrilases and a nitrile hydratase from a single source bacterium - *R. palustris* - to cary out useful transformations of nitroaromatic compounds.

The specific objectives of this study were:

- To clone, purify and biochemically characterize the complete set of nitroreductase enzymes from *R. palustris* to break down the toxic nitroaromatic comounds.

- To clone, purify and biochemically characterize the complete set of nitrilase enzymes from *R. palustris* and explore their degradation of the aromatic and aliphatic nitriles and in producing valuable carboxylic acids.

- To clone, purify and biochemically characterize the single nitrile hydratase enzyme from *R. palustris* and study its ability to degrade the aromatic and aliphatic nitriles

CHAPTER 2

MATERIALS AND METHODS

Materials and methods

2.1 Materials

Materials and Chemicals used in this project were obtained from different companies such as Sigma-Aldrich, Fisher Scientific, Promega, Invitrogen, Oxoid, Qiagen and Acros Organics.

2.2 Microorganisms

The different bacterial strains used in this study are listed in (Table 2.1).

Table 2.1: Strains used in this study

Strain	Source
***Rhodopseudomonas palustris* (CGA009)**	Prof. D. K Newman California Institute of Technology
***Escherichia coli* DH5α™**	Invitrogen
***Escherichia coli* BL21 (DE3)**	Invitrogen
***Escherichia coli* TOP 10**	Invitrogen
***Escherichia coli* Origami™B (DE3)**	Invitrogen
Escherichia coli Rosetta	Invitrogen

2.2.2 Media Preparation

The preparation of culture media was preformed following the manufacturer instruction using distilled water (dH_2O). Media sterilization was attained by autoclaving the prepared media at 121ºC for 20 minutes.

2.2.2.1 Antibiotics

Antibiotics from (Sigma-Aldrich) were prepared using sterilized distilled water (dH_2O) and antibiotic stock solutions (1000x concentrated) were then filter sterilized using (0.2 µm) syringe filters. Antibiotic stock solutions were stored at 4ºC and the final concentration of antibiotic used in different media was between 50-100 µg ml^{-1} for Carbenicillin.

2.2.2.2 Media for growth of *R. palustris*

R. palustris routine growth was done using liquid peptone yeast extract (PYE) supplemented with succinate (5g/L of peptone (Becton), 5g/L yeast extract (Oxoid) and 5g/Lsuccinic acid (Oxoid). The different components were mixed together with dH_2O and sterilized by autoclaving at 121 ºC for 20 min then stored at room temperature. Solid peptone yeast extract media was prepared with the addition of 13g/L agar (Melford) to the liquid form. Antibiotic supplementation was preformed once needed after media autoclaving (50 ºC)

Rhodobacter capsulatus vitamins (RCV) minimal media (Weaver et al. 1975) was used for the growth of *R. palustris*. The media was prepared by mixing the following (final concentrations); sodium succinate (30 mM), $(NH_4)_2SO_4$ (7.5 mM), $MgSO_4.7H_2O$ (1 mM), $CaCl_2.2H_2O$ (0.5 mM), Na_2.EDTA (0.05 mM), NaCl (1 mM), $FeSO_4$. $7H_2O$ (0.04 mM), $MnSO_4$ (0.01 mM), $NaMoO_4$. $2H_2O$ (3.3 mM), $ZnSO_4$. 7 H_2O (0.9 mM), $Cu(NO_3)_2$. $2H_2O$ (0.2 mM), Thiamine HCl (6 µM), Biotin (0.2 µM) and Nicotinic acid (8 mM) with dH_2O. Then RCV media were sterilized by autoclaving at 121ºC for 20 minutes and stored at room temperature. Other supplements were added after autoclaving and when the media reached 50 ºC. This included potassium phosphate buffer pH 7 (0.64 M), Sodium bicarbonate (10 mM final), vitamin mixture (p-aminobenzonoic acid (17 µM), Vitamin B_{12} (0.01 µM) and Calcium pantothenate (4 µM). In the experiment where different aromatic substrates were tested, 3 mM benzoate was supplemented with 3 mM aromatic substrate as the sole carbon source. After the addition of aromatic compounds, the media was adjusted to pH 7. Samples were taken at different times after inoculation (0 time, 60, 120 hours), then samples were centrifuged and supernatants were stored at -20°C until analysis by H1-NMR.

2.2.2.3 Growth of *E. coli*

E. coli was grown on LB agar with different types of antibiotic based on the experiment and cultured at 37 ºC. The antibiotic was added after autoclaving and plates were stored at 4ºC before use. For *E. coli* grown in liquid cultures, the flasks were incubated shaking at 250 rpm under 37ºC.

2.2.2.4 Growth of *R. palustris*

R. palustris was grown phototrophically under anaerobic conditions in liquid RCV media. The media was placed on a magnetic stirring plate (Stuart) to agitate the culture and prevent biofilm formation. Energy saving bulbs (15W LED) were used at 18 cm distance from growth vessels and the cultures were grown at 30 ºC. *R. palustris* grown on RCV agar plates were initially inoculated from glycerol stock and and the culture was kept in the dark at 30 ºC inside a closed container.

2.3 DNA extraction and manipulation

Different reagents and kits were used and they were mainly from New England Biolabs, Promega, Qiagen and Sigma-Aldrich.

2.3.1 Plasmids

Plasmids used in this study are listed in Table 2.3

2.3.2 Preparation of DNA

DNA preparation was done according to Promega and Qiagen manufacturer's instructions:

2.3.2.1 Extraction of genomic DNA

Bacterial genomic DNA was extracted using Wizard® Genomic DNA Purification Kit (Promega) following the manufacturer instruction. DNA concentrations were determined by measuring absorbance at 260 nm using a Nanodrop spectrophotometer (Thermo Fisher Scientific).

Table 2.3 Plasmids used in this study

Plasmid	Description	Resistance	Source
pET21a (+)	**Contain T7 promoter that is induced by IPTG with His-tag at the C-terminal. Used for protein over expression.**	**Ampicillin**	**Novagen**
pBAD4285	**pBAD/HisB containing the *rpa4285* gene cloned into *Xho*I/ *HindIII* restriction sites**	**Ampicillin**	**R. Salmon University of Sheffield**
pET0599	**pET21a (+) containing *rpa0599* gene cloned into *Nde*I/*Xho*I *restriction* sites**	**Ampicillin**	**R. Salmon University of Sheffield**
pET0711	**pET21a (+) containing *rpa0711* gene cloned into *Nde*I/*Xho*I *restriction* sites**	**Ampicillin**	**This study**
pET1392	**pET21a (+) containing *rpa1392* gene cloned into *Nde*I/ *Not*I *restriction* sites**	**Ampicillin**	**This study**
pET1563	**pET21a (+) containing *rpa1563* gene cloned into *Nde*I/ *Not*I *restriction* sites**	**Ampicillin**	**This study**
pET1711	**pET21a (+) containing *rpa1711* gene cloned into *Nde*I/*Xho*I *restriction* sites**	**Ampicillin**	**This study**
pET2416	**pET21a (+) containing *rpa2416* gene cloned into *Nde*I/ *Not*I *restriction* sites**	**Ampicillin**	**This study**
pET2805-2806	**pET21a (+) containing *rpa2805-rpa2806* gene cloned into *Nde*I/*Xho*I *restriction* sites**	**Ampicillin**	**This study**
pET2805-2806-2807	**pET21a (+)containing *rpa2805-rpa2806-rpa2807* gene cloned into *Nde*I/*Xho*I *restriction* sites**	**Ampicillin**	**This study**
pET3215	**pET21a (+) containing *rpa3215* gene cloned into *Nde*I/*Xho*I *restriction* sites**	**Ampicillin**	**This study**
pET3408	**pET21a (+) containing *rpa3408* gene cloned into *Nde*I/*Xho*I *restriction* sites**	**Ampicillin**	**This study**
pET4166	**pET21a (+) containing *rpa4166* gene cloned into *Nde*I/*Xho*I *restriction* sites**	**Ampicillin**	**This study**

pET4285	**pET21a (+) containing *rpa4285* gene cloned into *Nde*I/*Xho*I *restriction* sites**	**Ampicillin**	**This study**

2.3.2.2 Extraction of plasmid DNA

Microbial plasmid was isolated using QIAprep® Spin Miniprep Kit (Qiagen) 27106 product following manufacturer instruction.

2.3.3 DNA manipulation techniques

Plasmid DNA manipulation was done following (Sambrook et al., 1989) protocol.

2.3.3.1 Polymerase Chain Reaction (PCR) amplification

Primers were obtained from Sigma-Aldrich and 100 µM stock primers were prepared and stored at -20°C. For gene cloning Accuzyme DNA polymerase (Bioline) was used to amplify the gene under investigation in 20 µl final volume. Reactions were prepared as explained in manufacturer's instructions (0.1 µg of template DNA was used, 10 µM primer stock, Accuzyme and dNTPs). Because *R. palustris* genome has high G-C content PolyMate (Bioline) was added in the reaction to increase the DNA yield. PCR was performed using Techne Techgene Thermal Cycler (Techne). First 5 minutes denaturation step at 95°C was carried out then Accuzyme was added (0.5 µl). The reaction went through the following cycle for 30 cycles

Denaturing	96 °C	1 minute
Annealing	60 °C	2 minutes
Elongation	72 °C	2 minutes

Followed by a final extension of 72 ^{o}C for 5 minutes. QIAquick® PCR Purification Kit (Qiagen) was used to purify and concentrate PCR product. PCR products were visualized by agarose gel electrophoresis pre-stained with ethidium bromide.

The success of gene cloning procedure in *E. coli* was confirmed by PCR also using *Taq* DNA polymerase master mix, primer mix and a single bacterial colony. The reaction was started by denaturation at 96^{o}C for 1 minute followed by 30 cycles of

Denaturing	96 °C	15 seconds
Annealing	62°C	1 minutes
Elongation	72 °C	30 seconds

A final extension at 72 °C for 5 minutes was carried out at the end. Agarose gel electrophoresis was also used to visualize PCR product. Primers used in this study are listed in (Table 2.4).

2.3.3.2 Agarose Gel Electrophoresis

DNA samples were analyzed using 0.7 % agarose gel electrophoresis. 0.7 % [w/v] agarose was added to 1x TAE buffer (40 mM Tris-acetate, 1 mM ethylenediaminetetraacetic acid (EDTA) pH 8.0). The mixture was dissolved by heating in the microwave for 2 minutes and after that the mixture was allowed to cool (~50 °C) to add 200 ng/ml ethidium bromide. The mixture then was poured into a gel casting tray with fitted gel comb. DNA sample was loaded into the gel after the addition of 5 x DNA loading buffer (Tri-Colour, Bioline) and DNA Ladder (Hyperladder I, Bioline) was also loaded in the gel. DNA Sample migration through the gel was carried out in 1 x TAE buffer at 110 v for 40 minutes and the bands were viewed using an ultraviolet (UV) light source (Gene Flash Gel Documenting System, Syngene).

Table 2.4 Full list of Primers used in this study

Gene	Primer sequence	Used for
RPA0711	F: 5'- ATTACGCATATGACCGACCCGGCCGAGATCGCCGCCGCC-'3	Cloning and unsuccessful protein over expression
	R: 5'- TTCTATCTCGAGGCGCGACAGAACGATGCGCCCCGCCGT -'3	
RPA1392	F: 5'- ATACGCCATATGACGCCATCACCTTGCTGCTGACCCGAA-'3	Cloning and unsuccessful protein over expression
	R: 5'-TTACAGGGCCGCCAAATGCCGCACATGAGCTTCAGGATC-'3	
RPA2805-RPA2806	F: 5'- GCTTAGCATATGGCCGACCATGAGCATCATCAC -3'	Cloning and protein over expression
	R: 5'- AATATACTCGAGCGCGCGCTCCAGATAGGAGTC -'3	
RPA1711	F: 5'- ATTACGCATATGATGACCGACGCGCCCGCGACCACCGCT-'3	Cloning and protein over expression
	R: 5'- ATACATATCTCGAGCTCCACGAACGTCGCGACCTCGCCGAG-'3	
RPA3215	F: 5'- ATTACGCATATGCAATACGACGACGTGGTCCGCGGCCGC -'3	Cloning and unsuccessful protein over expression
	R: 5'-CATTACCTCGAGGCGGTCGAAGCCGACGAACCG-3'	
RPA3408	F: 5'- ATTAATCATATGACCGGGCCCGGCCCGACGCCGGA -'3	Cloning and unsuccessful protein over expression
	R: 5'- CCGGCCCTCGAGGAACCGCGTTACGATCGCGTTCAGTTC-3'	
RPA4285 pET21a(+)	F: 5' - ATTATACATATGACGCTGCCCGATCCCCACCTGCTGTT -3'	Cloning and protein over expression
	R: 5'- TCCAATCTCGAGCAGCACGCGGCAGGCGTCCTCGAAGG -'3	
RPA0599	F: 5'-AGTATA GCTAGC ACCGAAGCGGTGCCGTTCAA -'3	Cloning and protein over expression
	R:5'- AATATA GCGGCCGC TGATTGCCGGACCAGATG -'3	
RPA1563	F: 5'-GCCGCGCATATGCTTCCTCACTTCAAAGCCGCT -'3	Cloning and protein over expression
	R: 5'- AATATAGCGGCCGCAAGGACTACGGGCGCCGC -'3	
RPA2805-RPA2806-RPA2807	F: 5' - GCTTAGCATATGGCCGACCATGAGCATCATCAC -3'	Cloning and protein over expression
	R: 5'- AATATACTCGAGACGCGGCGGTGACTCAGC -'3	
RPA2416	F: 5'- GCCGCGCATATGTCGCAACTGCTGAAGGTCGCT -3'	Cloning and protein over expression
	R: 5'- AATATAGCGGCCGCGTAGTTGCCGGCCATCGC -'3	
RPA4166	F: 5'- GCGGCGCATATGGCTAAGTTGAAAGTCGCGGC -3'	Cloning and protein over expression
	R: 5'- AATATACTCGAGGGCTCCGGCGTCGCCTGCA-'3	
RPA4285 in pBAD	F: 5'- ATTATACTCGAGAAGCTCGACGCTGCCCGAT -3'	Cloning and protein over expression
	R: 5' -TTAATGAAGCTTTCACAGCACGCGGCAGGC -'3	

2.3.3.4 DNA Digestion with Specific Restriction Enzymes

Amplified DNA samples and plasmid DNA were digested using certain restriction enzymes and buffer (NEB) as recommended by the manufacturer's guidelines. All restriction digestion reactions were carried out at 37 °C for either 2 hours or overnight then the enzyme activity was inactivated at 65 ^{o}C for 20 minutes. Finally, QIAquick® PCR Purification Kit (Qiagen) was used to purify the samples.

2.3.3.5 Plasmid DNA Phosphatase treatment

The phosphate group at the 5´ end of plasmid DNA vector was prevented to re-ligate after restriction digestion by using Antarctic Phosphatase (NEB). The phosphatase removed the phosphate group at the 5´ phosphoryl termini which is required by ligases to ligate the digested vector and such reaction prevented the self-ligation of vector itself. Phosphatase treatment was carried out as described in manufacturer's guidelines and phosphatase was inactivated at 65 ^{o}C for 20 minutes and the sample was purified by QIAquick® PCR Purification Kit (Qiagen).

2.3.3.6 Ligation of Digested DNA fragments

Ligation was carried out in many different insert to vector ratio 1:1, 3:1, 5:1, and 7:1. DNA band intensity in agarose gel was used to estimate DNA concentration. Band intensity was compared to Hyperladder I (Bioline) molecular weight standard of known concentration. 10 ng of vector DNA was added in the reaction but insert concentration was calculated using the following equation:

$$\frac{\text{ng of vector} \times \text{kb size of insert} \times \text{molar ratio of insert:vector}}{\text{kb size of vector}} = \text{ng of insert}$$

Ligation reaction mixture contained 1 µl of 10X T4 DNA ligase buffer (NEB) and 0.5 µl of T4 DNA ligase (NEB) in addition to the 10 ng of vector and the calculated

insert. The final volume was made up to 10 µl with sterile dH_2O and a reaction control was prepared with no insert added to asses self-ligation level of the vector and the level of un-digested plasmid. Reaction mixture was incubated either at room temperatures for 1 hour or at 4 ^oC for 18 hours before being transformed into chemically competent *E. coli*.

2.4 Preparation and transformation of chemically competent cells

2.4.1 Preparation of chemically competent *E. coli*

Competent *E. coli* cells were prepared by the following Hanhan (1983) method to create RF buffer solutions (Hanahan, 1983). First *E. coli* cells were grown in 50 ml LB broth media till they reached mid-exponential phase (OD_{600} 0.6). This OD correlates to ~ 4-7 x 10^7 viable cell ml^{-1} density. Then, cells were centrifuged at 6000 x g for 20 minutes at 4° C and the pellets were resuspended using 50 ml ice cold RF1 solution pH 5.8 (100 mM KCl, 50 mM $MnCl_2$ $4H_2O$, 30 mM CH_3COOK, 10 mM $CaCl_2$-$2H_2O$ and 15 % (w/v) glycerol). Afterwards, the cell suspension was incubated on ice for 15 minutes, centrifuged as mentioned above and re-suspended in 8 ml RF2 solution pH 6.8 (10 mM MOPS, 10 mM KCl, 75 mM $CaCl_2$-$2H_2O$, and 15 % (w/v) glycerol). Lastly, cells were kept on ice for 20 minutes, aliquoted as 100 µl in small eppendorf tubes and stored at -80°C.

2.4.2 Transformation of chemically competent *E. coli*.

The transformation of competent *E. coli* started with the addition of 2 µl of purified plasmid or 5 µl of ligation mixture to 100 µl competent cells after being thawed on ice. The mixture was kept on ice for 30 minutes then a heat shocking procedure was carried out at 42 °C for 50 second followed by ice incubation for two minutes. LB broth was added in the volume of 850 µl to the mixture tube and the tube was incubated at 37°C for 45 – 60 minutes. The culture then was centrifuged to

harvest the cells at 16000 x g for 5 minutes and a fresh 100 µl LB was added to the pellets to re-suspend. The culture was plated in an LB agar plate supplemented with the antibiotic that corresponds to the vector selection marker. Culture plates were then incubated at 37 °C for 18 hours. For transformation using ligation mixture, a control was made where no genomic DNA insert was added to the vector and only digested vector was added to the competent cells. This helped in the estimation of vector self-ligation and level of transformation for the vector itself.

2.5 Over-expression of Recombinant Protein

Protein over expression was carried out using different *E. coli* strain and two different expression vectors; the pET21a(+) and pBAD vectors.

2.5.1 pET21(+) system

The pET21 vector (Novagen) containing the T7 promoter was induced by IPTG to overexpress proteins under study. This vector will allow the recombinant protein to have 6-histidine amino acid tag incorporation at the C-terminus of the protein. First, the gene under investigation would be amplified using PCR as described earlier. The primers used in cloning were designed to contain specific restriction sites that correspond to the vector restriction site and the stop codon in the gene under study was removed in the reverse primer design to allow for the addition of 6-histidine tag in protein C- terminus. After cloning the constructs were analyzed by sequencing to ensure proper gene incorporation. Then, BL21 (DE3) overexpression strain of *E. coli* would be transformed with the vector and would be grown under two different temperature conditions (25 ^{o}C and 37 ^{o}C) and under variable time intervals (1,3,5 and over night) and 9 ml samples are taken at each time point. The culture was grown at 37 ^{o}C for almost 1 hours and 30 minutes to $OD_{(600)}$ of 0.6 then the culture was induced using 400 µM IPTG. The collected samples for

each temperature and time point were visualized using SDS-gel electrophoresis. The SDS-gel would determine for us the appropriate growth condition to conduct the batch culture overexpression experiment. The cells were in 2L LB broth batch cultures and cell pellets were collected by 4 ^{o}C centrifugation at 10000 x g for 10 minutes. The collected pellet was stored at – 20 ^{o}C for subsequent expremints. To overproduce cells containing nitroreductase protein LB media was supplemented with final concentration 20 µg/ml riboflavin 5` phosphate sodium sulphate hydrate, while supplemented with 100 µM $CoCl_2$ in overproducing cells containing nitrile hydratase protein.

2.5.2 pBAD/HisB system

The pBAD/HisB vector (Novagen) under the control of *araBAD* promoter was used specially when overexpressed recombinant protein in pET vector system yielded insoluble proteins. In pBAD/HisB vector the 6-histidine tag was incorporated at the N-terminal end after removing the start codon from the gene under study in PCR procedure. After Sequencing the construct to ensure the gene to be in frame, the construct was transformed into *E. coli* (TOP10) strain. Arabinose was used to induce the expression of the protein which was tightly controlled by arabinose concentration. Different arabinose levels were used to induce protein expression which in turn can alter the overexpression and solubility altitudes of the protein under study (Guzman et al. 1995). TOP10 cells were grown under two different temperature conditions (25 ^{o}C and 37 ^{o}C), under variable time intervals (1, 3, 5h and over night) and different arabinose concentrations (0.002%, 0.02%, 0.2% and 2%). The culture was grown at 37 ^{o}C for almost 1 hours and 30 minutes to OD $_{(600)}$ of 0.6 then the culture was induced by the different arabinose concentration and 9ml culture samples were taken at different time point for each concentration and temperature. The collected samples were visualized using SDS-gel electrophoresis. Cells were grown in 2L batch cultures

after defining the proper growth condition and the pellets were collected by 4 ^{o}C centrifugation at 10000 x g for 10 minutes. The pellet was stored at – 20 ^{o}C until needed.

2.5.3 Preparation of cell free extracts

The preparation of cell free extract from the 2 L batch culture was done before the procedure of protein purification to allow the content of *E. coli* cell to be released from microbial cells. The stored pellets were re-suspended in 15-30 ml phosphate binding buffer (section 2.8.5.1). The re-suspended pellet was sonicated at 16 micron amplitude (Soniprep 150 ultrasonic disintegrator, SANYO) for 20 seconds to break the cells. This procedure was repeated for four times before the final centrifugation at 18000 x g for 30 min under 4 ^{o}C temperature. After centrifugation the supernatant was collected to be used later in protein purification.

2.5.4 Protein purification

An automated protein purification system known as Akta Prime plus purification system (GE Healthcare) was operated to monitor protein purification from cell free extract supernatant.

2.5.4.1 Nickel Affinity Chromatography

A commercial 5 ml column HisTrap^{TM} HP (GE Healthcare, UK) was used to purify recombinant proteins under study following the manufacturer instructions. Cell free extract supernatant of nitroreductase was injected onto the column after initial injection with binding buffer (20 mM sodium phosphate buffer, 500 mM NaCl, 30 mM imidazole, pH 7.4) to calibrate the column. After cell free extract injection the column was also injected with binding buffer to get rid of all weakly bounded proteins, then 50 ml of elution buffer was gradually injected in 0-500 mM imidazole

concentration. Protein samples were collected in 1 ml fractions that would be analysed later to check protein purity Different eluted protein fractions were collected in a volume of 1 ml.

Nitrilase purification was performed by following the Kiziak et al (2005) method. Cell free extract was injected to the column with binding buffer 20 mM Tris/HCl pH 7.5, 150 mM NaCl, 1 mM DTT and 50 mM Imidazole then eluted with 20 mM Tris/HCl pH 7.5, 100 mM NaCl, 1 mM DTT and 500 mM Imidazole(Kiziak et al., 2005). While nitrile hydratase was purified using binding buffer 10 mM potassium phosphate buffer pH 7.5, 100 mM NaCl, 0.5 mM DTT, 40 mM butyric acid and 30 mM Imidazole and eluted with 10 mM potassium phosphate buffer pH 7.5, 100 mM NaCl, 1 mM DTT, 40 mM butyric acid and 500 mM Imidazole.

2.5.4.2 Gel filtration chromatography

The gel filtration chromatography was performed using AKTA purifier system on a 10x300 Superdex 200GL column. Flow rate was 0.5ml/min of elution buffer (20 mM tris-HCl pH 7.5, 100 mM NaCl, 1 mM DTT). Column was calibrated under the same conditions using Ferritin 440 kDa, Aldolase 150 kDa, Ovalbumin 44 kDa and Ribonuclease 12.5 kDa.

2.5.4.3 Protein concentration and desalting

The fractions with pure protein were collected in a vivaspin column (Sartorius, UK) to concentrate the protein. The Vivaspin column has a molecular weight cut off value where it can be used with different protein size. The Vivaspin column also helps in desalting the protein fraction to yield a pure protein that can be used in subsequent experiments. After collecting the pure fractions in the Vivaspin column , the column was centrifuged at 8000 x g for 20 minutes then the sample was washed with exchange buffer in a volume 3X the protein fraction volume.

2.6 Characterisation of Recombinant Proteins

2.6.1 Measuring Soluble Recombinant Protein Concentration

Soluble protein concentration was measured using the Bradford assay method (Bradford, 1976) and the Bio-Rad reagent (Biorad Inc, USA) for routine lab experiments. A 1 ml cuvette was used to make a mixture of 200 µl of Bio-Rad dye reagent concentrate, 20 µl of purified protein and 800 µl of milli-Q H_2O. Protein concentration was measured using spectrophotometer at OD_{595} nm and the OD value was used to calculate protein concentration in mg using this formula (OD_{595} X 15/ volume of protein (µl). For biochemical assays and sensitive NMR assays a more accurate protein concentration measuring procedure was used. The purified recombinant protein (10 µl) was mixed with dH_2O (990 µl) using a quartz cuvette and A UV spectrophotometer (UV-24001 UV-Vis recording spectrophotometer) (Shimadzu). The concentration in Molar was measured after taken UV spectrum from 270-330 nm using the following formula ((Absorbance at 280nm – Absorbance at 320nm/ Extinction Co-efficient of protein) X 100).

2.6.2 SDS-polyacrylamide gel electrophoresis

SDS polyacrylamide gel electrophoresis (SDS-PAGE) was used to visualize and assess protein quality and size. One dimensional SDS-PAGE was prepared using Bio-Rad MiniProtean 3 system according to manufacturer instruction. Resolving gel (12%) and stacking gel (6%) were prepared, resolving gel constitute of 30 % (w/v) acrylamide /0.8 % (w/v) bisacrylamide (2.5 ml), 1 M Tris-HCl pH 8.8 (2.35 mL), 10 % (w/v) sodium dodecyl sulphate (SDS) (62.5 µl), 10 % (w/v) ammonium persulphate (APS) (62.5 µl), 0.01 % N,N,N’,N’-Tetramethylethylenediamine (TEMED) (6.25 µl) and dH_2O (1.28 ml). The prepared resolving gel was mixed gently to prevent bubble formation and then was added to gel casting plate. A

stacking gel was prepared as soon as the resolving gel was settled by mixing the following 1 M Tris-HCl pH 6.8 (0.45 mL), 10 % (w/v) SDS (37.5 µl), 30 % acrylamide mixture (0.75 mL), 10 % (w/v) ammonium persulphate (APS) (37.5 µl), 0.01 % N,N,N',N'-Tetramethylethylenediamine (TEMED) (3.75 µl) and dH_2O (2.47 ml). After that, the gel was added slowly on top of the resolving gel and a comb was added to create loading wells. Gel was left to settle and protein samples were prepared.

The preparation of protein sample included mixing 20 µl protein sample with 20 µl loading buffer (2 % (w/v) SDS, 0.005 % [w/v] bromophenol blue, 5 % [v/v] 2-mercaptoethanol, 10 % (w/v) glycerol and 60 mM Tris-HCl pH 6.8) and sample boiling for 5 minutes. After that, the samples were centrifuged at 13000 x g for 10 minutes then sample was loaded into the wells of SDS gel. A Pre-stained Protein Ladder (PageRuler® Plus, Fermentas) was also loaded into the gel and the gel was electrophoresed at 180 V for 50 minutes. The gel was then stained with Coomassie brilliant blue dye (0.5 % (w/v) Coomassie Brilliant blue R [Sigma-Aldrich], 50 % [v/v] methanol and 10 % [v/v] glacial acetic acid) for 1 hour and de-stained by de-staining solution (40 % (v/v) methanol and 10 % (v/v) glacial acetic acid) to get rid of excess stain and gain visible protein bands.

2.7 Characterization of the purified protein

2.7.1 Molecular size analysis

The molecular weight of the purified protein was determined by mass spectrometry, carried out at the Biological Mass Spectrometry Facility, University of Sheffield by Dr. Simon Thorpe.

2.7.2 Flavin cofactor analysis

The purified enzyme was treated using 10% of Sodium dodecyl sulphate (SDS) for 10 min. The spectrum of released flavin was monitored using UV spectrophotometer between 300-600 nm (Fitzpatrick et al., 2003). The flavin: protein ratio was determined from the absorption of the purified enzyme at 446 nm and 280 nm, using absorption coefficients of 12,200 M^{-1} cm^{-1} for the flavin (FMN) and the extinction coefficients M^{-1} cm^{-1} for the protein (Emptage et al., 2009).

2.7.3 Cobalt cofactor analysis:

Spectrum of the purified enzyme was monitored by UV- spectrophotometer (Shimadzu) between 250-600 nm. The cobalt: protein ratio was determined from the concentration of cobalt in the protein sample to protein concentration measured by Bradford assay.

2.7.4 Metal analysis

The metal content of the purified protein was determined using induction-coupled plasma mass spectrometry (ICP-MS), carried out at the Biological Mass Spectrometry Facility, University of Sheffield by Dr. Neil Bramall

2.8. Biochemical Assays

2.8.1 Nitroreductase enzymatic assay

Nitroreductase activity was performed in a UV- spectrophotometer (Shimadzu) by measuring the decrease in A_{340}, indicating the nitroaromatic compound dependent oxidation of NADPH. The reaction mixture contained purified nitroreductase (RPA 1711 or RPA 4285) 2 μM, 0.05-0.7 mM nitroaromatic substrates, NADPH (0.15 mM), and Tris-HCl buffer (50 mM, pH 8) in a final volume of 1 mL quartz cuvettes. The reaction was started by addition of NADPH. Rates were

ccalculated using a molar extinction coefficient for NADPH of 6.22 mM^{-1} cm^{-1} at λ=340nm.

We investigated the effect of pH, temperature and NAD(P)H preference and concentration of the preferred substrate on nitroreductase activity by monitoring the change of enzymatic activity over the pH range of 7–9.5, and temperature range of 25-45 ◦C.

Once optimization of the conditions and protein concentration was determined, assays were carried out to determine the enzyme activity with varying concentrations of 2,4- DNT, 2,6 DNT, Potassium 4 –nitrophenyl sulphate and Methyl-4-nitrobenzoate and via consumption of NADPH at λ=340nm. Kinetic analysis of the purified nitroreductase with different substrates in the presence of NADPH was performed and the maximum reaction rate (Vmax) and Michaelis–Menten constants (Km) were calculated using non-linear regression in the Graph Pad Prism package software.

2.8.2 Nitrilase enzyme assay

2.8.2.1 Coupled assay

Nitrilase activity was determined by monitoring the loss of absorbance spectrophotometrically at 340 nm associated with oxidation of NADH to NAD^+ by glutamate dehydrogenase (GDH) producing glutamate from α-ketoglutaric acid and the ammonia released from the nitrilase reaction. In a typical assay, the reaction mixture contained purified nitrilase 5 µM, nitrile substrate 50 mM, 8 units GDH, 5 mM α-ketoglutaric acid , NADH 200 µM, 1 mM DTT and 50 mM HEPES, pH 7.5 in a final volume of 1 ml in a quartz cuvette. The reaction was initiated by addition of NADH. The rate was calculated using a molar extinction coefficient for NADH of 6.22 mM^{-1} cm^{-1} at λ=340nm (Seiner et al., 2010).

2.8.2.2 Berthelot (phenol) assay

The release of ammonia by the nitrilase reaction was colorimetrically determined using the phenol-hypochlorite method (Weatherburn, 1967) adapted for use in 96-well plates. A standard reaction mixture (100 µl) contained a final concentration of 50 mM potassium phosphate buffer (KPB) pH 7.6, 100 mM NaCl, 1 mM DTT, 50 mM nitrile substrate (stock 1 M dissolved in DMSO), and 5µM of enzyme. The reaction was incubated for 1 hour at 30°C. The reaction was stopped by the addition of 3.5 volumes of each reagent A (0.59 M phenol and 1 mM sodium nitroprusside) and reagent B (2.0 M sodium hydroxide and 0.11 M sodium hypochlorite), added sequentially. The resulting mixture was heated at 55°C for 5 min then incubated for 1 hour for colour stabilization. The absorbance at 600 nm was measured for 200 µl of the resulting reaction mixture using a Victor plate reader. Control reactions were carried out without enzyme. Standards were prepared using different concentration of ammonium chloride NH_4Cl.

2.8.2.3 *o*-Phthalaldehyde reagent assay

Nitrilase activity was also measured by the release of ammonia reacting with the *o*-Phthalaldehyde (OPA) reagent (200 mg mL^{-1}). OPA was dissolved in methanol then diluted (1:100) into 15 mM, pH 9.5 sodium tetraborate buffer). The reagent was stored at 5 ºC in the dark. The standard reaction mixture contained a final concentration of 50 mM nitriles (23 µl) (stock 1 M dissolved in DMSO), 207 µl from 5 µM enzyme in 10 mM KPB pH 7.2 and 1 mM DTT in a final volume 230 µl. The reaction was incubated for 18 hours at 30°C. The production of ammonia was then detected by mixing 140 µl of DMSO, 100 µl of OPA reagent, 50 µl overnight incubated reaction and 50 µl (10 % trichloroacetic acid (TCA)). The mixture was diluted into DMSO (1:2) and incubated for 10 min at room temperature. Ammonia concentration was measured by comparison to a standard curve prepared using different concentrations of NH_4Cl (2-12 mM) (Black et al., 2015).

2.8.3 Nitrile hydratase (NHase) assay

NHase was assayed for catalytic activity using different nitrile substrates. In this assay, the hydration of nitriles was measured spectrophotometrically by monitoring the formation of amide as indicated by absorption spectra changes between 200-450 nm using 10 mM potassium phosphate buffer pH 7.5, 0.5 mM DTT, 40 mM butyric acid, 0.1 μM enzyme and 0.5 mM nitrile substrate. The reaction mixture was incubated at 30°C. The conversion from nitrile to amide was measured after 0, 30, 60, 12,180, 240 and 300 min. The spectra were compared to 0.5 mM substrate and 0.5 mM amide alone.

2.8.4 Nuclear Magnetic Resonance (NMR)

R. palustris utilization of different nitriles as sole carbon source was monitored by 1H-NMR, where the presence of substrate spectral peaks was monitored in different samples with different time points. The mixture of each reaction was prepared using 3 mM substrate and supplemented with 3 mM benzoate then compare the spectral obtained with the benzoate alone to samples from culture media at different growth points. The samples were prepared in a 5 mm NMR tubes containing 450 μL reaction mixture, 50 μL D_2O and 2 μL trimethyl-silyl propionate (TSP) as a 0 ppm reference. All 1H-NMR data were collected at 25 °C on a Bruker Advance NMR spectrometer at 800 MHz. Processing and integration was performed using Bruker Topspin v1.3 software after manual baseline correction was done. NMR spectra were acquired with the help of Mrs. Andrea Hounslow in the departmental NMR facility.

CHAPTER 3

CHARACTERIZATION OF PUTATIVE NITROREDUCTASES FROM *RHODOPSEUDOMONAS PALUSTRIS*

3 Characterization of putative nitroreductases from *Rhodopseudomonas palustris*

3.1 Introduction

As discussed in chapter 1, the nitroreductase superfamily comprises flavoproteins characterized by dependence on FMN or FAD as prosthetic group, and they use either NADH or NADPH as electron donor to reduce the toxic nitroaromatic and nitroheterocyclic compounds to non-toxic and corresponding amine products in living organisms.

Nitroreductases have been functionally characterized into two main types: oxygen-insensitive (type I) and oxygen-sensitive (type II) (Kobori et al., 2001, De Oliveira et al., 2010b). Nitroreductase type I is common in bacteria and fungi (Song et al., 2015, De Oliveira et al., 2007), however type II nitroreductase can be found in various organisms, especially in eukaryotes. Type II nitroreductases catalyze one-electron reductions producing a nitro anion radical that reacts with oxygen forming a superoxide radical to regenerate the nitro group (Peterson et al., 1979, Guillen et al., 2009, De Oliveira et al., 2010b). Type II nitroreductases are oxygen-sensitive and have not been cloned from bacteria until recently (Bang et al., 2012, Whiteway et al., 1998, de Oliveira et al., 2010a). According to the amino acid sequence similarity with *Escherichia coli*, type I nitroreductases can be categorized into two major groups, NfsA (group A) and NfsB (group B) (Bryant et al., 1981, Whiteway et al., 1998, Race et al., 2005, De Oliveira et al., 2010b) .

Bacterial nitroreductases have been characterized and proven effective in bioremediation of nitroaromatic compounds which are normally toxic and mutagenic such as in *E. coli* (Kobori et al., 2001, Bryant et al., 1981), *Mycobacterium smegmatis* (Manina et al., 2010, Park, 2014), *Pseudomonas putida* (Caballero et al., 2005), *Lactobacillus plantarum* (Guillen et al., 2009) and *Gluconobacter oxydans 621H*

(Yang et al., 2016). Six putative nitroreductase genes *rpa0711*, *rpa1392*, *rpa1711*, *rpa3215*, *rpa3408* and *rpa4285* were annotated in the completed genome sequence of *R. palustris* CGA009 (Larimer et al., 2004).

In this study, the genes encoding all of the annotated putative nitroreductases *rpa0711, rpa1392, rpa1711, rpa3215, rpa3408* and *rpa4285* from *R. palustris* were cloned and expressed in *E. coli*. Protein expression trials were unsuccessful with the transformed constructs: pET0711, pET1392, pET3215 and pET3408, whereas a high yield of protein was expressed from pET1711 and pET4285 constructs (Table 3.1). Therefore the biochemical properties of the purified enzymes RPA1711 and RPA4285 are described in this chapter.

The work of this chapter aimed to elucidate the substrate specificity and comparative kinetics of the two nitroreductases RPA1711 and RPA4285 with different nitroaromatic substrates, thus providing stronger evidence for the activity of nitroreductase from *R. palustris* to degrade the toxic nitroaromatic compounds to non-toxic products for bioremediation and for developing the biotechnological applications. To the best of our knowledge, nitroreductases from *R. palustris* CGA009 have never been studied before.

Table 3.1: Summary of nitroreductase genes in *R. palustris* genome cloned and overexpressed. All genes were cloned into the pET21a (+) vector and *rpa4285* gene was cloned in pBAD/His. The column labeled solubility indicates the soluble overproduced protein visualised on an SDS-PAGE gel.

	Genes	Cloned	pET21	Solubility	pBAD/His	Solubility
1	*rpa0711*	✓	✓	N/A	✖	✖
2	*rpa1392*	✓	✓	N/A	✖	✖
3	*rpa3408*	✓	✓	N/A	✖	✖
4	*rpa1711*	✓	✓	Soluble	✖	✖
5	*rpa3215*	✓	✓	N/A	✖	✖
6	*rpa4285*	✓	✓	Insoluble	✓	Soluble

3.2 Results

3.2.1 Identification by bioinformatics analysis of potential nitroreductases in *R. palustris.*

The nitroreductase family comprises a conserved set of proteins that were originally discovered in eubacteria and have been grouped together based on their sequence similarity (De Oliveira et al., 2010b).

R. palustris putative nitroreductases RPA0711, RPA1392, RPA1711, RPA3215, RPA3408 and RPA4285 (Uniprot accession numbers Q6NBW5, Q6N9Z4, Q6N939, Q6N4W8, Q6N4D1 and Q6N1W7) are proteins of 223, 182, 232, 225, 164 and 196 amino acid residues with predicted molecular sizes 25, 19.76, 24.88, 25.11, 18.09 and 21.55 kDa respectively. These proteins are included in the nitroreductase Pfam family (PF00881). Members of this family are often homodimeric proteins, oxygen-insensitive NAD(P)H nitroreductases and use FMN as co-factor. The active sites are located at the interface of the dimers, and indeed the residues from both monomers contribute to the non-covalent binding of FMN (Manina et al., 2010) and they bind together with two FMN at the dimer interface (Haynes et al., 2002).

BLAST searches using the translated *R. palustris* nitroreductases DNA sequences showed high-scoring identites of various proteins of < 70% identity but most are uncharacterized or hypothetical proteins. The predicted sequences of the *R. palustris* nitroreductases were aligned with selected nitroreductases for which biochemical activity has been previously reported. Table 3.2 displays the percentage identity of these homologs. RPA1711 showed the highest overall identity of 35% with that of *Mycobacterium smegmatis* NfnB nitroreductase and 32% with *Bartonella henselae* str. Houston-1, and similar percentage of 31% identity between *R. palustris* nitroreductase RPA3215 with PnbA from *B. henselae,* but the enzyme activity of this

Table 3.2:Comparison of amino-acid sequence identity. Uniprot accession numbers: NfnB (A0R6D0), MhqN (P96692), NfsA (P17117), NfsB (P38489), PnrA (Q7B4Y3) , PnbA (*B. henselae*) (A0A0H3M323) and PnbA (*L. plantarum*) (F9US71).The highlighted boxes are the maximum identity percentage.

	Known Nitroreductases	RPA1711 % identity	RPA4285 % identity	RPA0711 % identity	RPA1392 % identity	RPA3215 % identity	RPA3408 % identity
1	**NfnB *Mycobacterium smegmatis***	**35**	**18**	**25**	**14**	**26**	**17**
2	**MhqN *Bacillus subtilis* (strain 168)**	**19**	**22**	**18**	**13**	**19**	**14**
3	**NfsA *Escherichia coli K12***	**18**	**11**	**22**	**20**	**19**	**16**
4	**NfsB *Escherichia coli* K12**	**19**	**26**	**20**	**23**	**17**	**18**
5	**PnrA *Pseudomonas putida* JLR11**	**22**	**18**	**21**	**21**	**19**	**14**
6	**PnbA *Bartonella henselae* str. Houston-1**	**32**	**17**	**21**	**16**	**31**	**16**
7	**PnbA *Lactobacillus plantarum* WCFS1**	**29**	**12**	**22**	**16**	**25**	**21**

nitroreductase is uncharacterised. 25% identity of *R. palustris* nitroreductase RPA0711 and *M. smegmatis* NfnB nitroreductase was also found. On the other hand, the RPA4285 and RPA1392 amino acid sequence showed the highest identity of 26% and 23% respectively with NfsB from *E. coli*. Furthermore, 21% identity was found with nitroreductase RPA3408 and PnbA nitroreductase from *L. plantarum*. These results suggest that these enzymes may perform similar functions.

3.2.2 Heterologous expression of *rpa1711* and *rpa4285* and purification of the recombinant proteins

In order to carry out biochemical analysis of these two putative nitroreductases and to determine their nitroaromatic compound preference, both *rpa1711* and *rpa4285* genes were cloned into expression vectors and the recombinant proteins were over-produced in *E. coli*. Firstly both nitroreductase genes were cloned into pET21a(+) but insoluble protein was produced in overexpression trials with *rpa4285* therefore, the gene was then cloned into the pBAD/HisB vector for overexpression.

3.2.2.1 Overproduction and purification of RPA1711

Primers pET1711 F + R were used to amplify the coding region of *rpa1711* from *R. palustris* genomic DNA by PCR, the product digested with *Nde*I and *Xho*I and sticky end cloned into digested pET21a(+). A C-terminal 6x His-Tag was fused in-frame to the *rpa1711* gene sequence as the stop codon of the *rpa1711* gene was removed. Successful cloning was confirmed by colony PCR using pET1711 F + R primers and DNA sequencing of the cloned PCR construct was performed to confirm the insert sequence contained no mutations and was in-frame with the C-terminal 6x His-Tag (Core Genomic Facility, University of Sheffield Medical School, UK). Figure 3.1a shows the pET1711 construct.

Overexpression trials using *E. coli* BL-21 (DE3) (pET1711) were performed at 37 ^{o}C and 25 ^{o}C to optimize the conditions for soluble protein production. The cells were grown to an OD (600nm) of 0.6 at 37^{o} C and induced with 400 μM IPTG; cultures were then grown in different temperatures at either 37 ^{o}C or 25 ^{o}C and at 1, 3, 5 and 24 hours after IPTG induction samples were taken. To assess RPA1711 production, a whole cell sample for each time point was run on an SDS-PAGE gel and subsequently, to calculate protein solubility level, cell free extracts (CFE) samples at the same points were also run on an SDS-PAGE gel. Cell free extract from induced pET1711 containing cells was passed into a His-trap column and protein was purified using an AKTA purification system. The results of the protein expression trials for RPA1711 can be seen in (Figure 3.1b). The highest protein level was obtained with a sample that was taken 1 hour after IPTG induction incubating at 37 °C; this condition was then used to overproduce large-scale amounts of RPA1711 for purification.

RPA1711 was purified on a nickel-affinity chromatography column and the fractions were eluted with a 0.02-0.5 M imidazole gradient. Large quantities of highly purified yellow coloured RPA1711 protein were obtained and visualized on an overloaded SDS-PAGE gel; the molecular weight of RPA1711 was estimated by SDS-PAGE to be about 25-30 kDa (Figure 3.1C). The expected molecular weight is 25.7 kDa based on the sequence.

3.2.2.2 Overproduction and purification of RPA4285

Initially RPA4285 was cloned into the *Nde*I and *Xho*I sites of the pET21a (+) vector, in a similar manner to RPA1711. When expressed in BL21 (DE3) cells, pET4285 produced large amounts of protein but on conducting solubility trials it was apparent a large amount of only insoluble protein was produced. The pET4285 construct was subsequently transformed into several BL21 strain derivatives (Rosetta

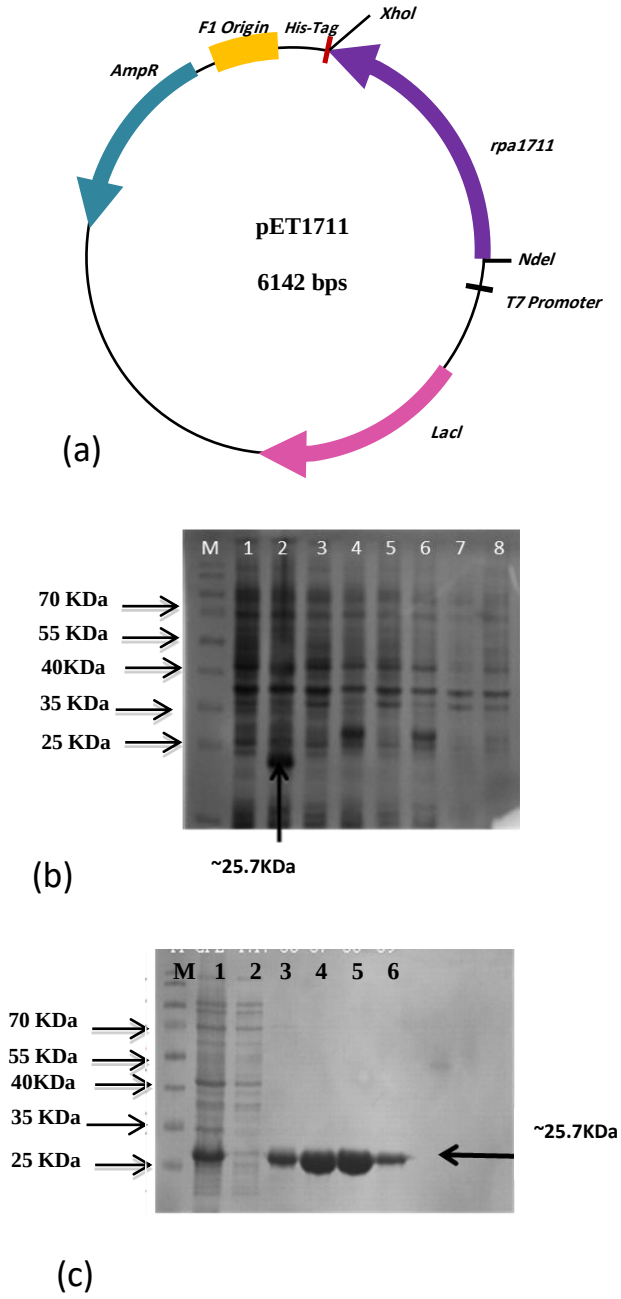

Figure 3.1 Protein overproduction and purification for RPA1711 protein. (a) Plasmid construct pET1711 including *rpa1711* gene (699bp) cloned into *Nde*I and *Xho*I sites of pET21 (+) and the expression was induced by 400 µM IPTG via of T7 promoter. (b) SDS-PAGE showing protein expression trials of RPA1711. M= pageRuler TM prestained protein ladder (Fermentas). Lane 1= control without induction , Lane 2=1h/25°C, Lane 3=1h/37°C Lane 4=3h/25°C, Lane 5=3h/37°C, Lane 6=5h/25°C, Lane 7=5h/37°C and Lane 8=24h/25°C. Lane 2 showing a high amount of protein expression at 25.7 kDa. (c) SDS-PAGE displaying protein purification of RPA1711 on His-trap columns. M= pageRuler TM prestained protein ladder (fermentas). Lane 1=Cell free extract , Lane 2= flow through and Lanes 3-6 containing eluted fractions from the Colum with a highly pure yellow protein size ~25.7 kDa in lane 4 and 5 which were used later in enzyme kinetics assay .

and BL21*) to improve solubility; unfortunately only insoluble protein was produced and thus a different expression strategy was undertaken.

The *rpa4285* gene was cloned into the *Xho*I and *Hind*III sites of the pBAD/HisB vector; the start codon was removed and the stop codon was retained since expression from this vector incorporated an N-terminal 6x His tag into the recombinant protein. The pBAD*4285* construct can be seen in Figure 3.2a. For increasing the solubility, changing vector systems and changing the position of the tag from C-terminus to N-terminus may help produce soluble protein. Expression from pBAD4285 was induced by arabinose via the *araC* promoter region.

Overproduction and solubility trials were carried out in the same manner as pET1711 (see section 3.2.2) but each culture was divided into three and induced with varying concentrations (0.2- 0.02- 0.002%) of arabinose to obtain the optimum concentration for soluble protein production. Protein expression trials showed that the best condition for overproduction of soluble RPA4285 was incubation at 37 ^{o}C for 24 hours after induction with 0.02% arabinose (Figure 3.2b). A very small amount of soluble protein was produced, as the SDS-gel shows, and so this meant several liters of culture needed to be grown for purification.

For purification *E. coli* cell free extract from of 4L growth was passed via a nickel-affinity chromatography column, to bind the his-tagged recombinant protein. Protein fractions were eluted with a 0.02-0.5 M imidazole gradient. Yellow fractions containing recombinant protein RPA4285 were obtained. Visualisation of the yellow fractions on an overloaded SDS-PAGE gel confirmed nitroreductase RPA4285 protein had been purified. The molecular weight of RPA4285 was estimated by SDS-PAGE to be about 22 kDa (Figure 3.2c).

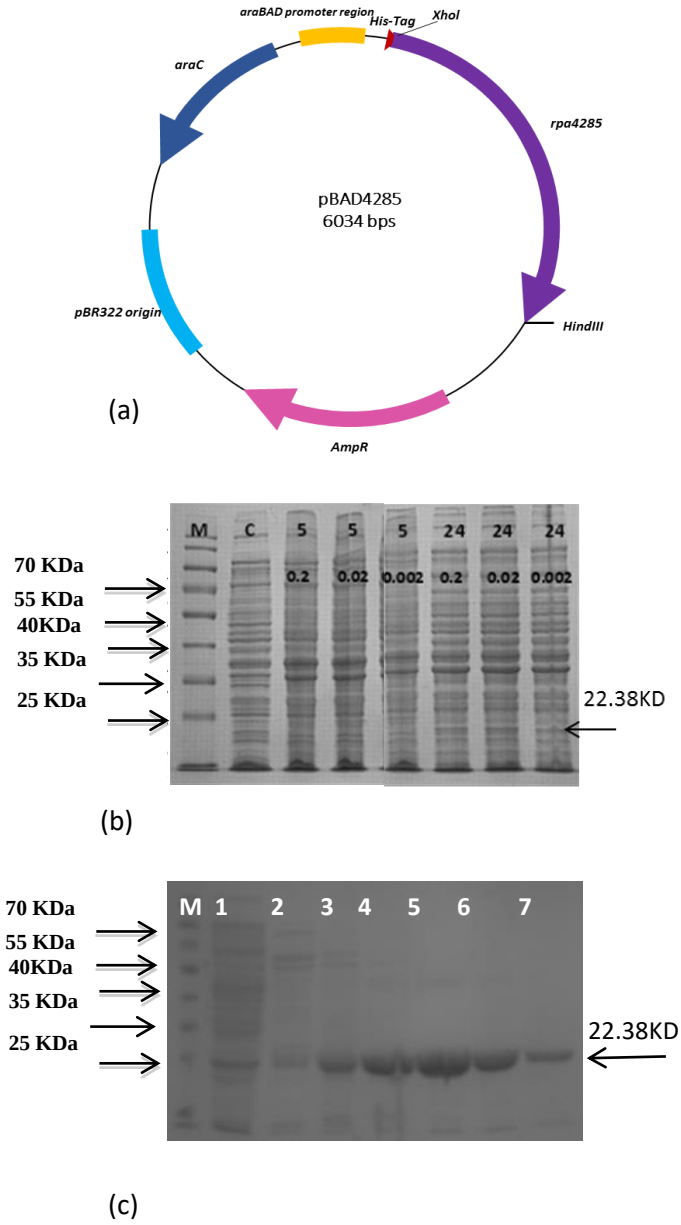

Figure 3.2: Overproduction and purification of RPA4285. (a)Over-expression constructs pBAD4285. The nucleotide sequence encoding the *rpa4285* gene was cloned into the *Xho*I and *HindIII* sites of pBAD/HisB thus, the expression of the gene was induced by arabinose through araC promoter and the recombinant protein had an N-terminal His-tag. (b) SDS-PAGE showing the protein expression trials of RPA4285. M= marker (PageRulerTM Prestained Protein Ladder (Fermentas)). Lane 1=C (control without arabinose. Samples were taken from cells incubated at 37^{o}C after 5 and 24 hours after arabinose induction with 0.2%, 0.02%, or 0.002%. Lanes 3-5 contain samples taken 5 hour after induction with 0.2% (lane 3), 0.02% (lane 4) and 0.002% (lane 5); lanes 6-8 represent 24 hours. The most expressed protein was produced 24 hours after induction with 0.02% arabinose shown in lane 7. (c) SDS-PAGE of purified RPA4285. M= marker, Lane 1 = Cell free extract loaded onto the His-trap column containing overproduced RPA4285. Lane= 2 Flow through and 3-7 containing purified RPA4285 eluted from the His-Trap column. Samples were used in biochemical assay.

3.2.3 Co-factor analysis

The purified proteins RPA1711 and RPA4285 were yellow, indicating the presence of the expected flavin co-factor, and analysis of their UV–visible spectrum identified two peaks of ~380 and ~450 nm in the 300–600-nm region, as is typical for flavin-containing proteins (Figure 3.3a and 3.3b).

All nitroreductase proteins utilize flavin as a cofactor. As the cofactor is important for catalysis, the ratio of protein: flavin was determined from the absorption of the purified enzymes. RPA1711 and RPA4285 were treated with 10% SDS to denature the aggregated proteins and release the cofactor. The UV–visible spectrum of the free form of released cofactor showed an absorbance maximum at 446 nm, which is typical of that for FMN and distinct from FAD (Figure 3.3a and 3.3b). The concentration of released FMN was measured by the extinction coefficient of FMN (ε = 12,200 M^{-1} cm^{-1}) at 446 nm. These results illustrate that RPA1711 and RPA4285 are flavoproteins associated tightly with FMN. On the basis of the UV–visible spectrum the molar ratio between FMN and RPA1711 protein was estimated at 0.97: 1, therefore suggesting that 1 mol of FMN binds to 1 mol of RPA1711, while half of this ratio 0.47:1 was estimated in RPA4285 protein, thus 0.5 mol of FMN binds to 1 mol of RPA4285. This suggests that only about 50% of the RPA4285 molecules have bound FMN.

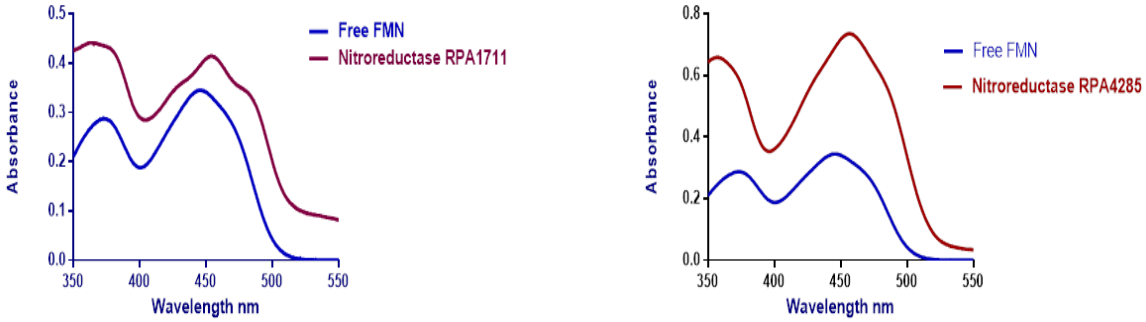

(a) (b)

Figure 3.3: Comparison of UV-Vis absorption spectra of purified nitroreductases. (a) RPA1711 480µM (red line), free FMN 3 µM (blue line) and (b) purified RPA4285 800 µM (red line), free FMN 3µM (blue line). The data is for a single batch of protein.

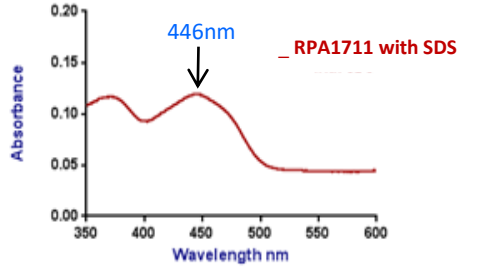

(a)

Protein concentration RPA1711= 10µM

The extinction coefficient of FMN

(ε = 12,200 M^{-1} cm^{-1}) at 446 nm

Δ 446nm= 0.119

1X 0.119/12200 = 0.00000975 M

= 9.75µM

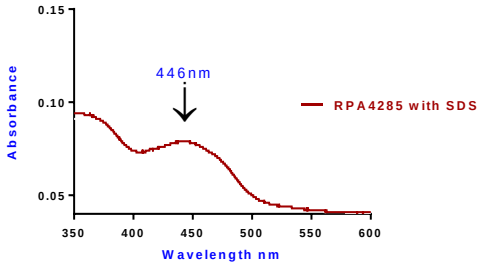

(b)

Protein concentration RPA4285= 10µM

The extinction coefficient of FMN

(ε = 12,200 M^{-1} cm^{-1}) at 446 nm

Δ 446nm= 0.058

1X 0.058/12200 = 0.0000047 M

= 4.7µM

Figure 3.4: UV- Vis spectrum of SDS-treated Nitroreductase RPA1711 and RPA4285. 10 µM with 10% SDS for 10 min , gives a spectrum with a 446nm maximum, typical of FMN with ratio (a) 1 mol RPA1711 per 1mol FMN and (b) 1mol RPA4285 per 0.5mol FMN. The data is for a single batch of protein**.**

3.2.4 Biochemical properties of nitroreductases RPA1711 and RPA4285

3.2.4.1 Screening of activity with nitroaromatic compounds

The effects of sixteen nitroaromatic substrates with different positions of the nitro group in the benzene ring on the enzymatic activity of the purified RPA1711 and RPA4285 were investigated spectrophotometrically (Shimadzu) by measuring the decrease of NADPH absorbance at λ=340nm. A standard reaction mixture for the enzyme assay contained 50 mM Tris-HCl (pH 8.5), 2 μM of purified nitroreductases RPA1711 or RPA4285, 0.7 mM of each nitroaromatic compounds and NADPH 150 μM in a final volume of 1 mL, in quartz cuvettes. All reactions were performed at 30°C for 3 min and reactions initiated by addition of NADPH. The RPA1711 enzyme was shown to be active with 4 substrates: 2,4-dinitrotoluene (2,4-DNT), 2,6-dinitrotoluene (2,6-DNT), potassium 4-nitrophenyl sulfate (P4NS) and methyl 4-nitrobenzoate (M4N). However, the activity of RPA4285 was shown only with 2,4-dinitrotoluene and 2,6-dinitrotoluene (Table 3.3). Kinetic parameters of purified enzyme RPA1711 were then determined with 2,4-dinitrotoluene (2,4-DNT) as substrates.

3.2.4.2 Kinetic parameters of purified RPA1711

3.2.4.2.1 NADH and NADPH comparison

Nitroreductases are enzymes with FMN co-factor that catalyze reduction dependent on NAD(P)H. This study was conducted to characterize each enzyme's co-factor dependency. 2,4-DNT was used as a model substrate in the reaction mixture containing 50 mM Tris-HCl (pH 8.5), 2 μM of purified enzyme and either 150 μM of NADH or NADPH was used separately. The results showed that the RPA1711 enzyme could use both NADPH and NADH as electron donors although using NADPH as reductant was 2 times more efficient than NADH (Figure 3.5).

Table 3.3 : The enzyme activity of RPA 1711 and RPA 4285 with nitroaromatic compound.

***ND non detectable** (can not measure the rate, the colour of the substrate interfere with UV spectrophotometer reading)

	Nitroaromatic subsrates	Activity RPA1711	Activity RPA4285
1	2,4-Dinitrotoluene	Yes	Yes
2	Methyl 4-nitrobenzoate	Yes	ND
3	2,6-Dinitrotoluene	Yes	Yes
4	Potassium 4-nitrophenyl sulfate	Yes	ND
5	2-Nitrophenol	*ND	ND
6	4-Nitrocinnamic acid	ND	ND
7	Nitrofurantoin	ND	ND
8	4-Nitrophenol	ND	ND
9	Nitrofurazone	ND	ND
10	Nitrobenzene	ND	ND
11	2-Nitrotoluene	ND	ND
12	2,4-Dinitrophenol	ND	ND
13	Furazolidone	ND	ND
14	2,4,6-trinitrotoluene	ND	ND
15	Trans-β-Nitrostyrene	ND	ND
16	4-Nitrotoluene	ND	ND

3.2.4.2.2 Optimum NADPH concentration

The optimization of NADPH concentration on the enzyme activity of RPA1711 was measured between 0.05 - 0.3 mM NADPH with 2,4-DNT as substrate. The reaction mixture was the same as in section 3.2.4.2.1. The reaction was started by addition of NADPH. The enzyme activity showed high rate in 150μM NADPH concentration and slightly increased above this concentration (Figure 3.6).

3.2.4.2.3 Effect of temperature on the RPA1711 nitroreductase activity

The effect of the temperature on enzyme activity was determined in reaction mixture containing 50 mM Tris-HCl (pH 8.5), 2 μM purified enzyme, 0.7 mM 2,4-DNT substrate and 150 μM NADPH and incubated in range of temperature 25 to 45°C. Purified RPA1711 was active between 25 to 45°C retaining the minimum of 67% relative activity between 25 and 45°C (Fig 3.7). Relative activities (%) were estimated as percentages of the maximum. Figure 3.7 shows the optimum temperature of the purified RPA1711 to be at 30°C.

3.2.4.2.4 Effect of pH on RPA1711 nitroreductase activity

The effect of pH on RPA1711 enzyme activity was measured in the range of pH 7-9.5, using 50 mM sodium phosphate buffer (pH 7.0–8.0), and 50mM Tris–HCl buffer (pH 8.5–9.5) Activity values were determined in each of these buffers containing 2 μM RPA1711, 0.7 mM 2,4-DNT, and 150 μM NADPH in a final volume of 1 ml at 30°C for 3 min. The reaction was started by adding NADPH and the best reduction rates with highest value 107.4 μmoles of NADPH oxidized min^{-1} mg of $protein^{-1}$ was achieved at pH 8. Purified RPA1711 displayed higher activity under neutral to alkaline conditions retained the minimum of 78% relative activity in Tris–HCl buffer at pH 9. Additionally, RPA1711 had considerably reduced activity below pH 8 (Figure 3.8).

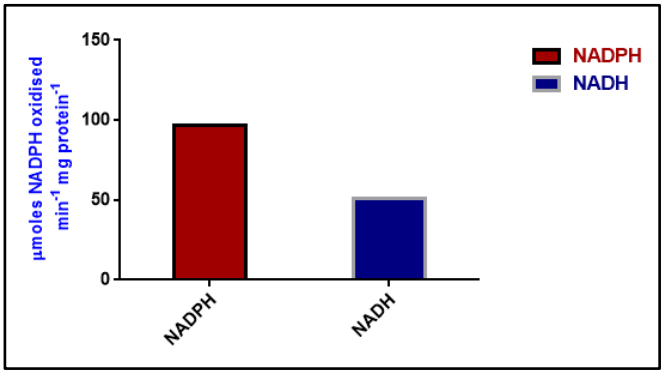

Figure 3.5: Nitroreductase RPA1711 preference for NADPH and NADH. A single assay is shown. NADPH oxidation rate measured using spectrophotometer in reaction mixture contained 50 mM Tris-HCl (pH 8.5), 2 µM purified enzyme, 0.7 mM 2,4-DNT substrate and the reaction started with 150 µM NADPH 30°C. The data is for a single batch of protein.

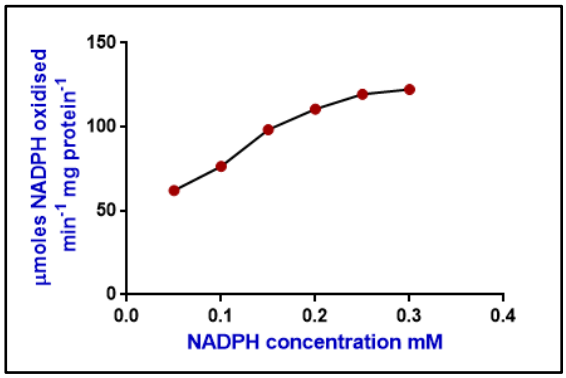

Figure 3.6: Optimum concentration of NADPH with RPA1711 enzyme activity. The figure shows the RPA1711 activity which correlated with NADPH oxidation, the rate was measured spectrophotometerically in reaction mixture contained 50 mM Tris-HCl (pH 8.5), 2 µM purified enzyme, 0.7 mM 2,4-DNT substrate and the reaction started with rang from 0.05 - 0.3 mM NADPH at 30°C. This assay was performed in duplicate for a single batch of protein with similar results.

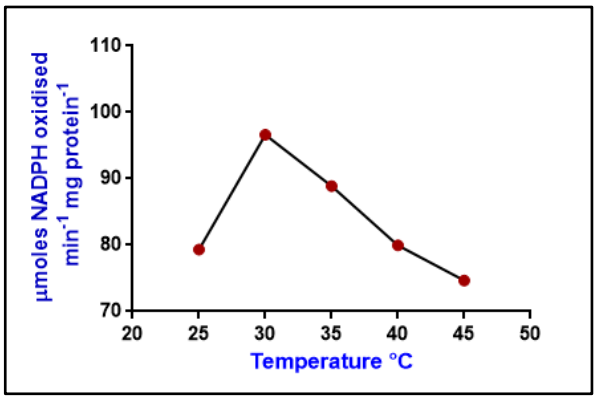

Figure 3.7: Effect of different temperatures on RPA1711 activity. The highest activity was when raction mixture incubated at 30°C. The reaction mixture containd 50 mM Tris-HCl (pH 8.5), 2 µM purified enzyme, 0.7 mM 2,4-DNT substrate was incubated at different temperature 25- 45°C. This assay was performed in duplicate for a single batch of protein with similar results.

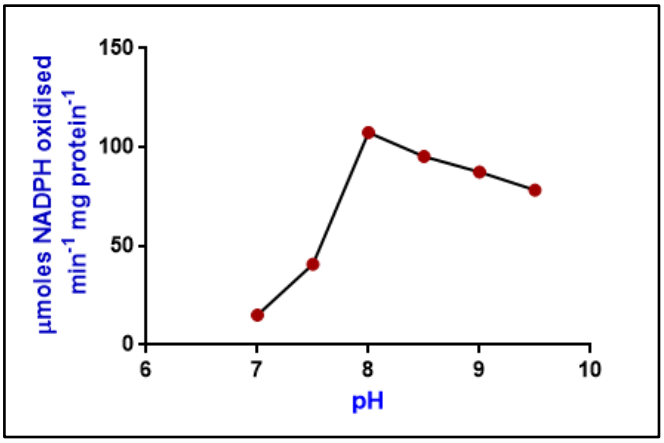

Figure 3.8: Effect of different pH values on RPA1711 activity. The RPA1711 activity rate was measured by spectrophotometer at 340 nm in reaction mixture contained 2 µM purified enzyme, 0.7 mM 2,4-DNT substrate and the reaction started with range from 0.15 mM NADPH at 30°C in range of buffer pH 7- 9.5. This assay was performed in duplicate for a single batch of protein with similar results.

The activity of RPA1711 decreased significantly at neutral pH to 14% of maximum activity at pH7 (Figure 3.8). The reduction rate was calculated as the μmoles of NADPH oxidized min^{-1} mg of $protein^{-1}$.

3.2.4.3 Enzyme kinetics of purified nitroreductases RPA1711 and RPA4285 with nitroaromatic substrates

To elucidate the substrate preference for both RPA1711 and RPA4285, the enzyme kinetics of the purified RPA1711 was analyzed for activity with the four nitroaromatic substrates 2,4-DNT, 2,6-DNT, P4NS and M4N while two nitroaromatic substrates 2,4-DNT and 2,6-DNT were used to analyze the enzyme kinetics of the purified RPA4285. The enzymatic assay was measured spectrophotometrically in the 1ml reaction by monitoring NADPH oxidation at λ=340 nm using purified recombinant RPA1711 or RPA 4285. The rate of NADPH oxidation was determined, and the reaction was initiated by the addition of the NADPH to the mixture. Kinetic data for NADPH oxidation and nitroaromatic substrates were fitted according to the Michelis-Menten equation.

The assays for RPA1711 with the nitroaromatic substrates can be seen in Figure 3.9. A summary of the kinetic parameters is shown in Table 3.5. Purified RPA1711 protein had good activity with all four nitroaromatic substrates and displayed a higher v_{max} when utilizing 2,4-DNT (140 μmol min^{-1} mg $protein^{-1}$) compared to 2,6-DNT (72 μmol min^{-1} mg $protein^{-1}$). However, the $k_m^{2,4\text{-DNT}}$ value (0.210 mM) was much larger compared to $k_m^{2,6\text{-DNT}}$ value (0.13 mM). The highest k_m value of 0.4 mM and a low v_{max} value of 55 μmol min^{-1} mg $protein^{-1}$ was found when RPA1711 catalyzed P4NS reduction. A non-saturating reduction rate was displayed when RPA1711 protein catalyzed M4N reduction, indicating a very low affinity. Therefore, no reliable kinetic parameters could be determined. .

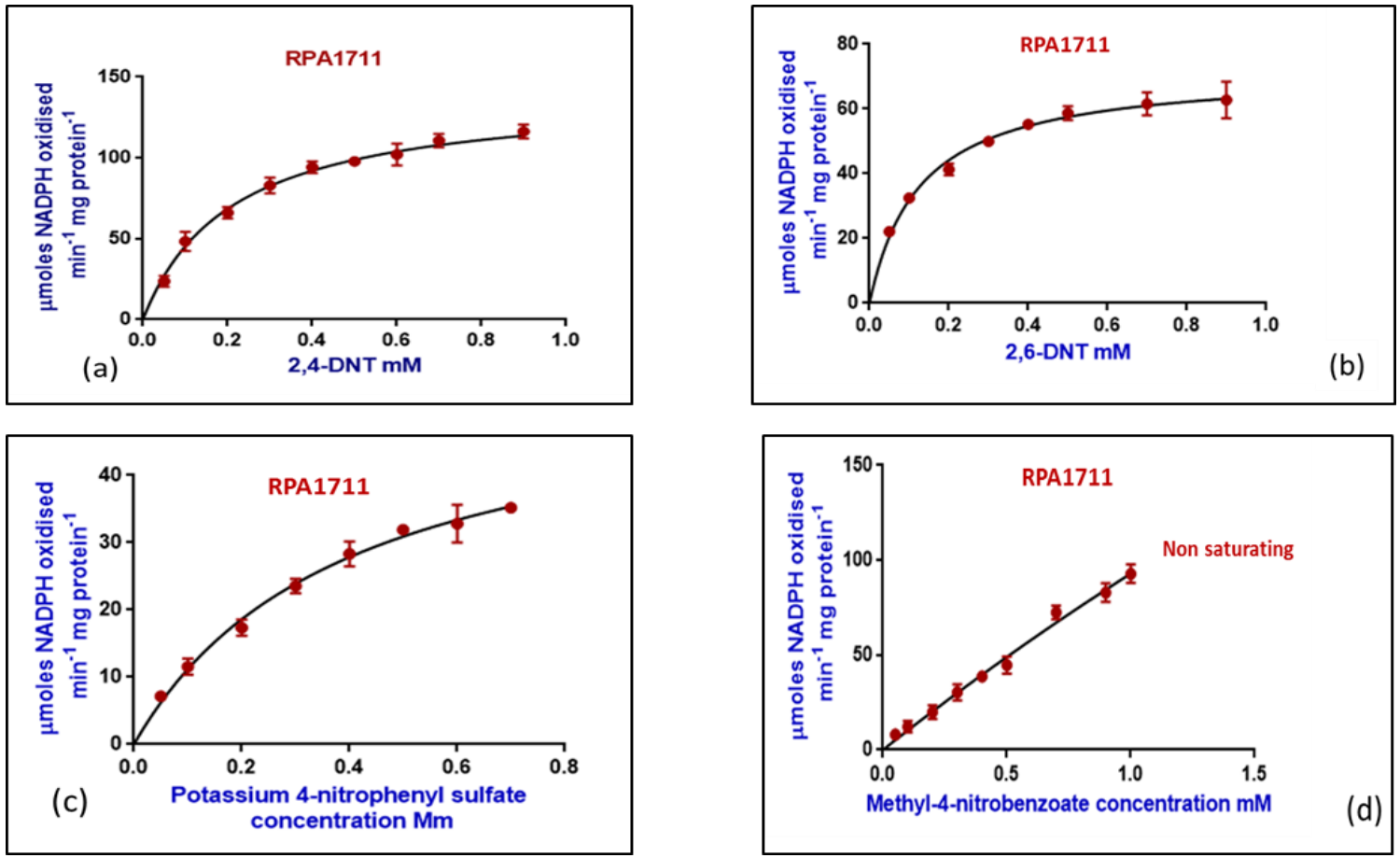

Figure 3.9: Enzyme Kinetic analysis with RPA1711. Enzyme activity of RPA1711 with four nitroaromatic substrates 2,4-DNT , 2,6-DNT, Methyl-4-nitrobenzoate and Potassium 4- nitrophenyl sulfate measured as NADPH oxidation. The data represent either two or three titrations with independently purified batches of protein. The data were fitted to the Michaelis Menten equation (the black solid line through the data points is the fit to the equation).

Due to the FMN ratio to the RPA4285 protein 0.5:1, protein RPA4285 activity was doubled to obtain the real activity of the RPA4285 enzyme. Assays of RPA4285 with the nitroaromatic ligands can be seen in Figure 3.10 with the kinetic parameters summarized in Table 3.5. These assays were carried out in the same manner as with RPA1711. Overall, purified enzyme displayed the highest V_{max} value (275 µmol min^{-1} mg $protein^{-1}$) when catalyzing 2,4-DNT reduction , but this was lowered by about 50% when reducing 2,6-DNT (134 µmol min^{-1} mg $protein^{-1}$). However, the comparison of V_{max}/K_m when catalyzing 2,4-DNT and 2,6-DNT reduction gave similar values. Furthermore, no activity was detected when RPA4285 was used with P4NS and M4N as substrates.

Table 3.5 illustrates the full kinetic analysis for both nitroreductase RPA1711 and RPA4285 with the nitroaromatic ligands. Despite a higher V_{max} value for RPA4285 compared to RPA1711, it was obvious when analyzing the kinetic parameters from these assays that RPA1711 had a much lower Km (i.e. higher affinity) with the 2,4-DNT and 2,6-DNT substrates than RPA4285. The specificity (kcat/km) for each of the substrates 2,4-DNT and 2,6-DNT was thus lower for RPA4285 than RPA1711. For both enzymes 2,4-DNT was the most preferred ligand.

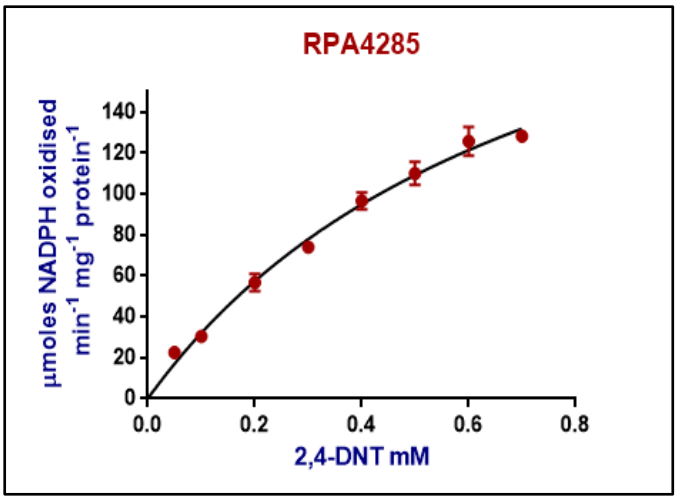

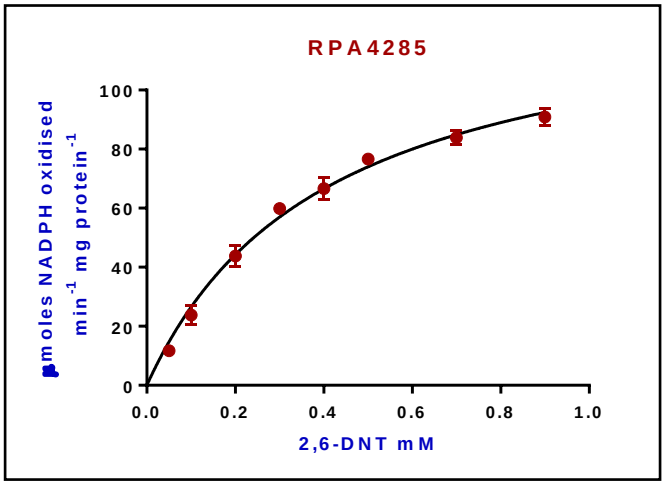

Figure 3.10: Enzyme kinetic analysis with RPA 4285. Enzyme activity of RPA4285 with two nitroaromatic substrates 2,4-Dinitrotoluene and 2,6-Dinitrotoluene measured as NADPH oxidation. The data were fitted to the Michaelis Menten equation.

Table 3.5:Kinetic parameters of RPA1711 and RPA4285 nitroreductase activity with nitroaromatic substrates. Rates were measured by monitoring the NADPH oxidation in UV absorbance at 340nm wavelength for each substrate.

	Substrate	K_m mM		Vmax µmol min^{-1} mg $protein^{-1}$		V_{max}/K_m UNITS		K_{cat} min^{-1}		Specificity K_{cat}/ K_m mM^{-1} min^{-1}	
		RPA 1711	RPA 4285	RPA 1711	RPA 4285	RPA 1711	RPA 4285	RPA 1711	RPA 4285	RPA 1711	RPA 4285
1	2,4 Dinitrotoluene	0.21±0.02	0. 76±0.11	140±3.6	275±25	0.67	0.362	70	137.5	350	180.26
2	2,6 Dinitrotoluene	0.13±0.01	0.41±0.04	72±1.8	134±5.6	0.57	0.326	36	67	285.7	163.41
3	Potassium-4-Nitrophenyl sulfate	0.4±0.05	N/A	55±3	N/A	0.14	N/A	27.5	N/A	69.6	N/A
4	Methyl-4-Nitrobenzoate	8.77±5.9 NS	N/A	908±564 NS	N/A	107.7 NS	N/A	592 NS	N/A	∞	N/A

2.3 Cloning and overproduction of *rpa0711, rpa1392, rpa3215 and rpa3408*

Other hypothetical nitroreductase genes in *R. palustris* genome were cloned and overexpressed in order to carry out biochemical characterisation and assay. The *rpa0711, rpa3215 and rpa3408* genes were cloned into the *Nde*I and *Xho*I sites of the pET21a (+) vector, while *rpa1392* was cloned into *Nde*I and *Not*I sites of the pET21a (+) vector and a 6x histidine tag was incorporated for each gene (Figure 3.11a, 3.11b, 3.11c and 3.11d). Successful cloning was confirmed by colony PCR using primers (data not shown). Constructs were sequenced (Core Genomic Facility, University of Sheffield Medical School, UK) to confirm no mutations and the insert sequence was in-frame with the 6x His-tag. Each construct pET0711, pET1392, pET3215 and pET3408 was subsequently transformed into three *E. coli* strains (BL21 (DE3), Rosetta and BL21*). More conditions of IPTG (400 µM and 1000 µM) concentration and (25-37°C) temperature were subsequently tried with these constructs. Unsuccessful and very low protein expression yields were obtained in protein expression trials, so work with these proteins was not pursued.

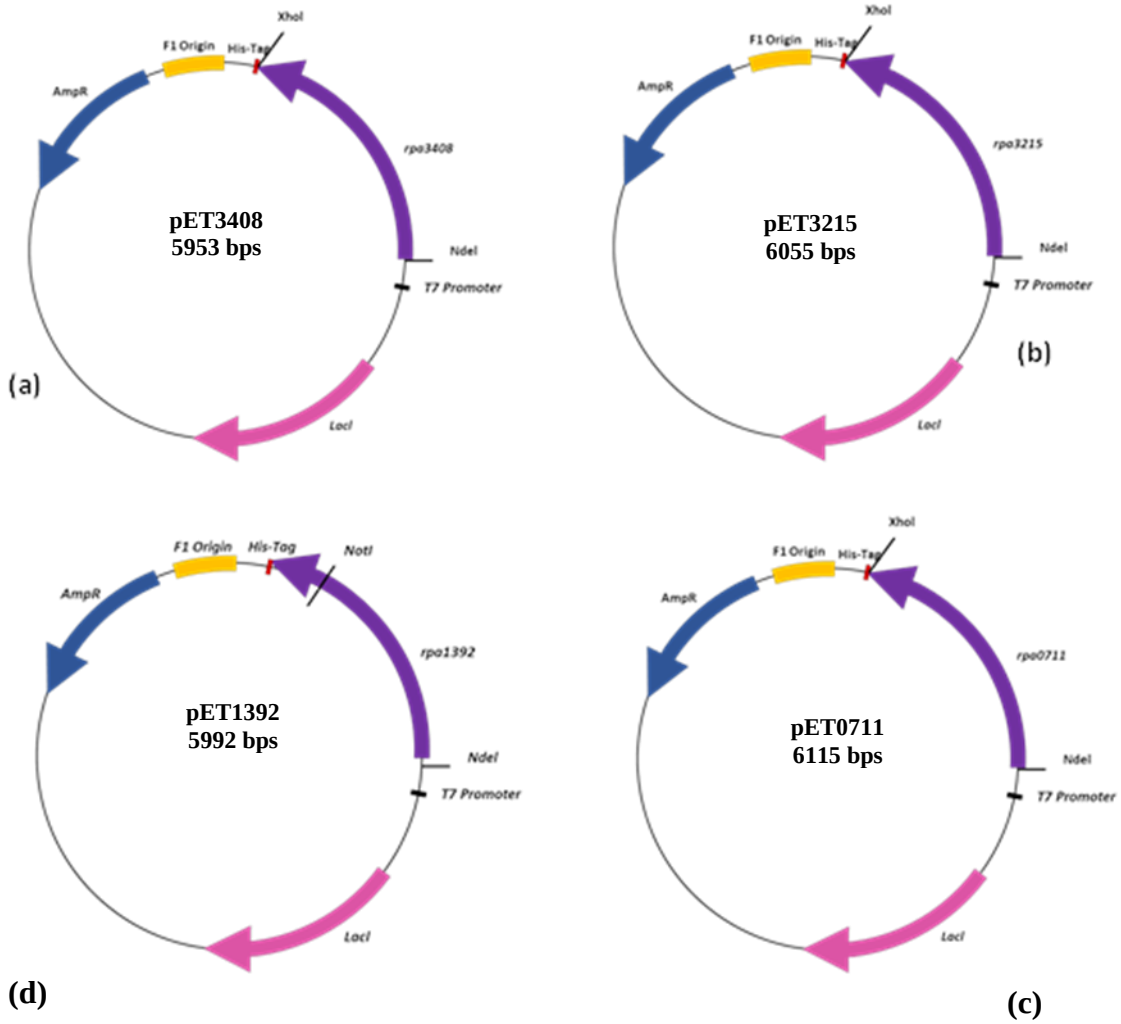

Figure 3.11: Plasmid construction *of rpa0711, rpa1392, rpa3215* and ***rpa3408*:**Genes were amplified from *R. palustris* genomic DNA with restriction sites for *Nde*I/*Xho*I in (a), (b) and (c) while using *Nde*I/*Not*I in (d). The genes fragments were ligated into pET21a (+), which encode 6x histidine tag.

3.3 Discussion

The nitroreductases RPA1711 and RPA4285 of *R. palustris* strain CGA009 were successfully cloned and expressed in this work. They are both flavoproteins with FMN as prosthetic group. These enzymes exhibit a number of similarities with other nitroreductases, which explains their substrate specificity with nitroaromatic ligands.

A phylogenetic analysis suggested RPA1711 to be closely related to the NfnB/PnbA nitroreductase while RPA4285 is closer to NfsB/MhqN (Figure 3.12). To better understand the substrate specificity of RPA1711 and RPA4285 we aligned the amino acid sequences of the *R. palustris* CGA009 with the most similar nitroreductases such as NfnB from *M. smegmatis* (Figure 3.13a), and NfsB from *E. coli*, (Figure 3.13b) respectively. The percentages of the identity were shown in Table 3.2. It is obvious that there are five conserved regions used for FMN binding in the protein sequences. First region residues in the C-terminal of the monomer are thought to interact with the phosphate group of the other monomer. Second region residues interact with benzene ring of FMN. Third conserved residues interact with the isoalloxazine ring system of FMN. Fourth conserved residues interact with ribityl chain of FMN and the last conserved region interact with the pyrimidine ring of the FMN (Parkinson et al., 2000).

The work in this chapter described the reactions of *R. palustris* nitroreductases with a series of nitroaromatic compounds including high explosives and toxic compounds for example (2,4,6-TNT, 2,4-DNT, 2,6-DNT). Putative nitroreductase genes were amplified from *R. palustris* genomic DNA and cloned into expression vectors; pET21a and pBAD/His. pBAD/His vector was used to clone *rpa4285*

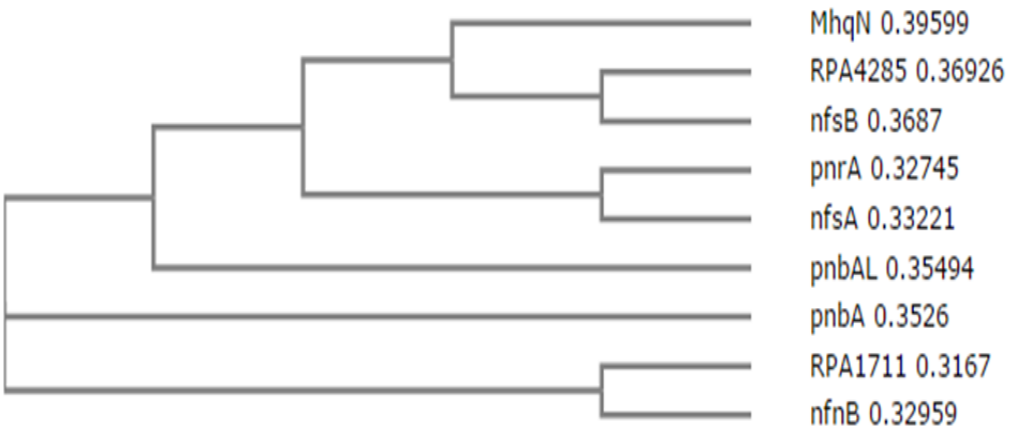

Figure 3.12: Phylogenetic tree of known nitroreductase and annotated nitroreductase RPA1711 and RPA4285.

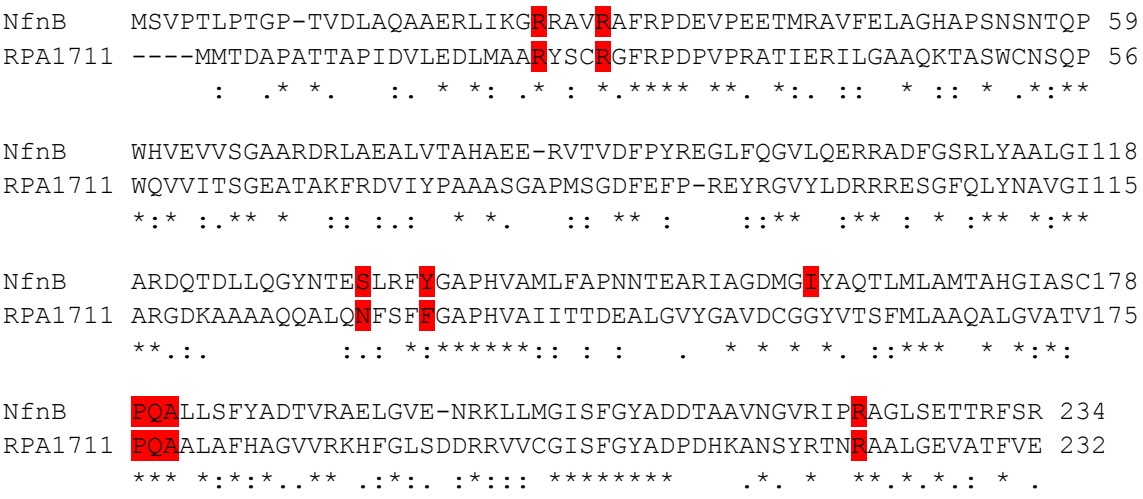

(a)

(b)

Figure 3.13: Alignment of Nitroreductase RPA1711 and RPA4285 sequence. (a) RPA1711 sequence with the NfnB family nitroreductases. (b) RPA4285 sequence with the NfsB family nitroreductases. The sources of the sequences were: NfnB from *M. smegmatis*, NfsB from *E. coli* .The red highlighted amino acids are conserved residues interacting with FMN in binding site. The software used for alignment was CLUSTALW.

because protein expression in pBAD/His system is highly controlled by arabinose titration which in turn changes protein expression levels in the cell. Whereas in pET21a expression system protein expression level in the cell is uncontrolled as IPTG concentration does not affect the expression. The controlled level of protein expression in Top10 *E. coli* cell enhances protein solubility using pBAD/His vector and the yields of the target protein can be increased to 100-fold by supplementing the culture with different concentrations of arabinose (Rosano and Ceccarelli, 2014, Guzman et al., 1995). In addition to that in pBAD/His vector the 6x Histidine tag is present in the N-terminus while in pET21a vector the 6x Histidine tag is located in the C-terminus.

Protein expression trials were successful with two nitroreductase proteins RPA1711 and RPA4285. Purified proteins were yellow in colour and biochemical studies were carried out to identify the co-factor. Absorption spectrum assay of co-factor content showed absorbance at 446 nm which is typical of FMN. Protein to liberated FMN ratio was obtained to be 1:1 and 1:0.5 in purified protein RPA1711 and RPA4285 respectively. As the FMN is non-covalently bound in the protein, the ratio can obviously be variable. In the nitroreductase Gox0834 from *Gluconobacter oxydans* 621H, the protein to FMN ratio was estimated to be 1:0.2 and after incubating the protein in 1M FMN the ratio increased to 0.7 mol, as well as, the ratio of nitroreductase from *Bacillus licheniformis* to FMN was 1:0.4, and after incubating the purified enzyme with 1 mM FMN the ratio was increased to 1:1. Furthermore, denatured *R. palustris* nitroreductase RPA4285 results showed high similarity with *Mycobacterium smegmatis* NfnB protein where 1 mol of NfnB binds to 0.54 mol of FMN (Park, 2014). Correspondingly the activity of RPA1711 was higher with nitroaromatic compounds than RPA4285. According to Bryant et al. (1981) nitroreductases type I can be classified to group A and group B. Both of these *R. palustris* enzymes belong to group B as amino acid sequence alignments showed 19 and

26% identity for RPA1711 and RPA4285 respectively, when compared to *E. coli* NfsB sequence group B (Table 3.2), that can utilize both NADPH and NADH as electron donor. Additionally, biochemical properties showed that nitroreductase RPA1711 could utilize both NADPH and NADH as electron source, preferring NADPH as a reductant. *Lactobacillus plantarum* nitroreductase PnbA could use either NADPH or NADH as electron donors even though using NADPH as reducing agent was approximately 2 times more efficient than NADH (Guillen et al., 2009). In *Mycobacterium smegmatis* nitroreductase NfnB both NADPH and NADH are used without any preferences except with the addition of benzothiazinone substrates that showed a significant increase in rate by using NADPH (Manina et al., 2010). On the other hand, and due to the similarity of *Pseudomonas putida* nitroreductase PnrA and *E. coli* group A, PnrA enzyme can utilize only NADPH to catalyze 2,4,6-trinitrotoluene (TNT) reduction (Caballero et al., 2005). From these features we can see that containing FMN as a co-factor and the ability to use NAPDH or NADH as electron donor are a common feature in subgroup B.

The optimal temperature of RPA1711 to reduce 2,4-DNT was 30°C, this reflects the optimum growth temperature of *R. palustris*, however 25°C was the optimum temperature of *Lactobacillus plantarum* nitroreductase PnbA (reduction of dichlorophenolindophenol) and *Pseudomonas putida* nitroreductase PnrA (reduction of TNT). Optimum pH of RPA1711 was 8 and the protein was active under alkaline conditions ranging from 8 to 9.5 which is similar to NfnB in *Mycobacterium smegmatis* and Gox0834 from *Gluconobacter oxydans* with nitroreductase activity ranging from pH 7.5 to 9.0 (Manina et al., 2010, Yang et al., 2016).

A wide range of aromatic compounds containing one or more nitro groups ($-NO_2$) which were in ortho or para position were screened with both recombinant proteins

RPA1711 and RPA4285. Enzymatic assay of RPA1711 and RPA4285 proteins showed high specificity with 2,4-DNT with a k_{cat}/K_m of 350 mM^{-1} min^{-1} and 180 mM^{-1} min^{-1} respectively , while NfnB from *M. smegmatis* was 84 mM^{-1} min^{-1} when reducing 2,4-DNT (Park, 2014). RPA1711 and RPA4285 were able to utilize 2,6-DNT in almost similar k_{cat}/K_m ratio to 2,4-DNT (Table 3.5). The substrate specificity ratio of RPA1711 is almost 2 times lower than ratio recorded for RPA1711. The two proteins only share 24% sequence identity, despite being identically annotated, therefore, it was to be expected that the two nitroreductases may have at least some preferences for distinct substrates (Table 3.2).

Moreover, the activity of RPA1711 and RPA4285 were affected by the position of the nitro group of the substrates. The best result was recorded with methyl (electon donating group) to the nitro group at the ortho-position, followed by para-position for RPA1711. Park (2014) suggests that NfnB from *M. smegmatis* has better catalytic utilization of substrates with electron-withdrawing group substituents *para* to the nitro group. Generally, the comparison (V_{max}/K_m) for reduction of 2,4-DNT or 2,6-DNT was much higher than other substrates or the enzymes were unable to reduce other nitroaromatic compounds. This may suggest that nitroreductases RPA1711 and RPA4285 and possibly the other nitroreductases annotated in *R. palustris* (Larimer et al., 2004), are specifically reducing nitro groups in ortho- positions. Unfortunately, the reduction of 2-nitrotulene was impossible to measure due to color interference in the UV spectrophotometer absorbance.

The work described here might help in characterization of enzymes which reduce nitro groups to amine groups and is important to complete our consideration of

nitroaromatic metabolism in bioremediation, for mediating the degradation of explosives and toxic compounds in the environment, also for prodrug activation.

CHAPTER 4

EVALUATION OF METHODS FOR DETERMINING THE ACTIVITY OF NITRILASES FROM *R. PALUSTRIS*

4. Evaluation of methods for determining the activity of nitrilases from *R. palustris*

4.1 Introduction

As described in Chapter 1 nitrilase enzymes catalyse the direct conversion of highly toxic and carcinogenic aliphatic and aromatic nitriles to the corresponding and valuable carboxylic acids with liberation of ammonia. Nitrilases are characteristically homooligomers with a single polypeptide (monomer) subunit with a molecular weight of 32-45 kDa. Usually, the nitrilase activity is associated with subunit oligomerisation (6-27 subunits) (O'Reilly and Turner, 2003, Williamson et al., 2010).

Nitrilases have a conserved catalytic triad (Glu, Lys, Cys) where the substrate binds to the cysteine. Nitrilases exhibit considerable differences in substrate specificity and the spectrum of substrate utilization can be narrow or broad. Nitrilases have been categorized into three groups, that include; aliphatic, aromatic, and arylacetonitrilases (Gong et al., 2012, Sonbol et al., 2016, Kim et al., 2009).

Nitrilase cloning, purification, functional mechanisms, screening pathways, biocatalytic properties and enzyme structure have been widely studied in a range of bacteria, including *Bradyrhizobium, Rhodococcus, Geobacillus, Pseudomonas, Acidovorax* and, *Streptomyces* (Rustler et al., 2008, Zhu et al., 2008, Thuku et al., 2007, Williamson et al., 2010, Kiziak et al., 2005, Chauhan et al., 2003, Nigam et al., 2009)

In this chapter, the genes encoding all of the annotated putative nitrilases *rpa0599, rpa1563, rpa2416* and the known nitrilase *rpa4166* from *R. palustris* were cloned and expressed in *E. coli.* Protein expression trials were successful with the transformed constructs pET0599, pET1563, pET2416 and pET4166 and good yields of proteins were expressed and purified from these constructs. The biochemical assays of the purified

enzymes RPA0599, RPA1563, RPA2416 and RPA4166 revealed that 4-Cyanopyridine was the preferred substrate for RPA0599, RPA1563, RPA4166 when compared with other nitriles using the OPA chemical assay.

4.2 Results

4.2.1 Identification and bioinformatics analysis of potential nitrilases in *R. palustris*

The sequence analysis of the complete genome of *R. palustris* CGA009 suggested the presence of four nitrilases. The *rpa0599, rpa1563,* and *rpa2416* genes were annotated as putative nitrilases, suggesting that nitrilases might be encoded by these genes, which hydrolyse nitriles to carboxylic acids and ammonia. On the other hand, the fourth gene *rpa4166* was previously studied by Xie et al. (2006) and its was characterized as a protein with nitrilase activity (Black et al., 2015, Xie et al., 2006).

R. palustris nitrilases RPA0599, RPA1563, RPA2416 and RPA4166 (Uniprot accession numbers Q6NC73, Q6N9I6, Q6N746 and Q6N284) are proteins of 291, 349, 317 and 579 amino acid residues respectively. These proteins are included in the nitrilase superfamily (EC:3.5.5.1). Members of this superfamily often have a conserved catalytic triad (E-K-C), and are homooligomeric α-β-β-α sandwich folded proteins.

BLAST searches using the translated *R. palustris* amino acids sequences showed high-scoring similarities of the different proteins of ≤ 70% identity to various nitrilases, but most are uncharacterized or hypothetical proteins. The predicted sequences of the *R. palustris* nitrilases were aligned with selected nitrilases in which enzymatic activity has been previously reported (Figure 4.1).

Table 4.1 shows the percentage identity of these homologs. RPA0599 showed the highest overall identity (36%) with that of *Caenorhabditis elegans* nft-1 nitrilase and

(31%) with Nit3 nitrilase from *Desulfococcus oleovorans*. On the other hand, the RPA1563 and RPA4166 share amino acid sequence identity 35 % with nitrilase blr3397 in *Bradyrhizobium diazoefficiens* and (30 and 35 %) identity with nitrilase from *Synechocystis* sp. PCC6803 respectively. Furthermore, BLAST alignments showed the highest identity of 50% of the RPA4166 amino acid sequence with Nit from *Pseudomonas aeruginosa*. The percentage identity of the RPA2416 amino acids sequence identity was 28 and 24% to Nit3nitrilase from the *Desulfococcus oleovorans* and nft-1 from *Caenorhabditis elegans* respectively.

RPA2416 protein has two domains and each domain contains conserved catalytic triad residues. BLAST search alignment for both domains showed identity of 35% between the two domains and each domain shares identity with nitrilase PYRAB13990 from *Pyrococcus abyssi;* 34 and 38% to domain α and β respectively. While domain α and domain β share identity ≤ 87% and ≤ 73% respectively with the putative or hypothetical amidohydrolase in many organisms such as *Bradyrhizobium* sp., *Tardiphaga* sp.,*Agrobacterium* sp. and *Rhizobium* sp., but unfortunately, uncharacterized amidohydrolases.

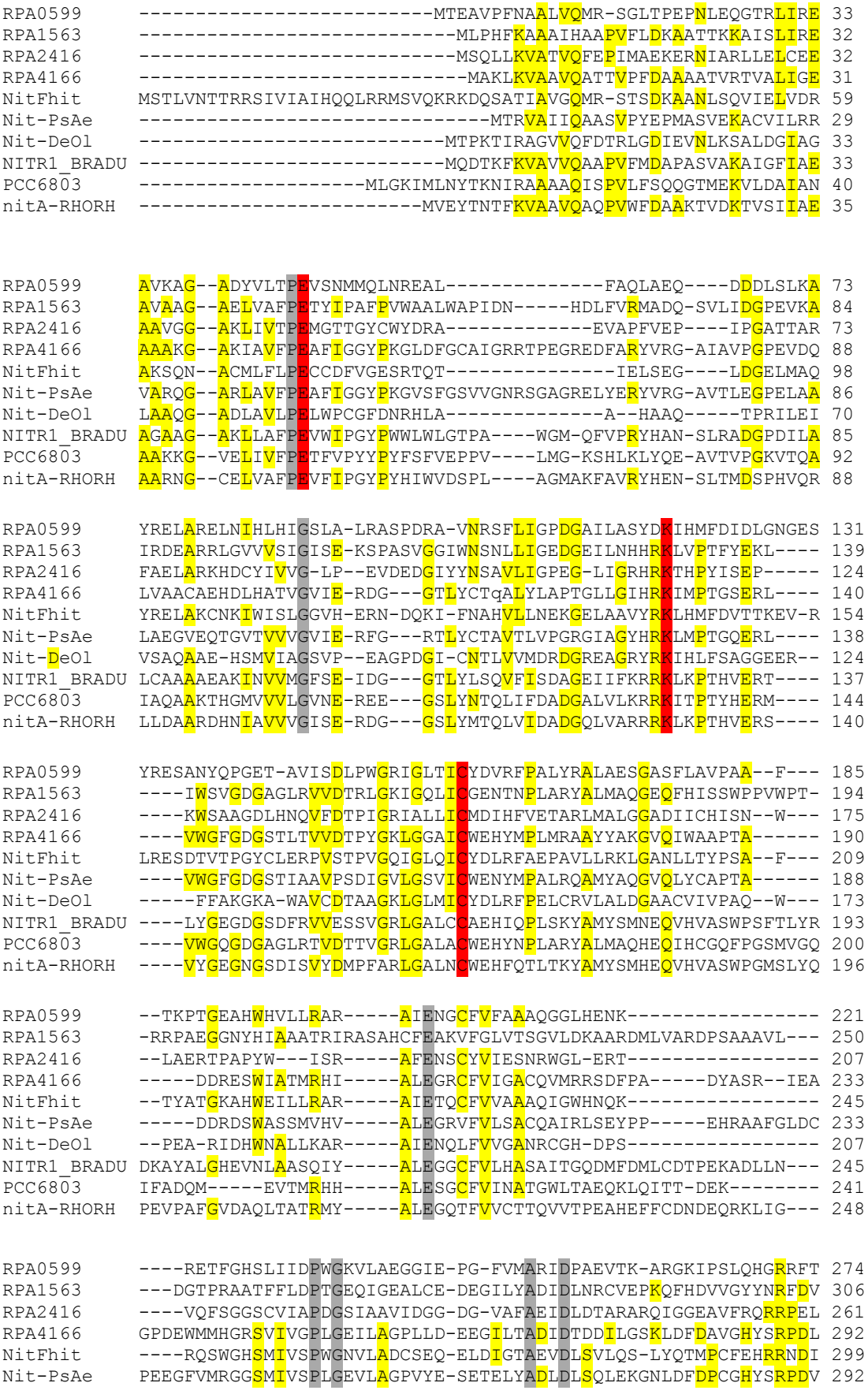
RPA0599 ----------MTEAVPFNAALVQMR-SGLTPEPNLEQGTRLIRE 33
RPA1563 ----------MLPHFKAAAIHAAPVFLDKAATTKKAISLIRE 32
RPA2416 ----------MSQLLKVATVQFEPIMAEKERNIARLLELCEE 32
RPA4166 ----------MAKLKVAAVQATTVPFDAAAATVRTVALIGE 31
NitFhit MSTLVNTTRRSIVIAIHQQLRRMSVQKRKDQSATIAVGQMR-STSDKAANLSQVIELVDR 59
Nit-PsAe ----------MTRVAIIQAASVPYEPMASVEKACVILRR 29
Nit-DeOl ----------MTPKTIRAGVVQFDTRLGDIEVNLKSALDGIAG 33
NITR1_BRADU ----------MQDTKFKVAVVQAAPVFMDAPASVAKAIGFIAE 33
PCC6803 ----------MLGKIMLNYTKNIRAAAAQISPVLFSQQGTMEKVLDAIAN 40
nitA-RHORH ----------MVEYTNTFKVAAVQAQPVWFDAAKTVDKTVSIIAE 35
RPA0599 AVKAG--ADYVLTPEVSNMMQLNREAL--------------FAQLAEQ----DDDLSLKA 73
RPA1563 AVAAG--AELVAFPETYIPAFPVWAALWAPIDN-----HDLFVRMADQ-SVLIDGPEVKA 84
RPA2416 AAVGG--AKLIVTPEMGTTGYCWYDRA-------------EVAPFVEP----IPGATTAR 73
RPA4166 AAAKG--AKIAVFPEAFIGGYPKGLDFGCAIGRRTPEGREDFARYVRG-AIAVPGPEVDQ 88
NitFhit AKSQN--ACMLFLPECCDFVGESRTQT----------------IELSEG----LDGELMAQ 98
Nit-PsAe VARQG--ARLAVFPEAFIGGYPKGVSFGSVVGNRSGAGRELYERYVRG-AVTLEGPELAA 86
Nit-DeOl LAAQG--ADLAVLPELWPCGFDNRHLA--------------A--HAAQ-----TPRILEI 70
NITR1_BRADU AGAAG--AKLLAFPEVWIPGYPWWLWLGTPA----WGM-QFVPRYHAN-SLRADGPDILA 85
PCC6803 AAKKG--VELIVFPETFVPYYPYFSFVEPPV----LMG-KSHLKLYQE-AVTVPGKVTQA 92
nitA-RHORH AARNG--CELVAFPEVFIPGYPYHIWVDSPL----AGMAKFAVRYHEN-SLTMDSPHVQR 88
RPA0599 YRELARELNIHLHIGSLA-LRASPDRA-VNRSFLIGPDGAILASYDKIHMFDIDLGNGES 131
RPA1563 IRDEARRLGVVVSIGISE-KSPASVGGIWNSNLLIGEDGEILNHHRKLVPTFYEKL---- 139
RPA2416 FAELARKHDCYIVVG-LP--EVDEDGIYYNSAVLIGPEG-LIGRHRKTHPYISEP----- 124
RPA4166 LVAACAEHDLHATVGVIE-RDG---GTLYCTqALYLAPTGLLGIHRKIMPTGSERL---- 140
NitFhit YRELAKCNKIWISLGGVH-ERN-DQKI-FNAHVLLNEKGELAAVYRKLHMFDVTTKEV-R 154
Nit-PsAe LAEGVEQTGVTVVVGVIE-RFG---RTLYCTAVTLVPGRGIAGYHRKLMPTGQERL---- 138
Nit-DeOl VSAQAAE-HSMVIAGSVP--EAGPDGI-CNTLVVMDRDGREAGRYRKIHLFSAGGEER-- 124
NITR1_BRADU LCAAAAEAKINVVMGFSE-IDG---GTLYLSQVFISDAGEIIFKRRKLKPTHVERT---- 137
PCC6803 IAQAAKTHGMVVVLGVNE-REE---GSLYNTQLIFDADGALVLKRRKITPTYHERM---- 144
nitA-RHORH LLDAARDHNIAVVVGISE-RDG---GSLYMTQLVIDADGQLVARRRKLKPTHVERS---- 140
RPA0599 YRESANYQPGET-AVISDLPWGRIGLTICYDVRFPALYRALAESGASFLAVPAA--F--- 185
RPA1563 ----IWSVGDGAGLRVVDTRLGKIGQLICGENTNPLARYALMAQGEQFHISSWPPVWPT- 194
RPA2416 ----KWSAAGDLHNQVFDTPIGRIALLICMDIHFVETARLMALGGADIICHISN--W--- 175
RPA4166 ----VWGFGDGSTLTVVDTPYGKLGGAICWEHYMPLMRAAYYAKGVQIWAAPTA------ 190
NitFhit LRESDTVTPGYCLERPVSTPVGQIGLQICYDLRFAEPAVLLRKLGANLLTYPSA--F--- 209
Nit-PsAe ----VWGFGDGSTIAAVPSDIGVLGSVICWENYMPALRQAMYAQGVQLYCAPTA------ 188
Nit-DeOl -----FFAKGKA-WAVCDTAAGKLGLMICYDLRFPELCRVLALDGAACVIVPAQ--W--- 173
NITR1_BRADU ----LYGEGDGSDFRVVESSVGRLGALCCAEHIQPLSKYAMYSMNEQVHVASWPSFTLYR 193
PCC6803 ----VWGQGDGAGLRTVDTTVGRLGALACWEHYNPLARYALMAQHEQIHCGQFPGSMVGQ 200
nitA-RHORH ----VYGEGNGSDISVYDMPFARLGALNCWEHFQTLTKYAMYSMHEQVHVASWPGMSLYQ 196
RPA0599 --TKPTGEAHWHVLLRAR-----AIENGCFVFAAAQGGLHENK---------------- 221
RPA1563 -RRPAEGGNYHIAAATRIRASAHCFEAKVFGLVTSGVLDKAARDMLVARDPSAAAVL--- 250
RPA2416 --LAERTPAPYW---ISR-----AFENSCYVIESNRWGL-ERT---------------- 207
RPA4166 -----DDRESWIATMRHI-----ALEGRCFVIGACQVMRRSDFPA-----DYASR--IEA 233
NitFhit --TYATGKAHWEILLRAR-----AIETQCFVVAAAQIGWHNQK---------------- 245
Nit-PsAe -----DDRDSWASSMVHV-----ALEGRVFVLSACQAIRLSEYPP-----EHRAAFGLDC 233
Nit-DeOl --PEA-RIDHWNALLKAR-----AIENQLFVVGANRCGH-DPS---------------- 207
NITR1_BRADU DKAYALGHEVNLAASQIY-----ALEGGCFVLHASAITGQDMFDMLCDTPEKADLLN--- 245
PCC6803 IFADQM-----EVTMRHH-----ALESGCFVINATGWLTAEQKLQITT-DEK-------- 241
nitA-RHORH PEVPAFGVDAQLTATRMY-----ALEGQTFVVCTTQVVTPEAHEFFCDNDEQRKLIG--- 248
RPA0599 ----RETFGHSLIIDPWGKVLAEGGIE-PG-FVMARIDPAEVTK-ARGKIPSLQHGRRFT 274
RPA1563 ---DGTPRAATFFLDPTGEQIGEALCE-DEGILYADIDLNRCVEPKQFHDVVGYYNRFDV 306
RPA2416 ----VQFSGGSCVIAPDGSIAAVIDGG-DG-VAFAEIDLDTARARQIGGEAVFRQRRPEL 261
RPA4166 GPDEWMMHGRSVIVGPLGEILAGPLLD-EEGILTADIDTDDILGSKLDFDAVGHYSRPDL 292
NitFhit ----RQSWGHSMIVSPWGNVLADCSEQ-ELDIGTAEVDLSVLQS-LYQTMPCFEHRRNDI 299
Nit-PsAe PEEGFVMRGGSMIVSPLGEVLAGPVYE-SETELYADLDLSQLEKGNLDFDPCGHYSRPDV 292

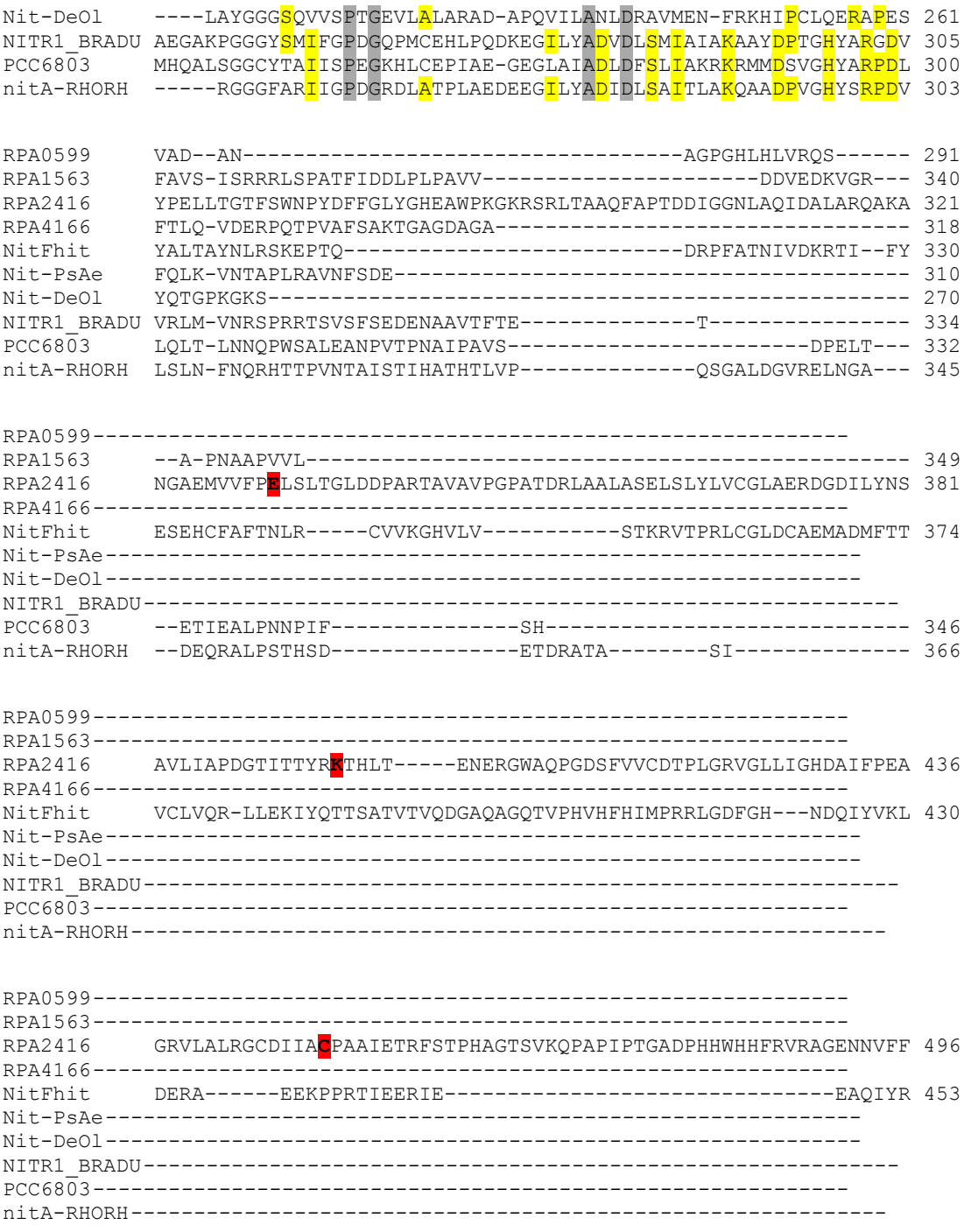

Figure 4.1: Alignment of RPA0599, RPA1563, RPA2416 and RPA4166 amino acids sequence. Red highlighted amino acids show catalytic triad residues ,gray highlighted 100% similarity and yellow highlighted sequence ≤ 90% similarity.

Table 4.1 Comparison of amino-acid sequence identity. Uniprot accession numbers and entry name: Nitrilase merR (Q55949), NitA (Q03217), Nitrilase Dole_1328 (A8ZYM7), Nitrilase blr3397 (Q89PT3), Nitrilase 4 PSPA7_3027 (A6V5Q2), nft-1 (O76463)

	Known Nitrilases	RPA0599 %	RPA1563 %	RPA2416 %	RPA4166 %
1	Nitrilase merR *Synechocystis* sp. PCC6803	21	30	20	35
2	NitA *Rhodococcus rhodococcus J1*	21	33	22	38
3	Nitrilase Dole_1328 *Desulfococcus oleovorans*	31	19	28	22
4	Nitrilas blr3397 *Bradyrhizobium diazoefficiens*	19	35	19	35
5	Nitrilase 4 PSPA7_3027 *Pseudomonas aeruginosa*	20	29	21	50
6	nft-1 *Caenorhabditis elegans*	36	18	24	21

4.2.1Recombinant expression and purification of nitrilase gene *rpa4166* and possible nitrilase genes *rpa0599, rpa1563 and rpa2416*

In order to carry out enzymatic analysis of these four enzymes to determine the nitrile preference, all genes *rpa0599, rpa1563, rpa2416* and *rpa4166* were cloned into pET21a (+) and recombinant protein was overproduced in BL21(DE3).

The *rpa0599, rpa1563, rpa2416* and *rpa4166* genes were amplified from *R. palustris* genomic DNA using primers pET21_0599 F + R for *rpa0599*, primers pET21_1563 F + R for *rpa1563*, primers pET21_2416 F + R for *rpa2416* and primers pET21_4166 F + R for *rpa4166*. These amplified genes were cloned into *Nhe*I and *Not*I , *Nde*I and *Not*I, *Nde*I and *Not*I and *Nde*I and *Xho*I sites of the pET21a (+) vector (Figure 4.2a, 4.3a, 4.4a) and 4.5 a respectively. A six histidine tag in the C-terminal was incorporated for all genes. The expression from pET21a (+) plasmid was induced by 400 µM IPTG via the T7 promoter. All constructs were sequenced (Core Genomic Facility, University of Sheffield Medical School, UK) to confirm the encoding genes were in-frame with the 6x histidine tag and that there were no mutations.

Constructs pET0599, pET1563, pET2416 and pET4166 were expressed individually using BL21 (DE3) cells and overexpression trials of *E. coli* BL-21 were performed to obtain the optimum temperature and time. Recombinant proteins were overproduced at 25 and 37°C at regular time intervals 1,3,5 hours and overnight after cells of 0.6 $OD_{(600)}$ were induced with 400 µM IPTG; a whole cell sample for each time point was taken and run on an SDS-PAGE gel to ensure the highest amounts of produced proteins. Protein overexpression and solubility trials showed that the most soluble protein was obtained at 3 hours at 25 °C post induction for RPA0599 and RPA4166 (Figure 4.2b, 4.5b), 5 hour at 25 °C post induction for RPA2416 (Figure 4.4b) and a very small amount of soluble

protein 1 hours at 25 °C post induction for RPA1563 was produced as the SDS – PAGE gel shows (Figure 4.3b), and so this meant several liters of culture needed to be grown for for purification. The protein solubility was also checked after sonication by running the sample on an SDS-PAGE gel.

Cell free extracts from induced pET0599, pET1563, pET2416 and pET4166 were passed individually through a nickel-affinity chromatography column and protein elution in 1 ml/minute samples was observed via UV readings. ~5 eluted protein fractions were detected in a UV single peak, both binding and elution buffers were supplemented with 1mM DTT to maintain protein stability. 8 µl of different fractions from each protein were run on SDS–PAGE gels (Figure 4.2c, 4.3c, 4.4c and 4.5c). Protein concentration was determined by using UV spectrophotometry and results for the concentration was 236 µM for RPA0599, 48 µM for RPA1563, 122 µM for RPA2416 and 180 µM for RPA4166. Purified protein fractions containing the C-terminal hexahistidine tagged protein were pooled and concentrated via viva-spin column using exchanged buffer X3 (50 mM Tris buffer, 50 mM NaCL and 1mM DTT pH 7.5). The concentrated proteins were subsequently measured using Bradford assay then stored in 50% glycerol at -20°C for subsequent biochemical assays.

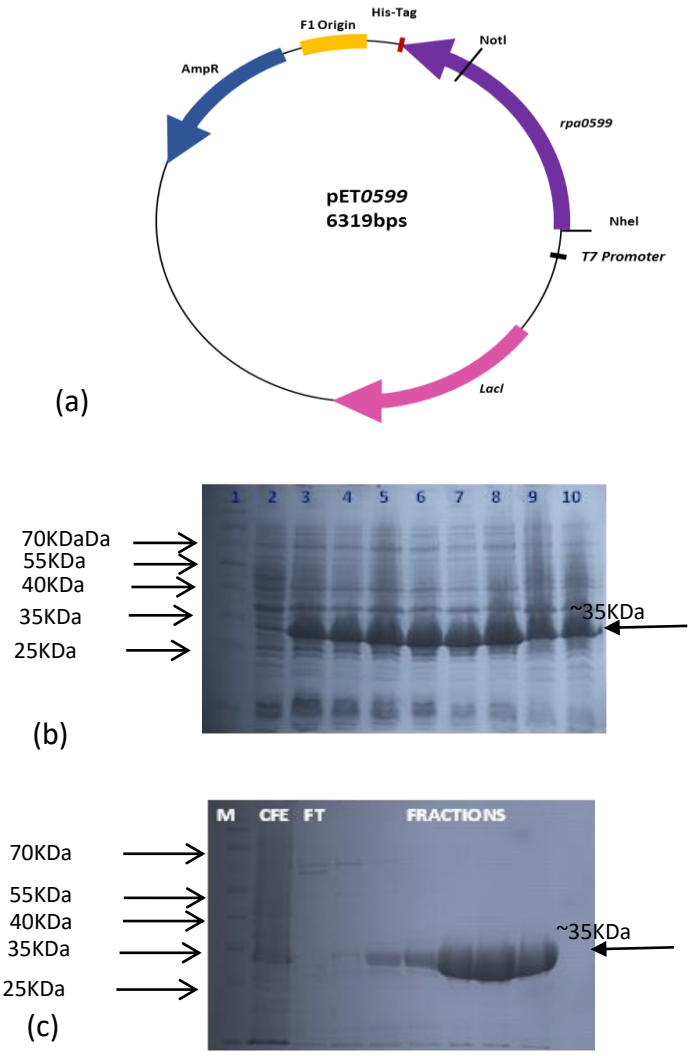

Figure 4.2 Overproduction and purification for RPA0599 protein. (a) over-expression construct pET0599. The nucleotide sequence including *rpa0599* gene was cloned into *Nhe*I and *Not*I sites of pET21a(+) . (b) SDS-PAGE showing expression trials of RPA0599. Lane 1= marker= pageRuler TM prestained protein ladder (Fermentas), lane 2 = control without induction , lanes 3,5,7 and 9 contain cells were induced with IPTG before incubation at 25°C at 1,3,5,24 hour interval respectively ,and lane 4,6,8 and 10 contain cells incubated at 37°C at 1,3,5,24 hour interval after IPTG induction respectively. Lane 5 shows the highest amount of protein expression at ~35 kDa. (c) SDS-PAGE showing HisTrap purification of RPA0599 protein. M = PageRulerTM Prestained Protein Ladder (Fermentas), lane 2= cell free extract, lane 3= flow through and lane 4-9 purified fractions of recombinant protein RPA0599 at ~35 kDa eluted via His-trap column on an imadazole gradient. Highly pure protein size ~35 kDa was shown in lane 8 which was used later in enzymatic assay.

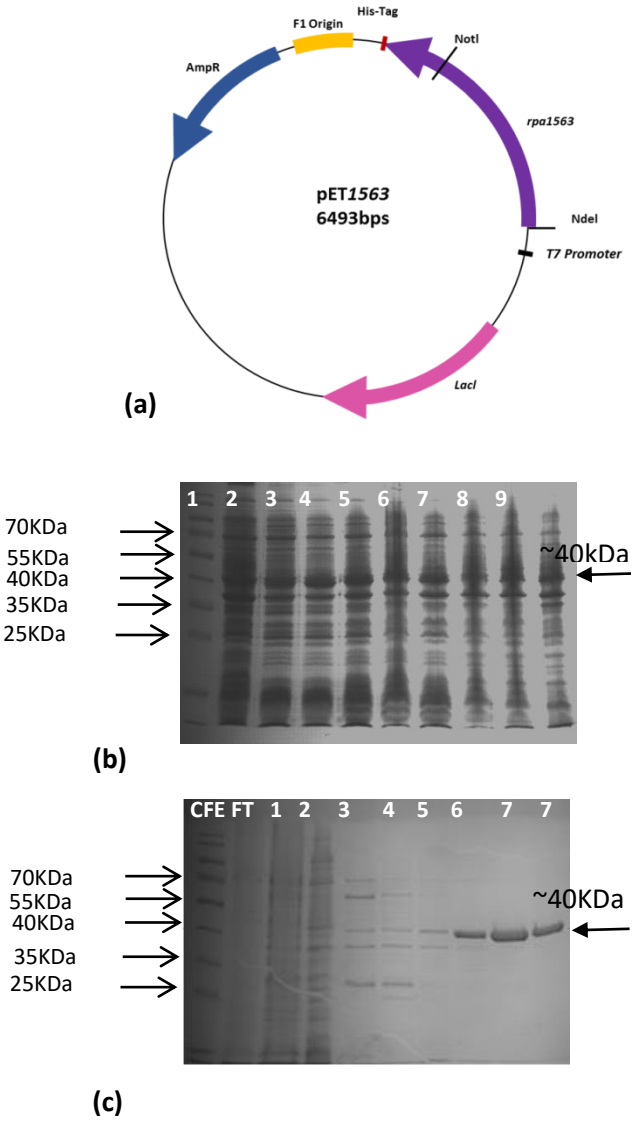

Figure 4.3 Overproduction and purification for RPA1563 protein. (a) over-expression construct pET1563. The plasmid pET1563 was made by cloning the *rpa1563* gene sequence into pET21a(+) between the *Nde*I and *Not*I restriction sites, *rpa1563* gene with C-terminal His-tag. (b) SDS-PAGE showing expression trials of RPA1563. M=marker= pageRuler TM prestained protein ladder (Fermentas), lane 1= control without induction , lanes 2,4,6 and 8 contain cells were induced with IPTG before incubation at 25°C at 1,3,5,24 hour interval respectively ,and lane 3,5,7 and 9 contain cells incubated at 37°C at 1,3,5,24 hour interval after IPTG induction respectively. Lane 2 shows low amount of protein expression at ~40 kDa. (c) SDS-PAGE showing HisTrap purification of RPA1563 protein. M = PageRulerTM Prestained Protein Ladder (Fermentas), lane CFE= cell free extract, lane FT= flow through and lane 1-7 purified fractions of recombinant protein RPA1563 at ~40 kDa eluted via His-trap column on an imidazole gradient. Highly pure protein size ~40 kDa was shown in lane 6 which was used later in enzymatic assay.

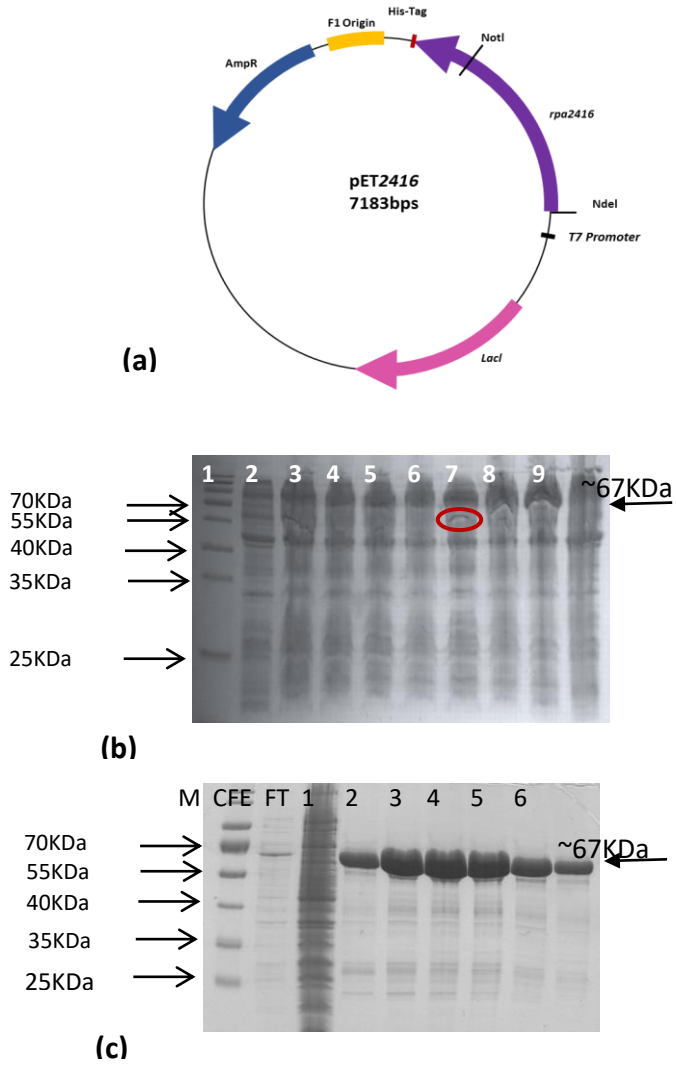

Figure 4.4 Overproduction and purification for RPA2416 protein. (a) over-expression construct pET2416. The plasmid pET*2416* was made by cloning the *rpa2416* gene sequence into pET21a(+) between the *Nde*I and *Not*I restriction sites, *rpa2416* gene with C-terminal His-tag. (b) SDS-PAGE showing expression trials of RPA2416. M=marker= pageRuler TM prestained protein ladder (Fermentas), lane 1= control without induction , lanes 2,4,6 and 8 contain cells were induced with IPTG before incubation at 25°C at 1,3,5,24 hour interval respectively ,and lane 3,5,7 and 9 contain cells incubated at 37°C at 1,3,5,24 hour interval after IPTG induction respectively. Lane 6 shows low amount of protein expression at ~67 kDa. (c) SDS-PAGE showing HisTrap purification of RPA2416 protein. M = PageRulerTM Prestained Protein Ladder (Fermentas), lane CFE= cell free extract, lane FT= flow through and lane 1-6 purified fractions of recombinant protein RPA2416 at ~67 kDa eluted via His-trap column on an imidazole gradient. Pure protein size ~67 kDa was shown in lane 6 which was used later in enzymatic assay.

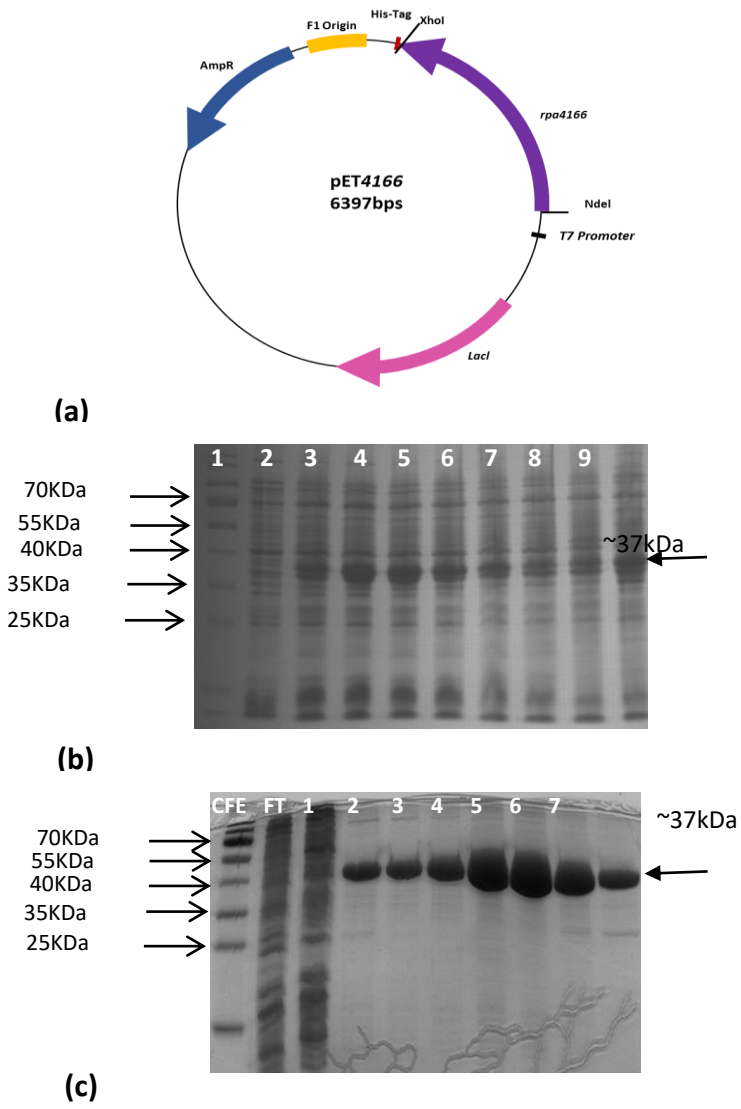

Figure 4.5: Overproduction and purification for RPA4166 protein. (a) over-expression construct pET4166**.** The plasmid pET4166 was made by cloning the *rpa4166* gene sequence into pET21a(+) between the *Nde*I and *Xho*I restriction sites, *rpa4166* gene with C-terminal His-tag**.** (b) SDS-PAGE showing expression trials of RPA4166**.** M=marker= pageRuler TM prestained protein ladder (Fermentas), lane 1= control without induction , lanes 2,4,6 and 8 contain cells were induced with IPTG before incubation at 25°C at 1,3,5,24 hour interval respectively ,and lane 3,5,7 and 9 contain cells incubated at 37°C at 1,3,5,24 hour interval after IPTG induction respectively. Lane 4 shows good amount of protein expression at ~37 kDa. (c) SDS-PAGE showing HisTrap purification of RPA1563 protein**.** M = PageRulerTM Prestained Protein Ladder (Fermentas), lane CFE= cell free extract, lane FT= flow through and lane 1-7 purified fractions of recombinant protein RPA4166 at ~37 kDa eluted via His-trap column on an imadazole gradient. Highly pure protein size ~37 kDa was shown in lane 5 which was used later in enzymatic assay.

4.2.3 Molecular weight and subunit structure

The purified nitrilases gave a single band on Coomassie blue stained SDS-PAGE gels for each enzyme with the predicted estimated subunit molecular weight. The molecular weight of the holoenzymes was estimated by analytical gel filtration to identify protein characteristics and apparent oligomeric molecular weight. Gel filtration was performed using an AKTA purifier system on a 10 x 300Superdex 200GL column. Column was calibrated by Ferritin 440kDa, Aldolase 150 kDa, Ovalbumin 44 kDa and Ribonuclease 12.5kDa (Figure 4.6). Samples of RPA0599, RPA1563 and RPA2416 nitrilases were supplied in 50% glycerol and the RPA4166 nitrilase sample was in 1M ammonium sulphate. To reduce glycerol concentration samples were diluted 5 fold and concentrated to about 0.5 ml using VivaSpin concentrators with MWCO 30000 Da. Elution profiles for the nitrilases are shown in (Figure 4.7 a, 4.7 b, 4.7 c and 4. 7 d). RPA0599 and RPA2416 showed a dimeric state with apparent molecular weight 71 kDa and 140 kDa respectively while RPA1563 showed oligomeric state of 18 (most likely 16) subunits with a wide peak which may be due to fast equilibrium between two forms. (Possibly between 12 mer-24 mer), the apparent molecular weight was 708 kDa. On the other hand, RPA4166 oligomeric state and apparent molecular weight was hard to identify as the protein exists in solution in the form of big aggregates of different sizes, and a small peak of a tetramer. These results obtained suggested that nitrilases RPA0599, RPA1563, RPA2416 and RPA4166 self-aggregated to the active form ranging from 2 to 27 subunits of identical size (Table 4.2).

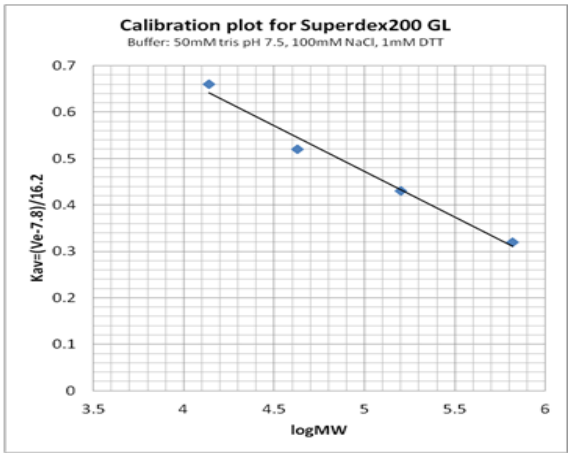

Figure 4.6: Calibration plot for Superdex 200GL. Column was calibrated using Ferritin 440kDa, Aldolase 150kDa, Ovalbumin 44kDa and Ribonuclease 12.5kDa.

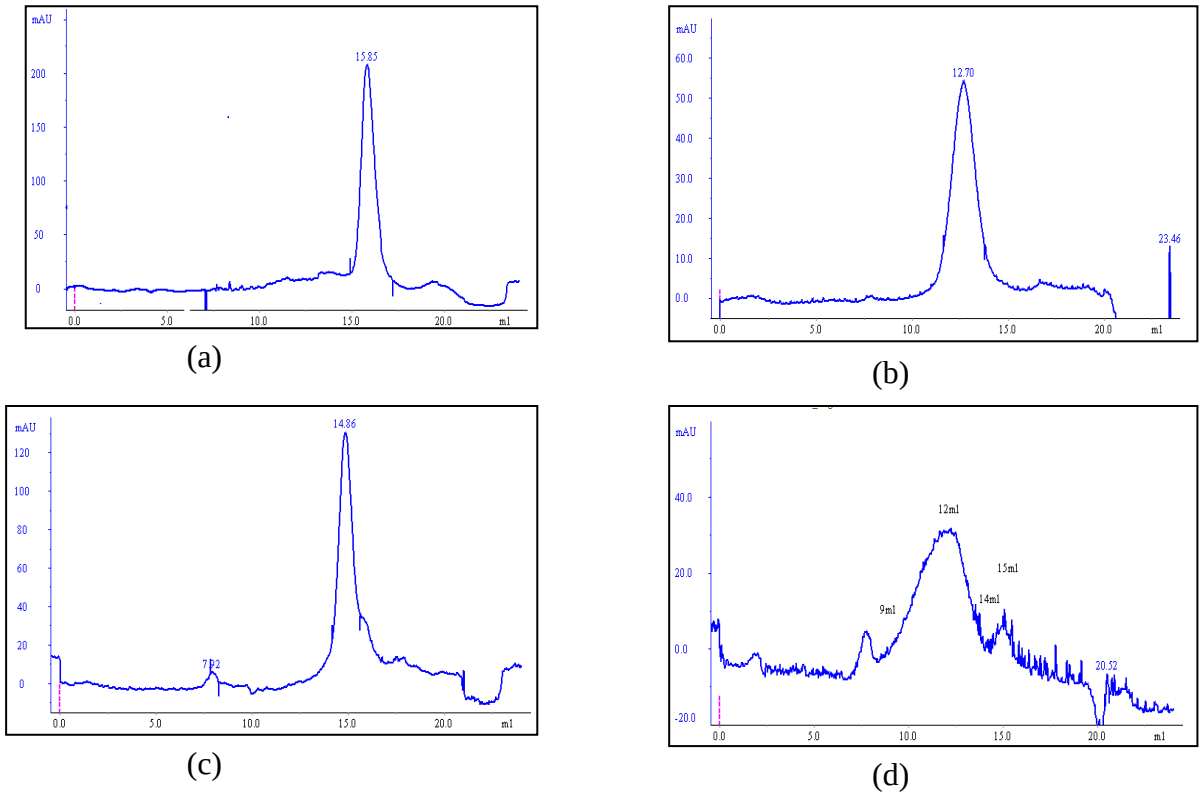

Figure 4.7:Estimation of oligomeric state of Nitrilase from *R. palustris* using gel filtration. (a) RPA0599 protein apparent weight is ~71 kDa. (b) RPA1563 protein apparent weight is ~708 kDa.(c) RPA2416 protein apparent weight is ~140 kDa. (d)RPA4166 protein apparent weight is ~1000 kDa. The data is for a single batch of protein.

Table 4.2: Comparison between predicted molecular weight and apparent molecular weight with oligomeric state for each nitrilase from *R. palustris* using gel filtration chromatography in AKTA purifier system using a 10 x 300 Superdex200GL column. The data is for a single batch of protein.

Protein	MW of monomer	Apparent MW	Oligomeric state
1- RPA0599	~35KDa	71kDa	dimer
2- RPA1563	~40KDa	708kDa	18 (most likely 16)
3- RPA2416	~67KDa	140kDa	dimer
4- RPA4166	~37KDa	1000kDa	~ 27

4.2.4 Determination of substrate Specificity for nitrilases RPA0599, RPA1563, RPA2416 and RPA4166

The catalytic activity of purified nitrilases toward a range of aliphatic and aromatic nitriles (Figure 4.8) was investigated by quantifying the amount of ammonia released during the hydrolysis, based on a continuous assay (GDH assay) and discontinuous assay (Berthelot method, and OPA method) in order to establish substrate specificity.

4.2.4.1 Continuous coupled assay

For determination of the catalytic hydrolysis of nitriles by nitrilases producing ammonia, the nitrilase enzyme was coupled with glutamate dehydrogenase (GDH). This method was designed as a spectrophotometric continuous coupled assay which continuously measures ammonia formation (Vergne-Vaxelaire et al., 2013). The ammonia formation is coupled to NADH oxidation, which was measured using a coupled enzyme system with nitrilase and GDH. Nitrilase hydrolyses nitriles to carboxylic acid and ammonia. GDH then converts liberated ammonia, α-ketoglutaric acid, and NADH to glutamate and NAD+ (Figure 4. 9). The rate of NADH oxidation was measured at 340 nm and the results are shown in (Figure 4.10). The reaction was initiated with 200 µM NADH to a reaction mixture containing 50 mM substrate, 8 units GDH, 5 mM α-ketoglutaric acid and 5 µM enzyme in 50 mM HEPES buffer pH 7.5. A control reaction was carried out using the same reaction mixture except the nitrile substrate which was substituted with water. Unfortunately, the control reaction as well as the tested reaction mixtures showed a similar rate of NADH oxidation and it was impossible to measure the kinetics for each substrate. For unknown reasons, NADH was being oxidized in absence

(a)Aromatic Nitriles

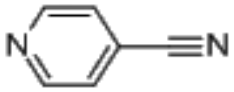

1

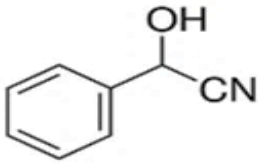

2

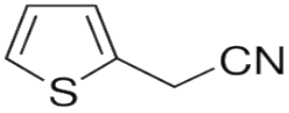

3

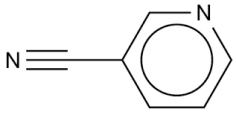

4

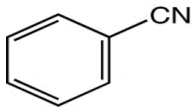

5

(b)Aliphatic Nitriles

6

7

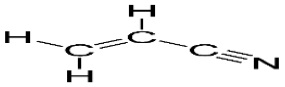

8

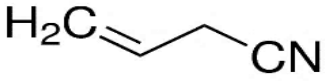

9

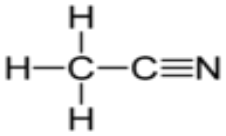

10

Figure 4.8: Aromatic and aliphatic nitriles used to screen each nitrilases RPA0599, RPA1563, RPA2416 and RPA4166. (a) Aromatic Nitriles (1) 4-Cyanopyridine, (2) Mandelonitrile (3) 2-Thiopheneacetonitrile (4) 3- Cyanopyridine, (5) Benzonitrile. (b) Aliphatic Nitriles (6) Fumaronitrile (7) Glutaronitrile (8) Acrylonitrile (9) Allyl cyanide and (10) Acetonitrile**.**

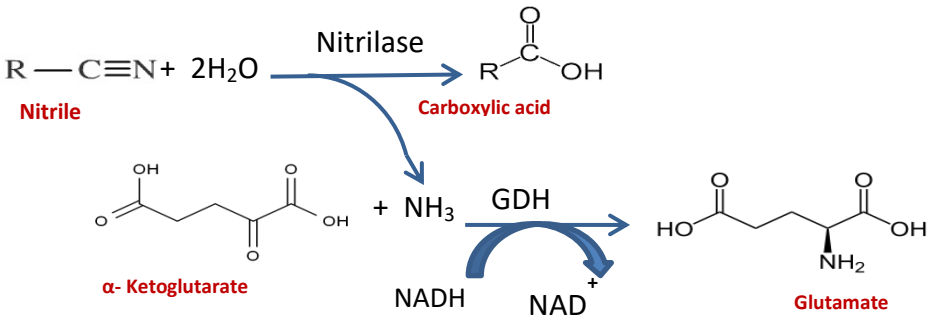

Figure 4.9: Continuous coupled enzyme assay mechanism.

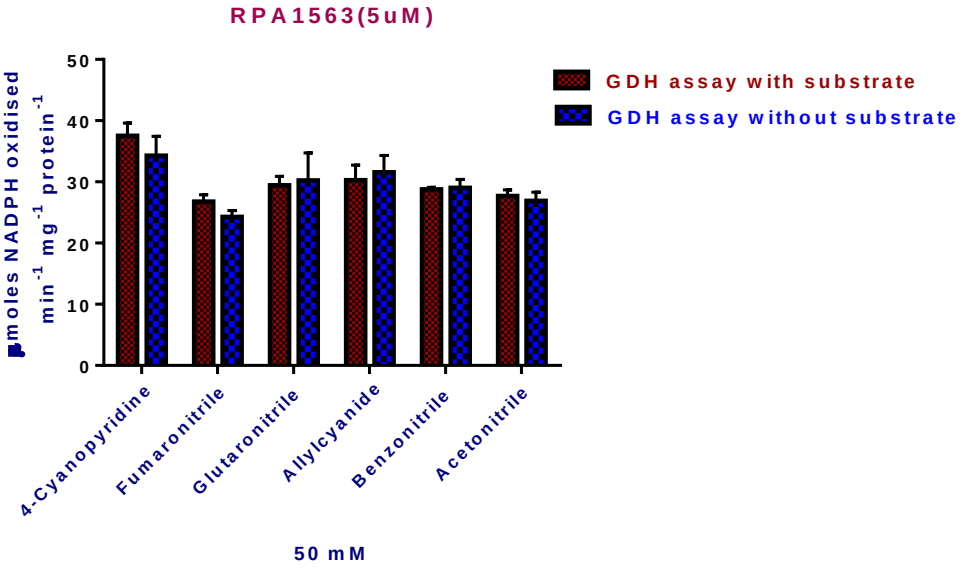

Figure 4.10: GDH continuous coupled assay of nitrilase RPA1563. Enzyme activity of RPA1563 with six nitriles was measured by detecting NADH oxidation in reaction mixture containing 50mM HEPES pH7.5, 8 units GDH, 5 mM α-ketoglutaric acid, 50 mM nitrile, 5 μM enzyme and 200 μM NADH. The assay was performed in duplicate of a single batch of protein.

of ammonia and the oxidation rate of NADH was similar in both, the control and reaction mixture. Despite many attempts, this problem could not be resolved. This leads to use of a chemical assay that detects ammonia through a colorimetric assay.

4.2.4.2 Colorimetric assays

There are well established chemical methods for detecting and quantifying ammonia that can be applied to nitrilase assays, but the disadvantage is that these methods are discontinuous. The reaction of the substrate and enzyme is set up and then terminated to measure the amount of ammonia produced. We tested two methods, one using the reaction of ammonia with alkaline phenol/nitroprusside, and the other based on the reaction of ammonia with o-phthalaldehye.

4.2.4.2.1 Berthelot method (phenol assay)

Weatherburn (1967) described a colorimetric assay method for the measurement of nitrilase activity (Berthelot method), where ammonia reacts phenol and sodium nitroprusside in alkaline solution sodium hydroxide and sodium hypochlorite. The liberated ammonia from the enzyme reaction reacts with the hypochlorite-alkaline phenol to form a blue indophenol dye that was detected here using a 96 wells plate reader at 600 nm to measure the NH_3 concentration. To test this assay, we first prepared a standard curve. Ammonia concentration was determined by using aqueous solutions of ammonium chloride standard curve, and deionised water was used as a blank (Table 4.3) and the results are shown graphically in (Figure 4.11a). The assay was linear with concentrations of ammonium ions up to at least 5 mM.

To test enzyme activity using this method, the reaction mixture contained 5 µM purified nitrilase and 50 mM nitrile compounds in 50 mM KPB pH 7.6 and incubated for

Table 4.3.Absorbance of standard curve of NH_4Cl solutions with both assays.

NH4Cl concentration mM	Phenol assay A600 nm	OPA assay A600 nm
0	0	0
0.1	0.13	0.02
0.5	0.20	0.04
1	0.72	0.06
2	1.28	0.09
3	1.93	0.14
4	2.89	0.18
5	3.44	0.22

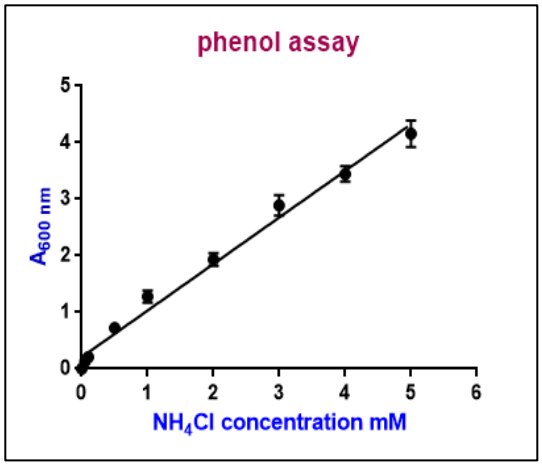

(a)

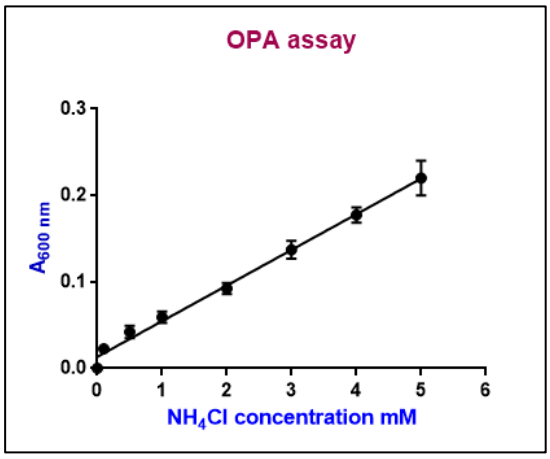

(b)

Figure 4.11: Calibration curves for both (a) Phenol assay and (b) OPA assay.

1 hour at 30°C, and then enzyme activity was stopped by the addition of reagent A (phenol and sodium nitroprusside). Equal volume of reagent B (sodium hydroxide and sodium hypochlorite) was then added to the mixture to develop the color. Then, the assay is heated for 5 min at 50 °C and left for 1 h at room temperature to stabilize the colour. A control reaction was prepared without the addition of enzyme and all assays were carried out in duplicate. Without enzyme, no colour development was noted.

The results (Fig. 4.12) showed that RPA4166 has the highest activity compared to the other nitrilases. The best substrate utilization activity was recorded for glutaronitrile showing 1.3 mM ammonia concentration, while the other nitriles showed ammonia concentration between 0.25- 0.4 mM (Figure 4.12d). RPA0599, RPA1563 and RPA2416 displayed weaker activity, but ammonia was produced with all of the screened aliphatic and aromatic nitriles used in this study. Overall the ammonia concentration recorded was less than 0.3 mM as shown in (Figure 4.12a, 4.12b and 4.12c). This method gave an insight into substrate utilization but did not provide detailed substrate utilization capability of the different nitrilases under investigation. The main problem with this method is that it is time-consuming to analyse the samples and requires a 50 °C heating step. The *o*-phthalaldehyde (OPA) method was used to overcome these issues.

4.2.4.2.2 Determination of ammonia by using OPA reagents

This method was used to confirm the nitrilase activity against ten nitrile substrates. In this assay, the reaction containing 5 µM enzyme with 50 mM nitrile substrate was incubated for 18 hours at 30°C and the liberated ammonia will react with a *o*-phthalaldehyde (OPA) reagent which produces a chromogenic reaction in the presence of 10% TCA. The produced chromophore may precipitate so 1:2 DMSO dilution was

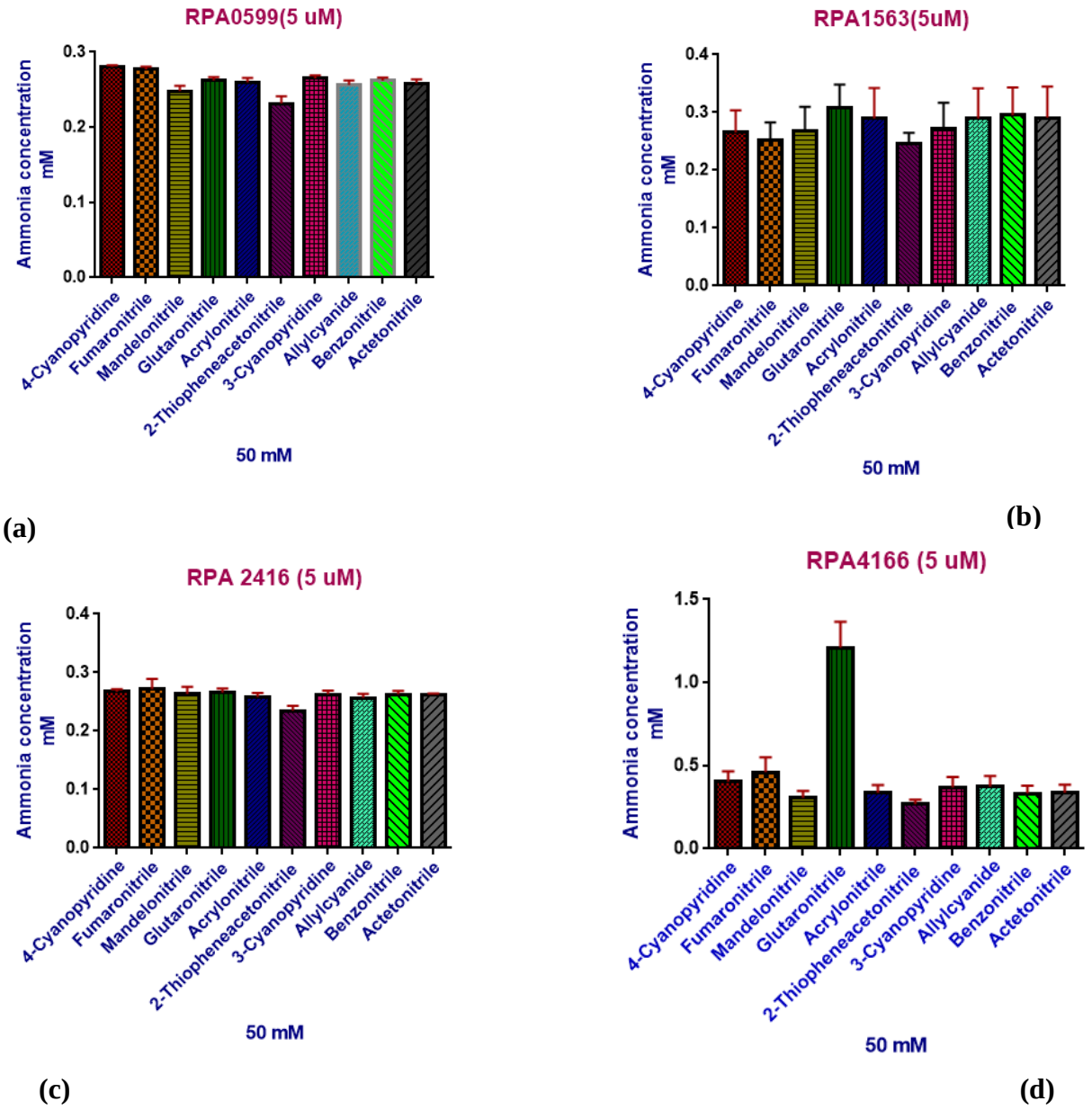

Figure 4.12: Screening of nitriles by using phenol assay. Enzyme activity was measured by detecting the relasing ammonia from starting reaction mixture containing 50 mM KPB pH 7.6, 50 mM nitriles, 1 mM DTT and 5 µM nitrilase. Reaction was stopped after one hour with reagent A then reagent B. All assays were performed in duplicate.

used and the blue colour was detected using a 96 well microplate reader. A standard curve (Table 4.3 and Fig. 4.11b) showed a linear response up to at least 5 mM ammonium chloride.

The results with the purified enzymes shown in Figure 4.13 suggested that this method is more sensitive in terms of the measured ammonia released, with much higher concentrations than with the phenol assay. RPA4166 showed the highest nitrilase activity followed by RPA1563. For RPA4166, 4-cyanopyridine was the preferred substrate with the highest ammonia concentration at 15 mM. RPA1563 and RPA0599 also showed high activity with 4-cyanopyridine (13 mM and 11 mM) respectively. RPA2416 was the only nitrilase that showed low activity with 4-cyanopyridine and the recorded ammonia concentration was below 2 mM. In general, all nitrilases have low activity with the remaining nitriles with slightly varying ammonia concentration that was ≤ 3 mM. The lowest ammonia concentration recorded for RPA4166 was for benzonitrile and acetonitrile with 1.4 mM for both substrates, while RPA0599, RPA1563 and RPA2416 showed the lowest activity with mandelonitrile, 2-thiopheneacetonitrile and acetonitrile with (1.3, 1.5 and 0.9 mM) respectively (Figure 413a, 4.13b, 4.13c and 4.13d).

4.2.3 Phenotypic growth studies

After analyzing nitrile utilization by detecting ammonia production using conventional method in vitro, the substrate uptake by wild type *R. palustris* was investigated *in vivo* to analyze their uptake rate using NMR.

R. palustris has the ability to grow on many different aromatic compounds under aerobic or anaerobic conditions, but its ability to grow with nitriles or metabolise them *in vivo* has never been specifically tested. Initial experiments to test growth on nitriles as sole carbon source yielded negative results. However, nitriles may be toxic and so we

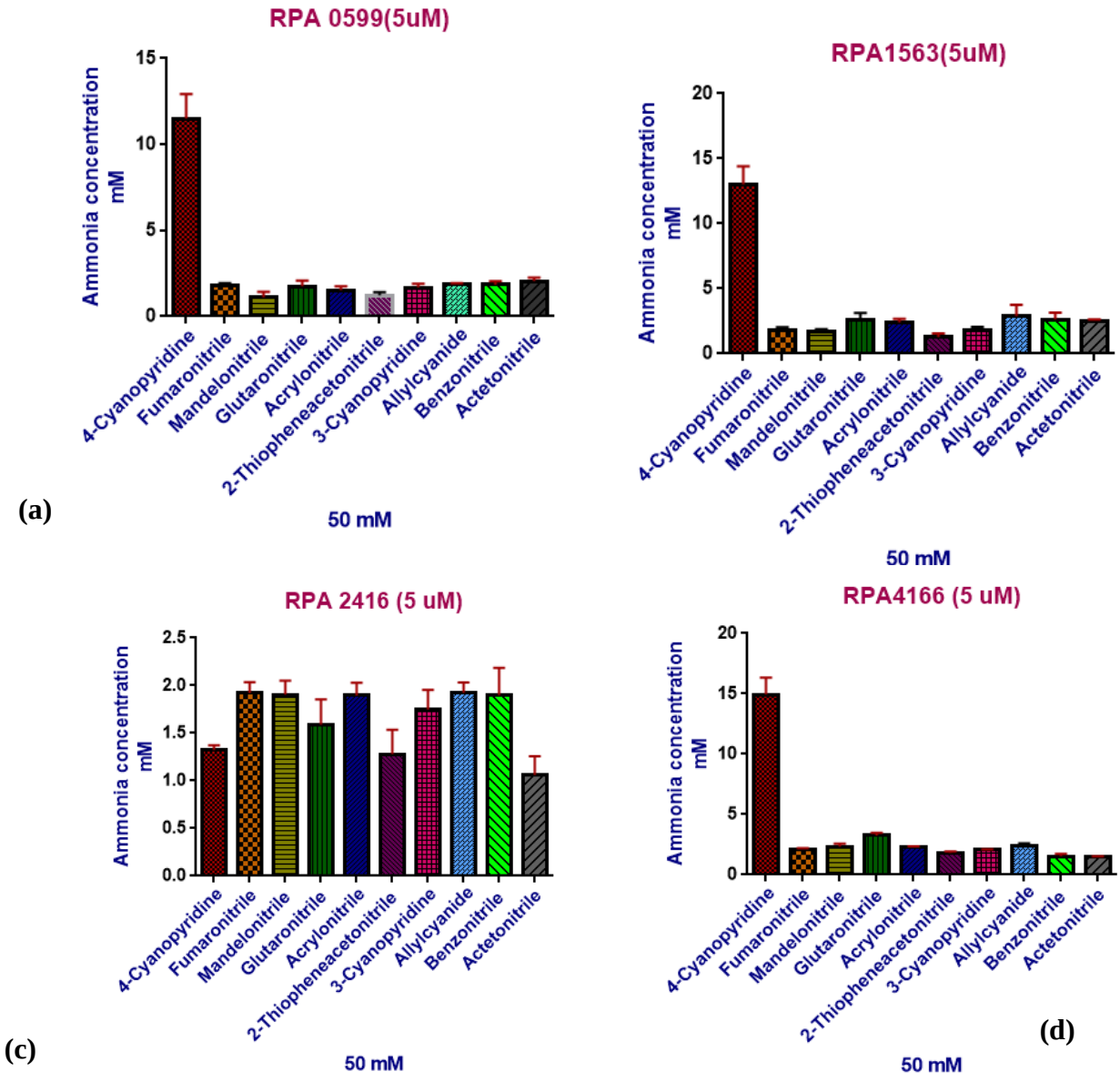

Figure 4.13 Screening of nitriles by using OPA assay. Enzyme activity was measured by detecting the releasing ammonia from starting reaction mixture containing 10 mM KPB pH 7.2, 50 mM nitriles, 1 mM DTT and 5 µM nitrilase. Released ammonia will react with OPA reagent then stopped with TCA and diluted 1:2 with DMSO. All assays were performed in duplicate using a single batch of enzyme.

tested whether there was any growth enhancement or inhibition resulting from inclusion of nitriles in media also containing the known carbon source benzoate. *R. palustris* strain CGA009 was grown anaerobically at 30ºC in photosynthetic minimal media (RCV). This medium was individually supplemented with 3 mM benzoate plus 3mM of each nitrile (benzonitrile, acetonitrile, 3-indoleacetonitrile or glutaronitrile were tested here) as the carbon source. A control growth was measured for *R. palustris* grown on 3mM benzoate only. RCV media was supplemented with freshly made 10 mM sodium bicarbonate and media pH was adjusted to pH 7.5. Growth OD was measured using anaerobic glass tubes containing a glass ball to agitate the culture and to prevent the formation of biofilm. *R. palustris* was able to grow on benzoate as expected and in the presence of benzonitrile with no growth inhibition but also no evidence of growth enhancement. The presence of acetonitrile caused some growth inhibition, while more severe growth inhibition was observed for 3-indoleacetonitrile or glutaronitrile (Figure 4.14). Samples (1 ml) were taken at different time intervals (0 hours, 60 hours and 120 hours) to analyze the nitrile concentration by NMR. The NMR spectra results revealed that 3-indo-acetonitrile, acetonitrile and benzonitrile were detected in low concentration due to their volatility even at time 0 hours (Figure 4.15d, 4.15c and 4.15b). For *R. palustris* grown on glutaronitrile in the presence of benzoate, the NMR spectra data revealed that only benzoate was consumed by *R. palustris* (Figure 4.15a) while glutaronitrile concentration remained the same (Figure 4.15e and Table 4.4). Therefore, these results do not provide any evidence for *in vivo* nitrile metabolism.

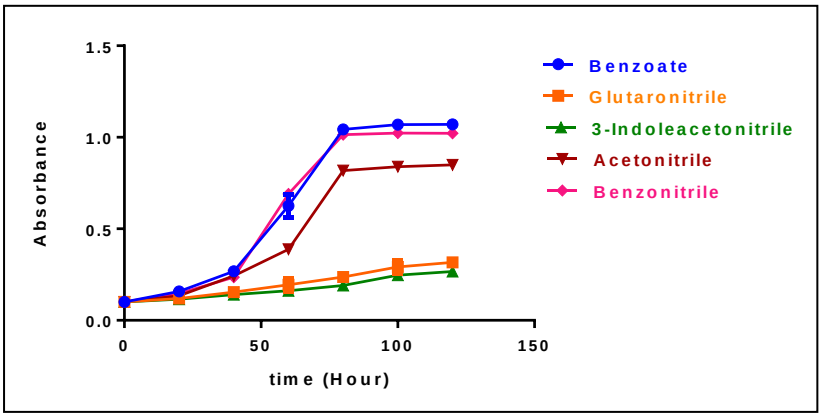

Figure 4.14: Growth curve of *R. palustrius* wild type with aromatic and aliphatic nitrile compounds. Cells were grown anaerobically on RCV media with 3mM nitriles as carbon source (acetonitrile, benzonitrile, glutaronitrile and 3-indoleacetonitrile) supplemented with 3mM benzoic acid for each. 3mM Benzoate only was used as control.

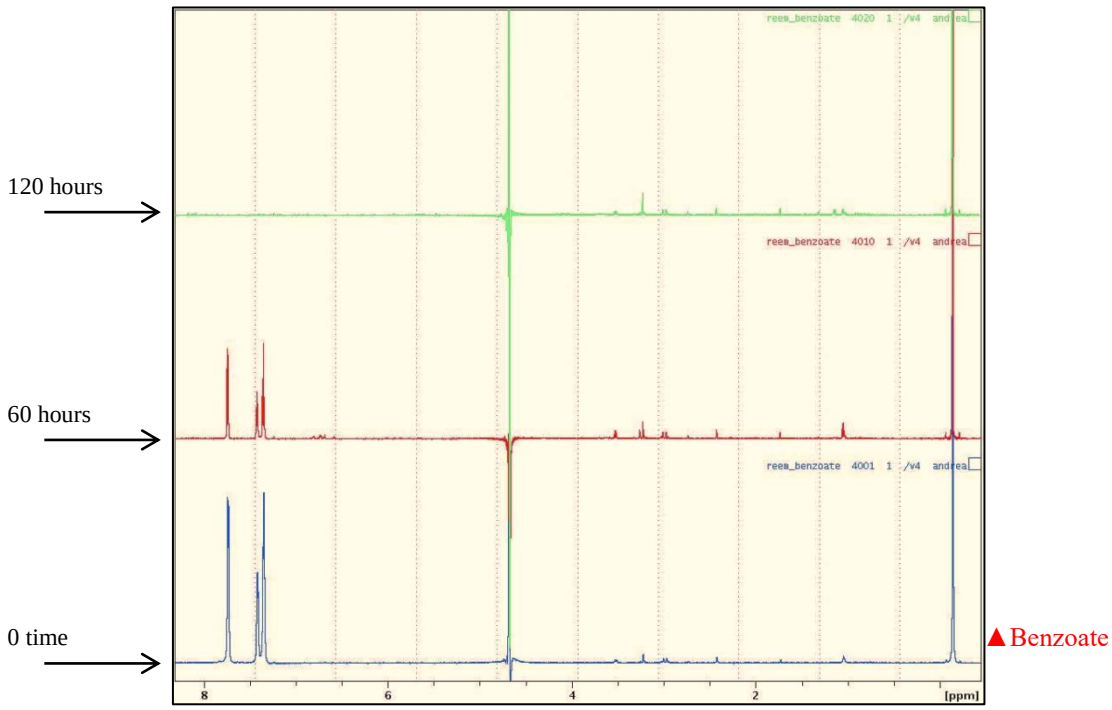
120 hours
60 hours
0 time
▲Benzoate
8
6
4
2
[ppm]

(a)

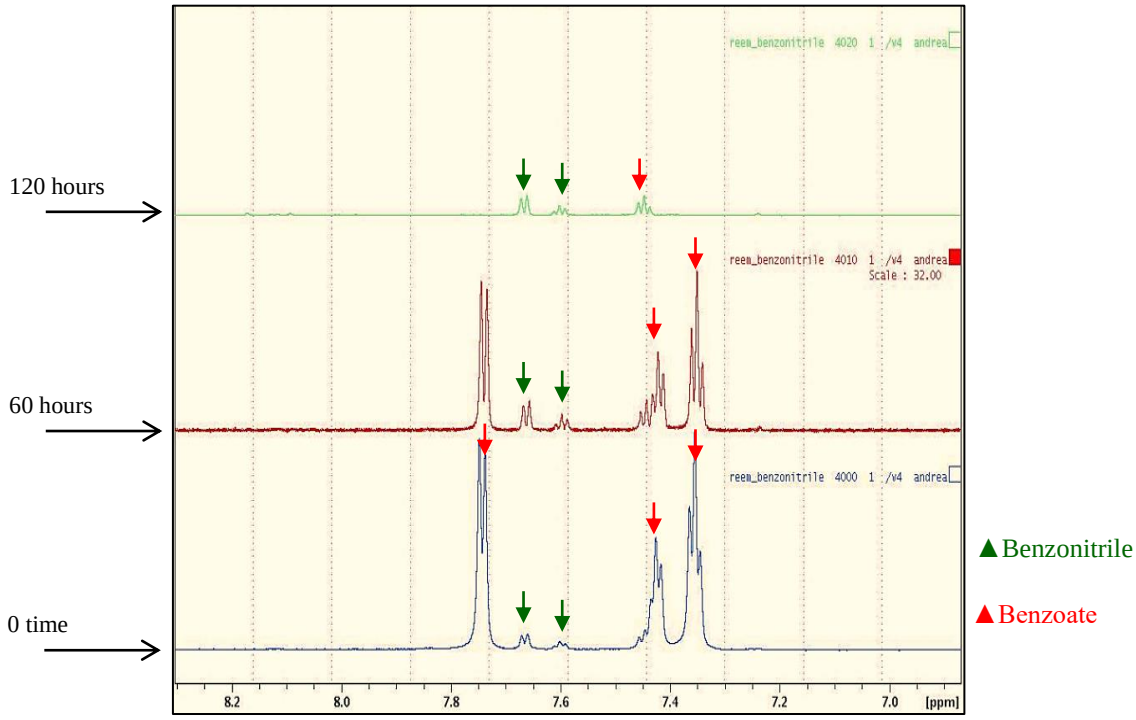
120 hours
60 hours
0 time
▲Benzonitrile
▲Benzoate
8.2
8.0
7.8
7.6
7.4
7.2
7.0
[ppm]

(b)

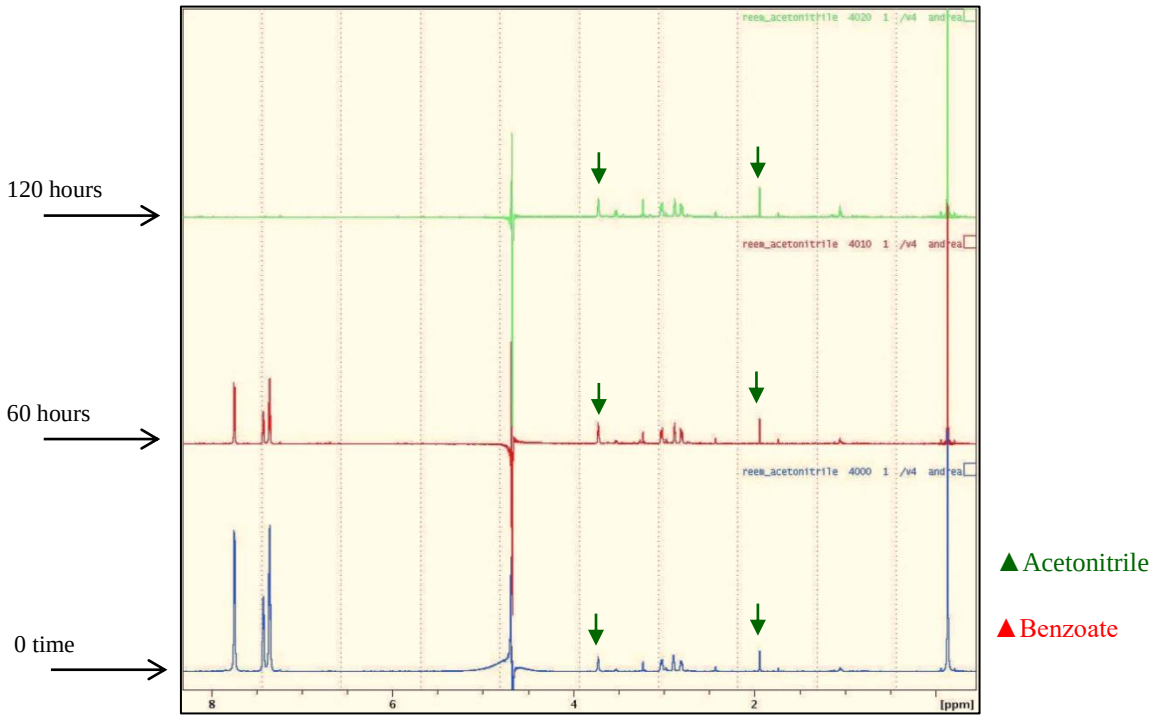
120 hours
60 hours
0 time
reem_acetonitrile 4020 1 /v4 andrea
reem_acetonitrile 4010 1 /v4 andrea
reem_acetonitrile 4000 1 /v4 andrea
8
6
4
2
[ppm]
▲Acetonitrile
▲Benzoate

(c)

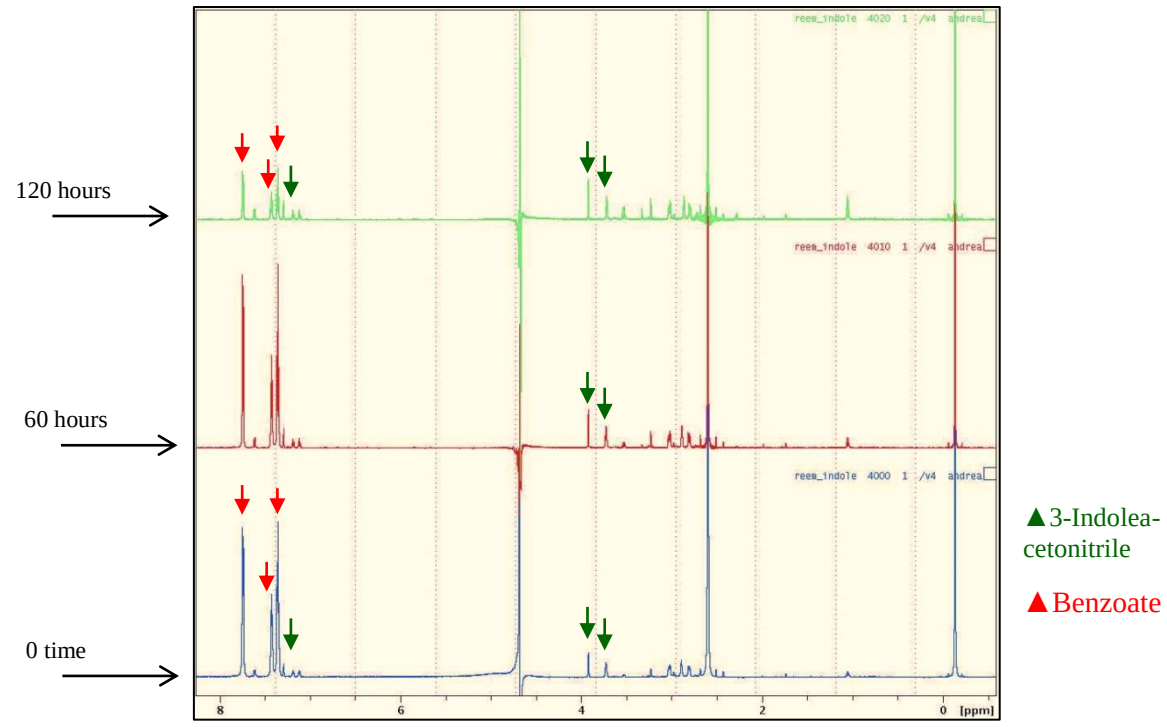
120 hours
60 hours
0 time
reem_indole 4020 1 /v4 andrea
reem_indole 4010 1 /v4 andrea
reem_indole 4000 1 /v4 andrea
8
6
4
2
0
[ppm]
▲3-Indolea-cetonitrile
▲Benzoate

(d)

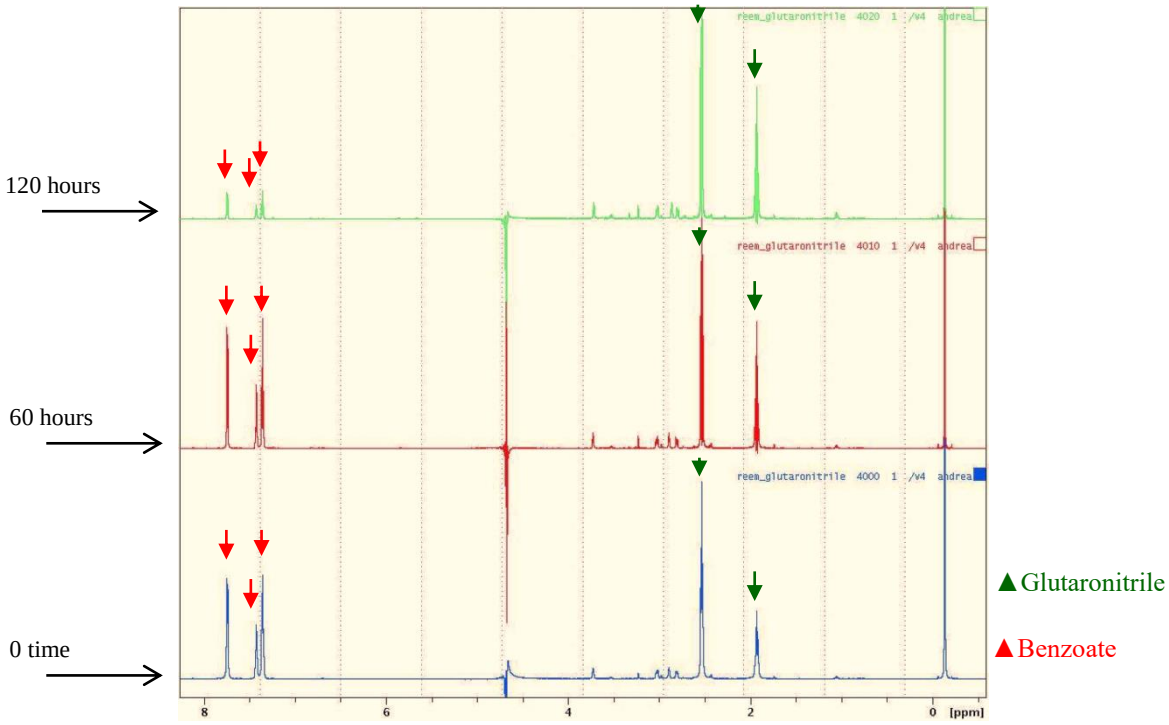

(e)

Figure 4.15: NMR Spectra of of *R. palustris* wild type growth with aromatic and aliphatic nitrile compounds. Cells were grown anaerobically on RCV media supplemented individually with 3mM benzoate and 3mM nitriles (a) Bnenzoate (control) ,(b) Benzonitrile, (c) acetonitrile ,(d) 3-Indolecetonitrile and (e) Glutaronitrile. The supernatant samples were taken at different intervals time: 0 time (blue line), 60 hours (red line) and 120 hours (green line).The data is for a single batch of sample.

Table 4.4: The utilization of aromatic and aliphatic nitriles and benzoate by *R. palustris.* Cells were grown anaerobically on RCV media supplemented individually with 3mM benzoate and 3mM nitriles. The supernatant samples were taken at different intervals time (0time, 60 and 120 hours).

Time	Benzoate concentration mM	Nitriles concentration mM
	[Benzoate] mM	
Zero time	3.5	
60 h	0.9	
120 h	0	
	Benzoate mM	Glutaronitrile mM
Zero time	2.7	2.5
60 h	2	2.4
120 h	0.5	2.5
	Benzoate mM	3-Indol-acetonitrile mM
Zero time	3.1	0.2
60 h	2.3	0.2
120 h	0.6	0.2
	Benzoate mM	Acetonitrile mM
Zero time	2.9	0.1
60 h	1.1	0.1
120 h	0	0.1
	Benzoate mM	Benzonitrile mM
Zero time	2.4	0.2
60 h	1.6	0.3
120 h	0	0.2

4.3 Discussion

The need for new nitrilases in the biotechnological industry comes from the insufficient stability of such enzymes in addition to their often low activity and substrate specificity (Heinemann et al., 2003). The *R. palustris* genome codes for 4 different nitrilases RPA0599, RPA1563, RPA2416 and RPA4166 and these were cloned, expressed and purified in this work and investigated to asses their substrate specificity.

Multiple sequence alignments using CLUSTAL W software was done and the results showed that the similarity percentage ranged from 18-50 % between the *R. palustris* nitrilases and the nitrilase superfamily group from eukaryotic and prokaryotic organisms Table 4.1. In addition, an inspection of the (E-K-C) catalytic triad showed that *R. palustris* nitrilases sequence displayed conservation of residues. Many studies of the aliphatic/aromatic nitrilases group suggested the presence of a conserved catalytic triad composed of Cysteine, Glutamate and Lysine residues (Pace and Brenner, 2001, Thuku et al., 2007) The same conserved triad was detected in all isolated nitrilases from *R. palustris* (Table 4.1).

Nitrilase genes were successfully cloned into the pET21a(+) expression vector. The recombinant proteins from *R. palustris* were expressed in *E. coli* BL21 cells and purified by nickel affinity chromatography followed by gel filtration chromatography in absence of substrate. In the native form nitrilase exists as either an inactive dimer or an active homooligomer (Thuku, 2006). Table 4.2 showed the gel filtration results where an active form was suggested for RPA4166 and RPA1563, whereas a possible non-active form was suggested for RPA0599 and RPA2416. However, the enzymes were reactivated by incubating for 1 and 18 hours with substrate in phenol and OPA assay respectively. Furthermore, a low concentration of DTT was added to the enzyme aliquots to avoid thiol

oxidation of the active site cysteine residue in the reaction mixture and hence reactivate and stabilize the nitrilase (Kiziak et al., 2005, Bayer et al., 2011) The addition of DTT in high concentration was avoided due to several studies that showed its ability to inhibit the enzyme activity (Winkler et al., 2006, Gong et al., 2012).

Published methods to assay nitrilase activity depend mainly on HPLC methods, either to detect the consumption of the nitrile or the appearance of the product carboxylic acid, or they depend on measuring the liberated ammonia in the hydrolysis reaction. The HPLC methods are probably most widely used but they require special equipment and columns. Moreover, continuous rate measurements are not possible with HPLC based assays. In contrast, ammonia production is technically easier to measure and there is the possibility of a continuous assay. In this chapter, three different methods were used to assay the activity of the nitrilase enzymes purified in this work and all methods used depends mainly on detecting ammonia production. We ideally wished to develop a continuous assay so true rates of the enzymes with different substrates could be compared and the kinetic parameters determined. However, in the GDH continuous assay method both control and test reaction showed a similar rate which indicated that in the absence of a nitrile substrate NADH was being oxidized and a true rate could not be calculated. A smaller background rate was observed in the control samples by Vergne-Vaxelaire et al., (2013) but as the rate was smaller it could be subtracted from the reaction rate (Vergne-Vaxelaire et al., 2013). It is possible to speculate on the origin of this background rate. One possibility is that there are traces of ammonium present in the commercial GDH enzyme preparation used. Commonly, such enzymes are purified using ammonium sulphate precipitation as one of the steps. Although it was not possible to obtain details of how the GDH was purified, this remains a likely problem. Therefore, if this assay is to be

used in future studies to measure rates continuously, it may be necessary to use highly purified and buffer exchanged GDH coupling enzyme.

The second method used was the Berthelot method (phenol assay) where the liberated NH_3 interacts with phenol/hypochlorite reagent and the activity was quantified colorimetrically at 600 nm. This method results showed quite high ammonia concentration in the assay of RPA1563 (0.32 mM) and a significant increase in RPA4166 (1.3 mM) with aliphatic glutaronitrile but less than 0.2 mM for RPA0599 and RPA2416. Glutaronitrile was also the preferred substrate with high relative activity for Nit1 protein that was isolated from metagenomic library grown on cinnamonitrile and other nitriles (Bayer et al., 2011). Nit1 was able to convert 2-methylglutaronitrile to 4-cyanopentanoic acid which can be used as a precursor for added value chemicals in pharmaceutical industry such as 1,5 dimethyl-2-piperidone (Bayer et al., 2011). Furthermore, a nitrilase isolated from *Rhodococcus rhodochrous* k22 showed 345% relative activity with glutaronitrile (Kobayashi et al., 1990).

The Berthelot method in general is a difficult assay as its uses corrosive chemicals, and required large amount of samples due to its low sensitivity (Banerjee et al., 2003). Also, one of the main disadvantages in this method is the need for at least 1 hour incubation time to develop a stable chromophore at room temperature. Another major disadvantage is the time sensitivity for reagent addition (Xue et al., 2016). Weatherburn (1967) found that the order of reagent addition did not interfere with the results and color formation but when there was a time gap of two minutes between the additions of reagent B to reagent A, the results showed a significant decrease in the absorbance of up to 8.5%. A 17% decrease in the absorbance was also found when the time interval of reagent addition was a round 5 minutes. All these issues will reflect on the apparent determined

ammonia concentration if the method is preformed manually (Weatherburn, 1967). Such difficulty was observed while preforming the experiments described here and that was reflected in the results as no major variations between tested substrates were recorded. Therefore, the OPA method was used where ammonia production was monitored using the single OPA reagent forming a colorless mixture, which eventually becomes strongly coloured after the addition of TCA. Overall the results showed high activity with aromatic 4-cyanopyridine for RPA4166, RPA1563 and RPA0599 with significant ammonia concentrations being reached. Similar results were recorded for a nitrilase isolated from *Aspergillus niger* which showed a maximum activity of 91.6 U mg^{-1} with 4-cyanopyridine followed by benzonitrile (Kaplan et al., 2006). The OPA method was able to detect low ammonia concentrations and a variation between different nitrile utilization was recorded. Sharma et al. (2012) showed that a high concentration of 4-cyanopyridine < 50 mM can inhibit the NHB-2 nitrilase activity in *Nocardia globerula* (Sharma et al., 2012), while no activity was recorded with nitrilase from *Rhodococcus rhodochrous* J1(Thuku et al., 2007)

On the other hand, very low activity was determined with RPA2416 that could be due to a side reaction and not ammonia production. Based on the results and it's sequence analysis, RPA2416 could be an amidohydrolayse. Therefore, further analysis is required if amides are a possible the substrate for RPA2416.

In general *R. palustris* nitrilases were shown to be active with aliphatic and aromatic nitriles and they could be characterized as aliphatic/aromatic nitrilases showing weak activity. RPA4166 has previously been investigated (Sharma et al., 2012, Xie et al., 2006, Black et al., 2015) and these authors proved that this enzyme is capable of utilizing both aromatic and aliphatic nitriles. RPA4166 activity was determined by investigating

ammonia production using OPA reagent assay against 38 nitriles and the results showed narrow substrate specificity and the highest activity was recorded for 4-nitrophenylacetonitrile followed by 3-phenylpropionitrile (Black et al., 2015) .

Nitrile substrate utilization by wild type *R. palustris* results showed that Glutaronitrile and 3- indoleacetonitrile are quite toxic, while the growth with Benzonitrile resulted in no inhibition but there was a slight inhibition with Acetonitrile. Furthermore, 1H-NMR spectroscopy analysis data of the culture supernatants showed an apparent decrease in the concentration of Benzonitrile, 3- indoleacetonitrile and Acetoniytile nitriles but this was due to the volatile nature of these compounds as only a small amount could be measured at zero time. Layh et al. (1994) showed that *Rhodococcus* sp. C3II are able to grow on racemic naproxen nitrile as a nitrogen source while using succinate as a carbon source and convert the naproxen nitrile to S-naproxen amide and subsequently S-naproxen (Layh et al., 1994). Also Howden et al (2009) proved that *Pseudomonas fluorescens PfSBW25* could grow on an aliphatic nitrile β-cyano-l-alanine and utilised it to produce ammonia which can subsequently be used as a nitrogen source (Howden et al., 2009).

Because of the complexity of nitrilases, low activity and substrate range for the purified nitrilases were recorded; further analysis is required in the future to look at the reaction product using HPLC, also a crystal structure for each enzyme could give an indication for the substrate selectivity and their binding and the active site capabilities.

CHAPTER 5

THE ROLE OF AN ACTIVATOR PROTEIN IN THE DEGRADATION OF AROMATIC AND ALIPHATIC NITRILES BY THE NITRILE HYDRATASE ISOLATED FROM *R. PALUSTRIS*

5 The role of an activator protein in the degradation of aromatic and aliphatic nitriles by the nitrile hydratase isolated from *R. palustris*

5.1 Introduction:

As described in Chapter 1 nitrile hydratase (NHase; EC 4.2.1.84) catalyzes the hydration of the aliphatic and aromatic nitriles some of which are toxic to the corresponding amide (Rzeznicka et al., 2010) and this reaction has potential applications in biotechnology in biosynthetic and bioremediation processes (Kamble et al., 2013). NHases are metalloenzymes that contain as a cofactor a non-corrinoid cobalt (III) ion (Liu et al., 2013, Sun et al., 2016) or non-heme iron (III) (Hashimoto et al., 1994, Nagasawa et al., 1987) at the active site. These enzymes consist of two-subunits α and β which are different in their amino acid sequence (Black et al., 2010). The metal ions in NHase cofactor are located in the α-subunits (Black et al., 2010, Xia et al., 2016).

The NHase activators are small proteins with a molecular weight of 14–17 kDa (Kataoka et al., 2006), often referred to as "P14K". These proteins are essential for the functional expression of NHase enzymes, for example for those in the Fe-NHases from *Pseudomonas sp*. B23 and *Rhodococcus sp*. N-774 (Hashimoto et al., 1994, Nagasawa et al., 1987) in addition to the Co-NHase from *Bordetella petrii, Pseudomonas putida and Rhodococcus rhodochrous* J1(Zhou et al., 2009, Sun et al., 2016, Liu et al., 2013). The NHase from *R. palustris* is thought to be a Co-NHase because it has a typical active site sequence of VCTLCSC at the active site of the α-subunit, where the metal ion is bound to the cysteine residues (Black et al., 2010). In Black et al. (2010) study the *R. palustris* NHase did not require an activator protein for activity while there is a putative activator protein encoded directly downstream of the β-subunit (Larimer et al., 2004) Nevertheless, at this time the possibility that activator is involved in cobalt trafficking or modulating

the activity of the *R. palustris* NHase α-β cannot be ruled out. The trafficking of metal ions into the NHase active site is thought to be mediated by the corresponding activator proteins acting as a "self-subunit swapping chaperone" (Black et al., 2010, Xia et al., 2016).

In this chapter the genes encoding the annotated NHase alpha subunit *rpa2805*, the NHase beta subunit *rpa2806* and a putative nitrile hydratase activator (P14K) or uncharacterized protein *rpa2807* from *R. palustris* were studied. We overproduced and purified two types of NHase; first by cloning the α- and β- subunit genes of the NHase and secondly by cloning the α- and β- subunit genes along with the P14K encoding gene. Both constructs were overexpressed individually in *E. coli*. The resulting proteins were purified and biochemically characterized.

This work is focused on the effect of the activator protein on the NHase of *R. palustris* CGA009 in catalyzing the transformation of various aromatic and aliphatic nitriles (mandelonitrile, benzonitrile, 4-cyanopyridine, 3-indoleacetonitrile, acrylonitrile and acetonitrile) to the corresponding amides. The *rpa2805* and *rpa2806* genes were previously cloned and the two subunit enzyme purified and biochemically characterized in another study (Black et al., 2010). However, these authors did not realize that a potential activator protein was encoded downstream of the beta subunit gene and so their enzyme preparation did not represent the native form of the enzyme.

5.2 Results

5.2.1 Identification and bioinformatics analysis of a potential nitrile hydratase activator "P14K" in *R. palustris*

The sequence analysis of the complete genome of *R. palustris* CGA009 showed that the *rpa2805* gene encodes the α-subunit, *rpa2806* gene encodes the β-subunit and the downstream gene *rpa2807* gene encodes a potential P14K type activator, which is not annotated as such in the genome sequence database (Uniprot accession numbers Q6N613, Q6N612 and Q6N611) (Figure 5.1) . The P14K activator belongs to "electron transport accessory proteins superfamily 50090" in the structural Classification of proteins (SCOP) database.

BLAST searches using the translated *R. palustris* DNA sequence of *rpa2807* showed high-scoring similarities to various potential P14K activators, but most are uncharacterized or hypothetical proteins. The predicted sequence of the *R. palustris* P14K activator was aligned with selected known P14K activators in which functional activation of NHase has been previously reported (Figure 5.2). This shows clear conservation of specific residues in this family of proteins.

Table 5.1 shows the percentage identity of these homologs. RPA2807 showed the highest overall identity (35-36 %) with that of Bpet1414 from *Bordetella petrii* and Pchl3084_3169 from *Pseudomonas chlororaphis* respectively, followed by the P14K activator from *Mycobacterium smegmatis*, while the identity to the NHase activators in *Pseudomonas putida*, *Rhodococcus rhodochrous* and *Bacillus* sp. RAPc8 was around 25%.

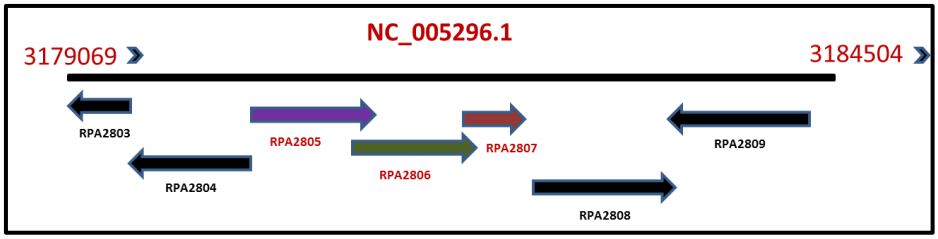

Figure 5.1 Cluster of overlapping nitrile hydratase genes found in the *R. palustris* CGA0009 genome. NHase α (*rpa2805*) , NHase β (*rpa2806*) and NHase activator P14K (*rpa2807).*

```
nhhG-Rr             --MSEDTLT--DRLPATGTAAPPRDNGELVFTEPWEATAFGVAIALSDQKSY-EWEFFRQ
P14k-Bac            MKSCENQPNESLLANMSEEVAPPRKNGELEFQEPWERRSFGMTLALYEEKLYSSWEDFRS
P14k-Myc            ---------------MKLHQTCTTDQAAPSFDHEWQRRAFGLALALSEFGHY-PWSEFQQ
2807                MSS---Q-SEAAAIAAHSVPGLPRDDDGPVFREPWEAHAFAMAVTLHGRGLF-TWPEWAA
Pch13084_3169       --------MNASMPHIPPIAGLSLDDEGPVFDKPWQAQAFSLLLHLHQTGLF-PWKDWVQ
Bpet1414            ----------MKDERFPLPEGSLKDLDGPVFDEPWQSQAFALVVSMHKAGLF-QWKDWAE
P14K-PsPu           -------------------MALCLTSLGSP-RRLPWWSACTRPVSFSGKTG---------P
                                                .         *   .

nhhG-Rr             RLIHSIAE-------A---NGCEAYYESWTKALEASVVDSGLISEDEIRERMESMAIID-
P14k-Bac            RLIEEIKGWETAKQKD---NSDWNYYEHWLAALERLVVETGMLNKRDVDTRTNEFLTGKR
P14k-Myc            SLIDAIGAWDASTGSDSDSHADWQYYDHWVAALEKVVAQRGLLAEAAGS-----------
2807                ALSAEIRRAQADGDPD----CGDTYYRHWLATLEQMVATKGVASLATQHRYRDAWDRAAD
Pch13084_3169       VFSDEIKASPAQPGES----VNDTYYRQWIAAMERMVTTLGLAGMEDITQRTEEWQQAYL
Bpet1414            TFTAEIDASPALPGES----VNDTYYRQWVSALEKLVASLGLVTGGDVNSRAQEWKQAHL
P14K-PsPu           RPSPPKSTLPRSAGES----VNDTYYRQWVSALEKLVASLGLVTGGDVNSRAQEWKQAHL
                                        **  *  ::*  *.  *:

nhhG-Rr             ----------------------------------------
P14k-Bac            DEVFY-----------------------------------
P14k-Myc            ----------------------------------------
2807                RTPHGRPIELQPGDFPQSEAFSAAESPPR----------
Pch13084_3169       NTPHGQPVTLLNASCPPAHGNGHEHLPRHEPVAISRATS
Bpet1414            NTPHGHPILLAHALCPPAIDPKHKHEPQRSPIKVVAAMA
P14K-PsPu           NTPHGHPILLAHALCPPAIDPKHKHEPQRSPIKVVAAMA
```

Figure 5.2: Alignment of RPA2807 (P14K activator) amino acid sequences. Blue line indicates the identity between the sequences.

Table 5.1 Comparison of amino-acid sequence identity. Uniprot accession numbers and entry name: Bpet1414 (A9IEG8_BORPD), P14K (O69769_PSEPU), nhhG (Q53039_RHORH), Pchl3084_3169 (J2YHE6_9PSED) , P14K (Q79M84_9BACI) , P14K (A0QPF4_MYCS2)

	Known P14K activator protein	RPA2807
1	**Bpet1414** ***Bordetella petrii***	**36%**
2	**P14K** ***Pseudomonas putida***	**25%**
3	**nhhG** ***Rhodococcus rhodochrous***	**26%**
4	**Pchl3084_3169** ***Pseudomonas chlororaphis***	**35%**
5	**P14K** ***Bacillus* sp. RAPc8**	**26%**
6	**P14K** ***Mycobacterium smegmatis***	**29%**

5.2.2 Cloning, expression and purification of the two subunit nitrile hydratase from genes rpa2805 and rpa2806

In order to carry out enzymatic analysis of NHase α-β enzyme to determine the nitrile preference, genes *rpa2805* and *rpa2806* were cloned into pET21a (+) and recombinant protein RPA2805- RPA2806 was overproduced in *E. coli* BL21(DE3).

R. palustris genomic DNA was used as a template to clone the NHase *α* and *β* genes, denoted as *rpa2805-rpa2806*, with the primers *rpa2805*-up and *rpa2806* down. The PCR products were digested with *Nde*I and *Xho*I, ligated into pET21a (+) to construct pET2805-2806 (Figure 5.3a). A six histidine tag in the C-terminal region of the beta subunit was incorporated. The expression from the pET21a (+) plasmid was induced by 400 µM IPTG via the T7 promoter. The construct was sequenced (Core Genomic Facility, University of Sheffield Medical School, UK) to confirm the encoding genes were in-frame with the 6x histidine tag and that there were no mutations.

Construct pET2805-2806 was expressed using *E. coli* BL21 (DE3) cells and overexpression trials were performed to identify the optimum temperature and time for protein production. Recombinant protein was overproduced in LB media supplemented with 100 µM $CoCl_2$ at 25 and 37°C and sampled at regular time intervals (1,3,5 hours and overnight) until cells reached 0.8 OD (600). IPTG was added to a final concentration of 400 µM; a whole cell sample for each time point was taken and run on an SDS-PAGE gel to determine the highest amounts of produced proteins. Protein overexpression and solubility trials showed that the most soluble protein was obtained overnight at 25 °C post induction. The β subunit at 25 kDa is very similar in size to the α subunit at 23.7 kDa and it was difficult to separate these proteins on the gel, but it appeared that there may be more beta subunit being produced compared to the alpha subunit (Figure 5.3b).

Cell free extracts from induced pET2805-2806 were passed individually through a nickel-affinity chromatography column and protein elution was observed via UV monitoring. Gold colour eluted protein fractions were detected in a single UV peak. Both binding and elution buffers were supplemented with 0.5 mM DTT (Liu et al., 2012, Xia et al., 2016) and 40 mM butyric acid to maintain protein stability as recommended by Nagasawa (1986). 8 µl of each of the peak fractions was run on SDS–PAGE gels. The purified NHase α-β enzyme was gold in colour and two distinct bands were clearly identified with molecular weights ~23.7 and ~25 kDa which confirmed the presence of α-subunit and β-subunit (Figure 5.3c).

Protein concentration was determined by using the Bradford assay which yielded a typical concentration of 3mg/ml. Purified protein fractions were pooled and concentrated via viva-spin column and buffer exchanged X3 into 10 mM potassium phosphate buffer pH 7.5, 100 mM NaCL, 0.5 mM DTT and 40 mM butyric acid. The concentrated proteins were subsequently measured using Bradford assay then stored in 50% glycerol at -20°C for subsequent biochemical assays.

5.2.3 Recombinant expression and purification of Nitrile hydratase gene *rpa2805 rpa2806* and *rpa2807*

The above results suggest that NHase α-β requires an activator protein for NHase α-β activation. Therefore, in order to elucidate the role of *rpa2807* (P14K activator) from *R. palustris* in the functional expression of NHase α-β, genes *rpa2805, rpa2806* and the *rpa2807* genes were cloned into pET21a (+) and recombinant protein of Rpa2805-Rpa2806- Rpa2807 was overproduced in *E. coli* BL21(DE3). *R. palustris* genomic DNA was used to clone the NHase *α , β and* P14K genes, denoted *rpa2805-rpa2806-rpa2807* using primers *rpa2805*-up and *rpa2807* down.

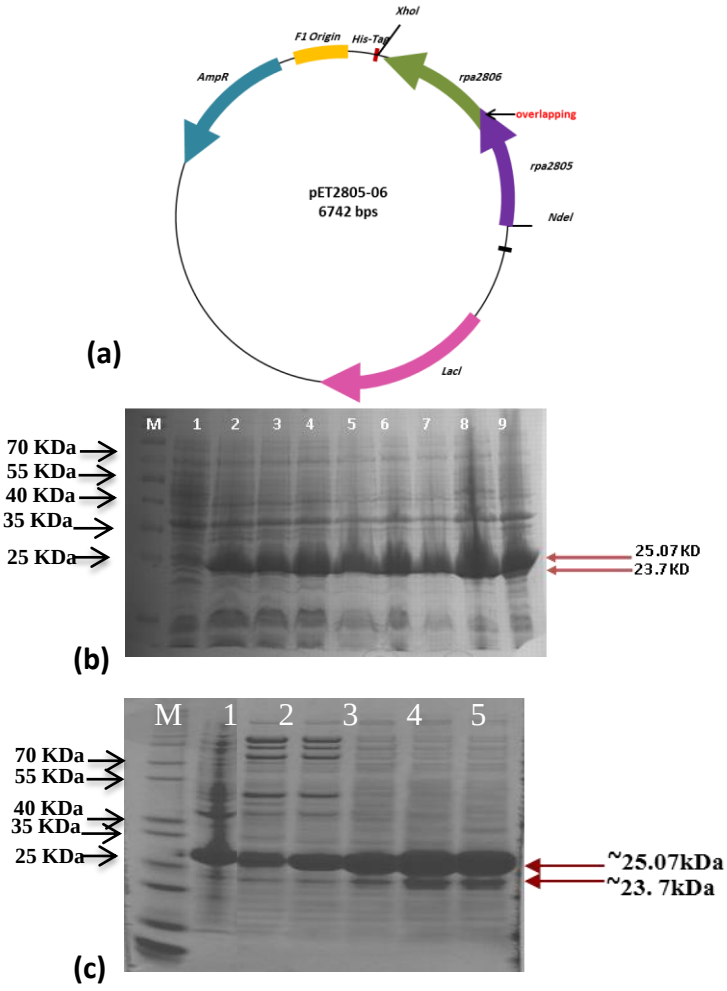

Figure 5.3 Overproduction and purification for NHase α-β protein. (a) over-expression construct pET2805-2806. The plasmid pET2805-2806 was made by cloning the *rpa2805-2806* genes sequence into pET21a(+) between the *Nde*I and *Xol*I restriction sites, *rpa2805-2806* genes with C-terminal His-tag. **(**b) SDS-PAGE showing expression trials of NHase α-β protein. M=marker= pageRuler TM prestained protein ladder (Fermentas), lane 1= control without induction , lanes 2,4,6 and 8 contain cells were induced with IPTG before incubation at 25°C at 1,3,5,24 hour interval respectively ,and lane 3,5,7 and 9 contain cells incubated at 37°C at 1,3,5,24 hour interval after IPTG induction respectively. Lane 8 shows 2 distinct bands; very low amount of protein expression (α subunit) at ~23.7 kDa and good amount of protein expression (β subunit) at ~25.07. (c) SDS-PAGE showing HisTrap purification of NHaseα-β protein. M = PageRulerTM Prestained Protein Ladder (Fermentas), lane 1= cell free extract and lane 2-6 purified fractions of distinctive two bands of recombinant protein NHase α-β at ~23.7 and ~25.07 kDa eluted via His-trap column on an imidazole gradient. Good amount of β subunit protein at size ~25.07 kDa and Low amount of α subunit protein at ~23.7 kDa were shown in lane 5 and 6 which were used later in enzymatic assay.

The sequence encoding the protein of interest was PCR amplified and sticky end cloned into the *Nde*I and *Xho*I sites of pET21a (+) to construct pET2805-2806-2807 including a six histidine tag in the C-terminal region of RPA2807 (Figure 5.4a). The expression of the cloned genes via the T7 promoter was induced with 400 µM IPTG and automated sequencing (Core Genomic Facility, University of Sheffield Medical School, UK) showed the encoding genes were correct and in-frame with the 6x histidine tag and that there were no mutations.

Construct pET2805-2806-2807 expression was carried out in the same manner as with construct pET2805-2806. Protein overexpression gel showed that the most protein expression was obtained at 5 hours at 25 °C post induction for NHase α-β-P14K (Figure 5.4b).

Purification of the cell free extract from induced pET2805-2806-2807 was carried out in the same manner with pET2805-2806. The purified NHase α-β-P14K enzyme was brownish in colour and three distinct protein bands were apparent, with molecular weights ~23.7, ~24.2 and ~16.2 kDa which confirmed the presence of the two main subunits and the activator (Figure 5.4c).

Protein concentration was determined by using Bradford assay and the concentration was 28 mg/ml for NHase α-β-P14K ten times more than NHase α-β. Purified protein fractions were concentrated and stored at the same manner in section (5.2.2).

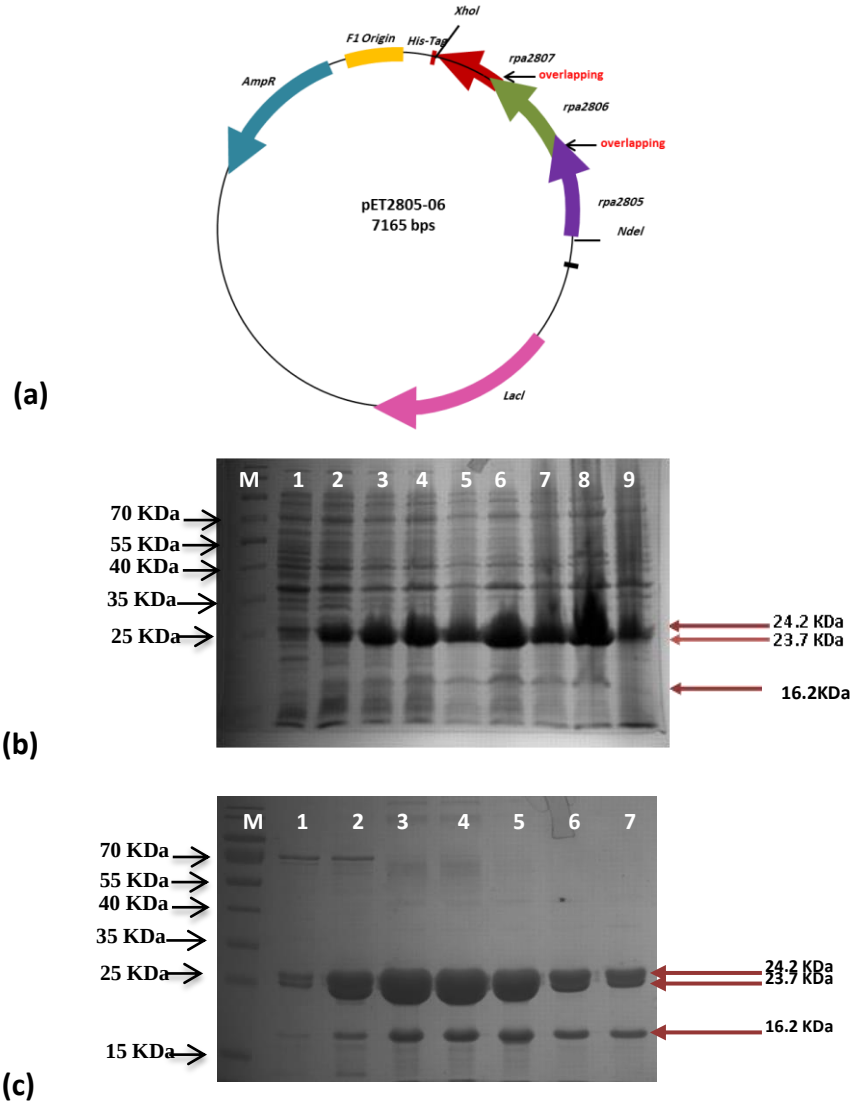

Figure 5.4 Overproduction and purification for NHase α-β-P14K protein. (a) over-expression construct pET2805-2806-2807. The plasmid pET2805-2806-2807 was made by cloning the *rpa2805-2806-2807* genes sequence into pET21a(+) between the *Nde*I and *Xol*I restriction sites*, rpa2805-2806-2807* genes with C-terminal His-tag. **(**b) SDS-PAGE showing expression trials of NHaseα-β- P14K protein. M=marker= pageRuler TM prestained protein ladder (Fermentas), lane 1= control without induction , lanes 2,4,6 and 8 contain cells were induced with IPTG before incubation at 25°C at 1,3,5,24 hour interval respectively ,and lane 3,5,7 and 9 contain cells incubated at 37°C at 1,3,5,24 hour interval after IPTG induction respectively. Lane 6 shows 3 distinct bands; of good amount of protein expression (α subunit) at ~23.7 kDa , (β subunit) at ~24.2 and P14K at ~16.2 KDa. (c) SDS-PAGE showing HisTrap purification of NHaseα-β-P14K protein. M = PageRulerTM Prestained Protein Ladder (Fermentas), lane 1-7 purified fractions of recombinant protein NHaseα-β-P14K at ~23.7 and ~24.2 kDa eluted via His-trap column on an imadazole gradient. Good amount of three bands of brownish highly pure protein size ~23.7, ~24.2 and 16.2 kDa was shown in lane 5 which was used later in enzymatic assay.

5.2.4 Characterization of the purified NHase α – β and NHase α – β-P14K

5.2.4.1 Determination of the molecular weight of the purified NHase α – β and NHase α – β-P14K

The apparent molecular mass of the purified NHase and NHase with the activator were determined by mass spectrometry by Dr Simon Thorpe (University of Sheffield) (Table 5.2). The determined molecular weight of the purified enzyme subunit α and β was 23.61 and 25.27 kDa (Figure 5.5) while the predicted molecular weight was 23.72 and 25.03 respectively. On the other hand the actual molecular weight of the purified NHase α - β- P14K was 23.61, 24.2 and 16.2 kDa, while the predicted molecular weight was 23.72 , 24.2 and 16.3 kDa respectively (Figure 5.6).

5.2.4.2 Metal analysis

The NHase from *R. palustris* can be predicted from primary sequence data to be a Co-centred NHase from the presence of the amino acid sequence VCTLCSC in the active site on the α subunit (Precigou et al., 2001, Black et al., 2010). Moreover the purified proteins were coloured; therefore, the UV–Vis absorption spectrum of both proteins were carried out. The results showed that NHase α-β exhibited one peak at 280 nm (protein absorbance) and very small peak above 300 nm, while that of NHase α-β-P14K showed one peak at 280 nm (protein absorbance) and an extra clear shoulder peak above 300 nm and a small peak at ~420 nm which is typical for a Co-NHase (Figure 5.7). The metal analysis done by Dr Neil Bramall using induction-coupled plasma mass spectrometry (ICP-MS) showed a considerably higher metal content in Nhase α-β-P14K protein when compared to the NHase α-β without activator. When the P14K activator was absent the Co concentration in the preparation was as low as 1.58 mg/l (Table 5.3) when 25 mg/l.

Table 5.2 Comparison of the actual size and predicted size of the molecular weight in NHase α-β and NHas α-β-P14K. The actual size was measured by mass spectrometry analysis and the predicted molecular weight size was determined using Expasy software.

protein	NHase α- β-P14K		NHase α- β	
	Predicted size kDa	Actual size kDa	Predicted size kDa	Actual size kDa
RPA2805	23.72	23.61	23.72	23.61
RPA2806	24.20	24.20	25.03	25.27
RPA2807	16.20	16.32	_____	_____

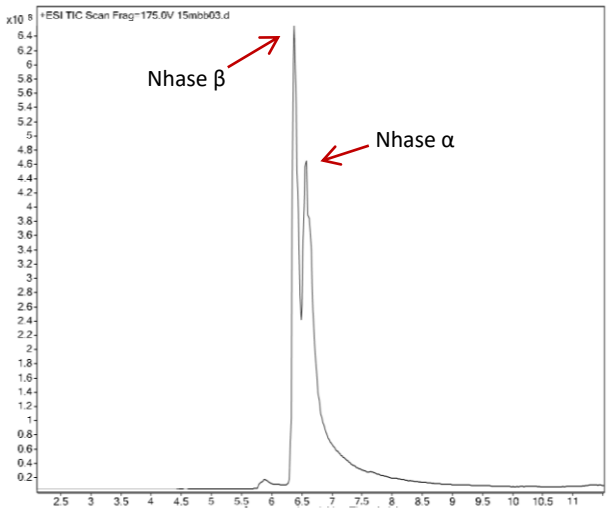

(a)

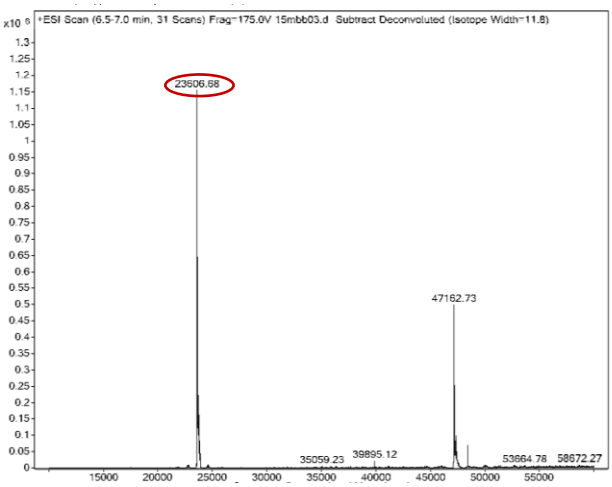

(b)

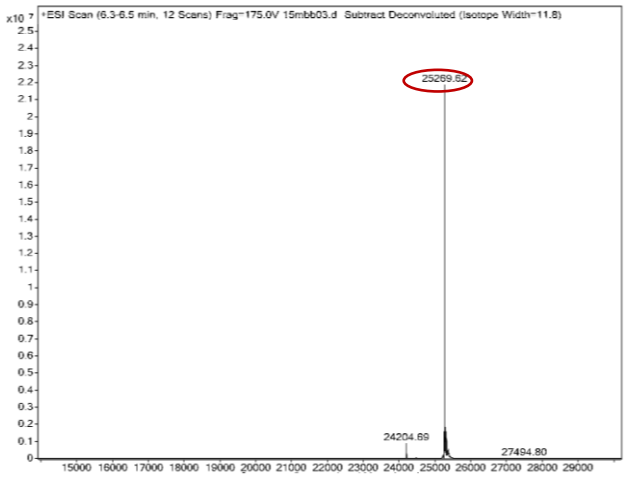

(c)

Figure 5.5 Mass spectrometry analysis of the molecular weight of NHas α-β. (a) two peaks of the two subunits α and β. (b) the highest peak with size 23.6 kDa similar to predicted molecular weight of α- subunit. (c) The highest peak with size 25.26 kDa similar to predicted molecular weight of β-subunit.the predicted MW was determined using Expasy software. The data is for a single batch of enzyme.

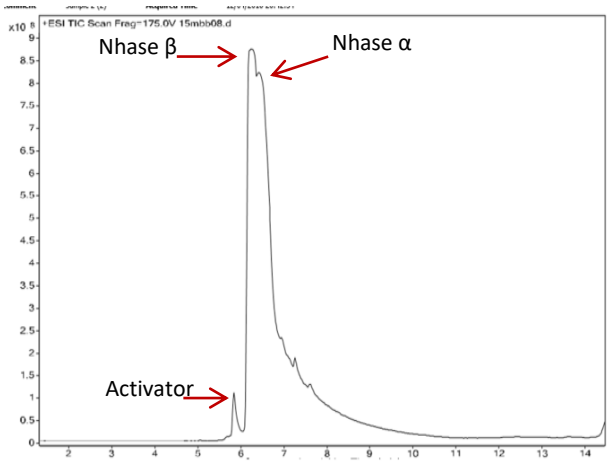

(a)

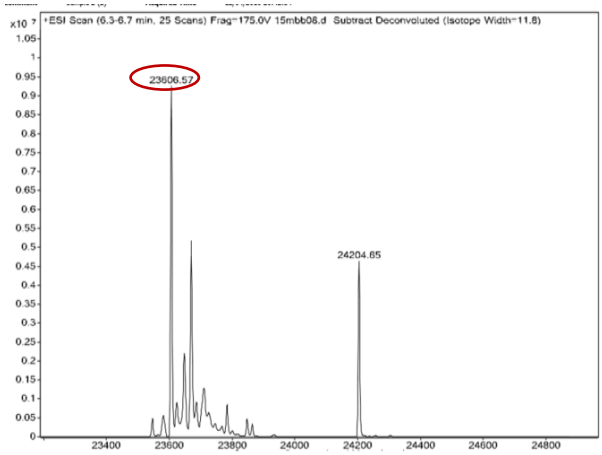

(b)

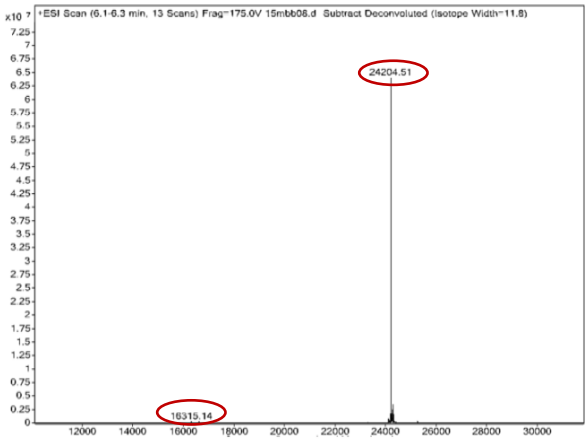

(c)

Figure 5.6 Mass spectrometry analysis of the molecular weight of NHase α-β-P14K (a) Three peaks of the two subunits α and β and P14K activator. (b) The highest peak with size 23.6 kDa similar to predicted molecular weight of α- subunit. (c) The highest peak with size 24.2 kDa similar to predicted molecular weight of β-subunit and a small peak at 16.3 kDa similar to predicted molecular weight of NHase activator P14K. The predicted MW was determined using Expasy software. The data is for a single batch of enzyme.

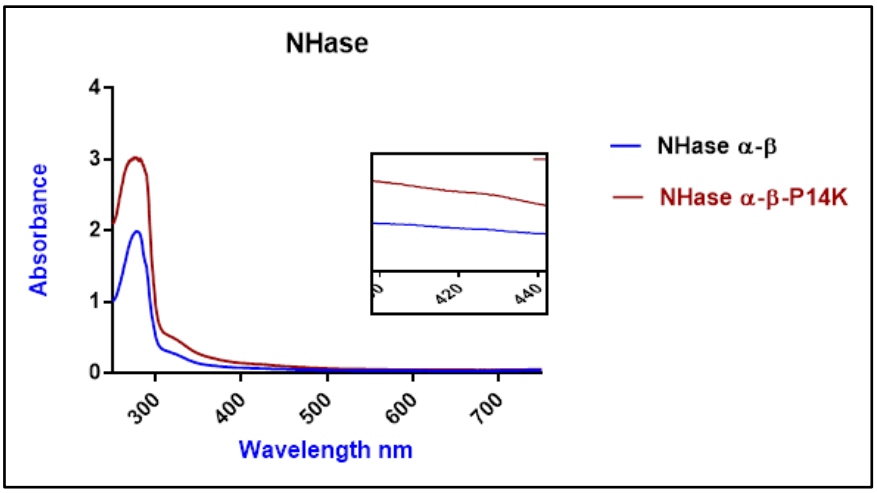

Figure 5.7 Absorption spectra of NHase α-β and NHase α-β-P14K. Blue and red lines represent the absorption spectra NHase α-β and NHase α-β-P14K respectively. The blue line sample contained 3 mg/ ml purified NHase α-β and the red line sample contained 28 mg/ ml purified NHase α-β- P14K both samples contained 50 mM Tris/HCl buffer pH 7.5, 0.5 mM DTT, 50 mM NaCl and 40 mM butyric acid pH 7.5 . The data of each sample are from single batch of enzyme.

Table 5.3 Metal analysis of NHase α-β and NHase α-β-P14K proteins by ICP-MS. The table showed the concentration in mg/l of Cobalt (Co), Copper (Cu), Zinc (Zn), Nickel (Ni) and Iron (Fe) for two samples. The NHase α-β sample contained 3 mg/ ml purified protein and the NHase α-β- P14K sample contained 28 mg/ ml purified NHase α-β- P14K both samples contained 50 mM Tris/HCl buffer pH 7.5 , 0.5 mM DTT, 50 mM NaCl and 40 mM butyric acid pH 7.5. The data of each sample are from single batch of enzyme

Protein	Co mg/l	Cu mg/l	Zn mg/l	Ni mg/l	Fe mg/l
NHase α-β	1.58	0.072	0.025	0.316	0.058
NHase α-β-P14K	24.9	0.113	0.105	1.56	0.294

However, the protein concentration in these samples were very different (only 3 mg/ml for the two subunit enzyme and 28 mg/ml for the three subunit enzyme), so this result is perhaps not so surprising. Nevertheless, as shown below, there is a difference in the protein: cobalt ratio in these protein preparations. Other metal concentration was also slightly affected when P14K was not present (Table 5.3). NHase proteins utilize cobalt as a cofactor for the enzymatic reaction. As the cofactor is essential for catalysis, the ratio (protein: cobalt) was determined. From the ICP-MS metal analysis results displayed the cobalt concentration in both NHase α-β and NHase α-β- P14K, while the protein concentration of both NHase was determined Bradford assay. Figure 5.8 showed the calculation of the ratio between cobalt and NHase α-β protein was estimated at ~0.5:1, therefore suggesting that 0.5 mol of cobalt binds to 1 mol of NHase α-β, while this ratio was ~1:1 in NHase α-β- P14K protein, thus 1 mol of cobalt binds to 1 mol of NHase α-β-P14K. This suggests that only 50% of the NHase α-β molecules have bound cobalt. This result illustrates the role of the P14K activator in the correct incorporation of cobalt into the enzyme.

5.2.4 Enzymatic assay of NHase α – β and NHase α – β- P14K

To determine the substrate activity spectrum of NHase with and without the activator from *R. palustris*, the activity of both purified enzymes was assayed spectrophotometrically by monitoring the amide formation from 6 different aliphatic and aromatic nitrile substrates (Figure 5.9) by monitoring the change in UV absorbance during this process (Figure 5.10 and 5.11).

This assay was specifically developed in this project as an alternative to the more commonly used HPLC and GC-MS methods, which require specialist equipment.

Cobalt Ratio in the protein:

1- NHase α - β

Cobalt MW 59 mg/ml= 1M

Cobalt in NHase α - β protein 0.0016 mg/ml= 0.00002712 M

Cobalt in NHase α - β protein = 27.12 µM

NHase α - β Protein concentration = 60 µM

NHase α - β Protein : Cobalt

60 µM : 27 µM ~ 1:0.5

2- NHase α-β - P14K activator

Cobalt MW 59 mg/ml= 1M

Cobalt in NHase α - β- P14K a protein 0.025 mg/ml= 0.0004237 M

Cobalt in NHase α - β- P14K protein = 423.7 µM

NHase α - β- P14K Protein concentration = 430 µM

NHase α - β- P14K Protein : Cobalt

430 µM : 423.7 µM ~ 1:1

Figure 5.8: Calculation of the NHase α- β and NHase α- β-P14Kprotein ratio to cobalt content in these proteins. The calculation of each enzyme is for a single batch of enzyme.

(a)Aromatic Nitriles:

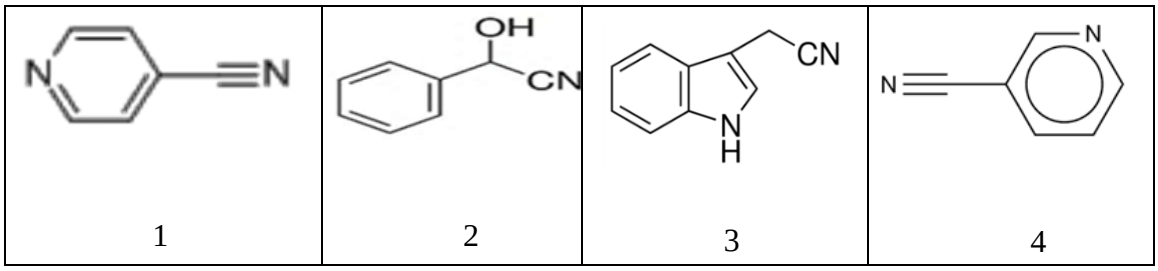

1 2 3 4

(b) Aliphatic Nitriles:

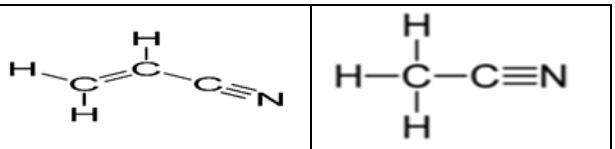

5 6

Figure 5.9 : Aromatic and aliphatic nitriles used to screen both NHase α- β and NHase α- β-P14K. (a) Aromatic Nitriles **(**1) 4-Cyanopyridine, (2) Mandelonitrile (3) 3-Indoleacetonitrile (4) Benzonitrile**.** (b) Aliphatic Nitriles (5) Acrylonitrile and (6)Acetonitrile.

The advantage is that the assay is easy to carry out using a standard recording spectrophotometer, but the disadvantage is the overlap between the absorption bands of the substrate and product and the protein itself (often around 280 nm). This was overcome to some extent by the use of a low concentration of enzyme and longer incubation periods to detect activity.

Each standard reaction mixture contained 0.5 mM DTT, 40 mM butyric acid, 0.1µM enzyme and 0.5 mM nitrile substrate. The assay was performed at 30°C in a final volume of 1 mL in quartz cuvettes. The assay baseline was set with the same reaction mixture but without substrate and the spectra were recorded between wavelengths 200 and 450 nm spectra were recorded between wavelengths 200 and 450 nm after 30, 60 120, 240 and 300 min incubation. Overall, NHase α – β and NHase α – β- P14K displayed activity with all tested aliphatic and aromatic nitrile substrates. Assays showed the highest activity of after 30, 60 120, 240 and 300 min incubation mixture but without substrate and the spectra were recorded between wavelengths 200 and 450 nm after 30, 60 120, 240 and 300 min incubation. Overall, NHase α – β and NHase α – β- P14K displayed activity with all tested aliphatic and aromatic nitrile substrates. Assays showed the highest activity of both enzymes with benzonitrile and the lowest activity was with mandelonitrile (Table 5.4).

NHase α – β- P14K showed ~ 100 % complete reaction with no remaining starting benzonitrile within 120 min while 60% formation of benzamide was recorded with NHase α – β after 120 min and 65% after 300 min (Figure 5.10c and Figure 5.11c) . A similar percentage of 90% conversion of 3-indoleacetonitrile to 3-indolacetamide was detected after 300 min with both enzymes (Figure 5.10a and 5.11a). In addition, 90% maximum possible acrylamide formation was recorded with NHase α – β- P14K and ~

60% of the acrylonitrile consumption was detected after 300 min (Figure 5.10f and 5.11f). Moreover, 77% and 66% of detectable nicotinamide was monitored after 300 min with NHase α – β- P14K and NHase α – β respectively (Figure 5.10b and 5.11b). 43% and 37% of acetonitrile hydration was observed after 300 min with NHase α – β and NHase α – β- P14K (Figure 5.10e and 5.11e) respectively. Furthermore, 38 % of mandelonitile conversion to mandelamide was detected with NHase without activator and half of this percentage was recorded with NHase with activator (Figure 5.10d and 5.11d).

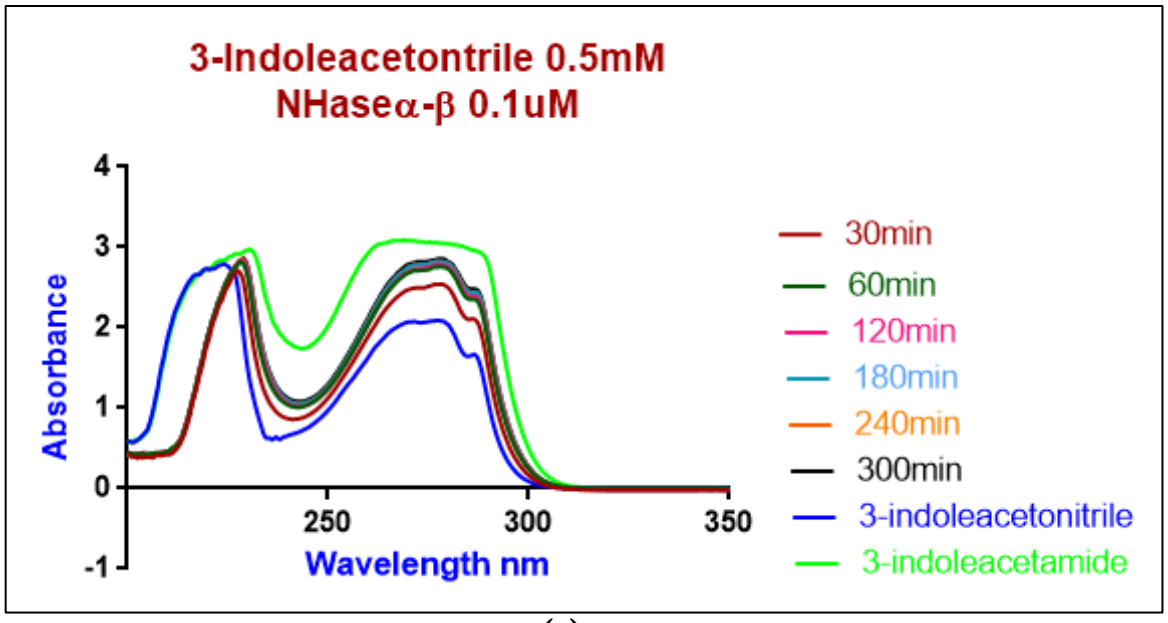
3-Indoleacetontrile 0.5mM
NHaseα-β 0.1uM
Absorbance
4
3
2
1
0
-1
250
300
350
Wavelength nm
30min
60min
120min
180min
240min
300min
3-indoleacetonitrile
3-indoleacetamide

(a)

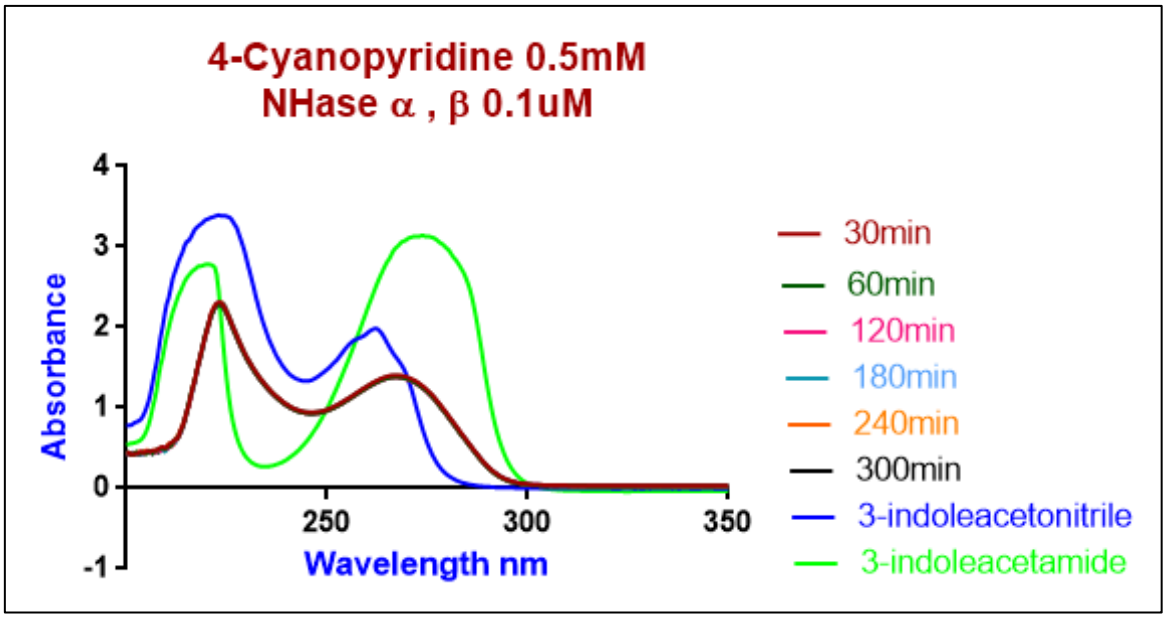
4-Cyanopyridine 0.5mM
NHase α , β 0.1uM
Absorbance
4
3
2
1
0
-1
250
300
350
Wavelength nm
30min
60min
120min
180min
240min
300min
3-indoleacetonitrile
3-indoleacetamide

(b)

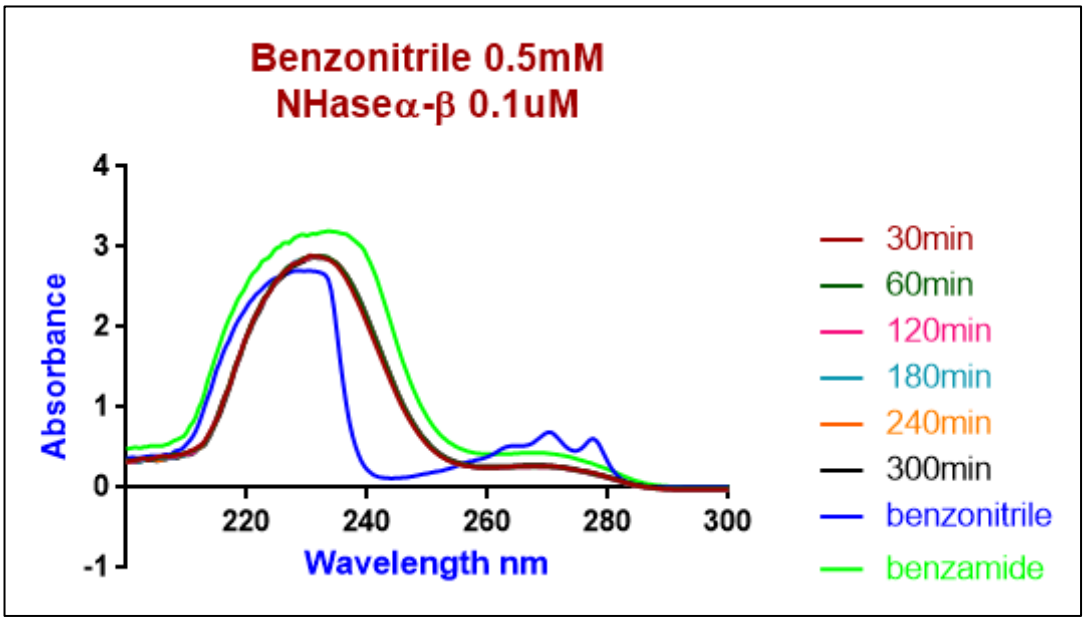
Benzonitrile 0.5mM
NHaseα-β 0.1uM
Absorbance
Wavelength nm
4
3
2
1
0
-1
220
240
260
280
300
30min
60min
120min
180min
240min
300min
benzonitrile
benzamide

(c)

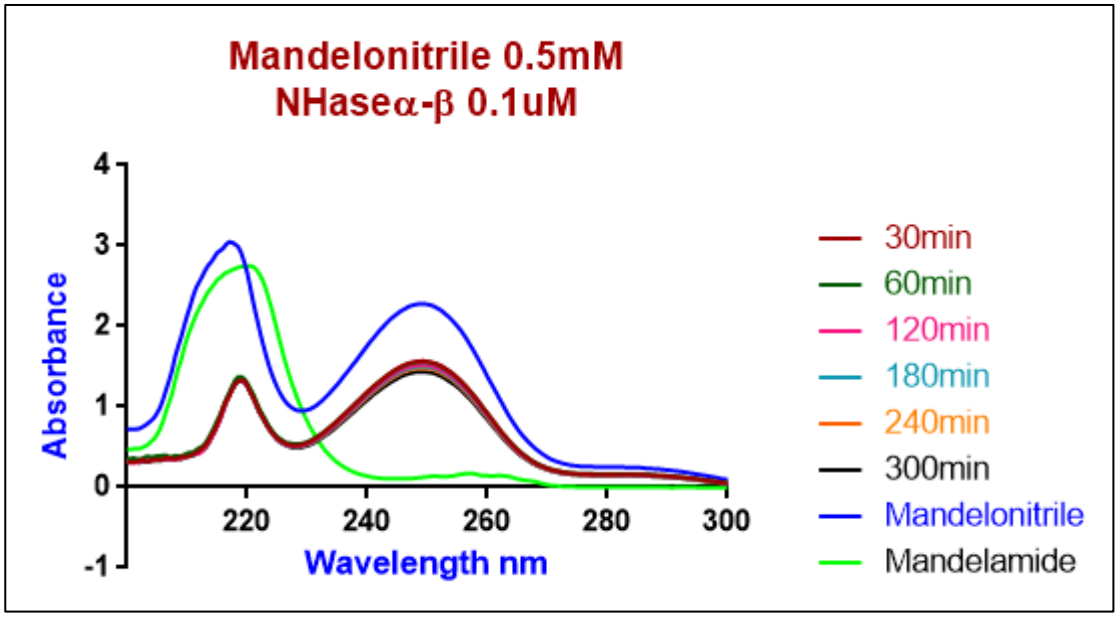
Mandelonitrile 0.5mM
NHaseα-β 0.1uM
Absorbance
Wavelength nm
4
3
2
1
0
-1
220
240
260
280
300
30min
60min
120min
180min
240min
300min
Mandelonitrile
Mandelamide

(d)

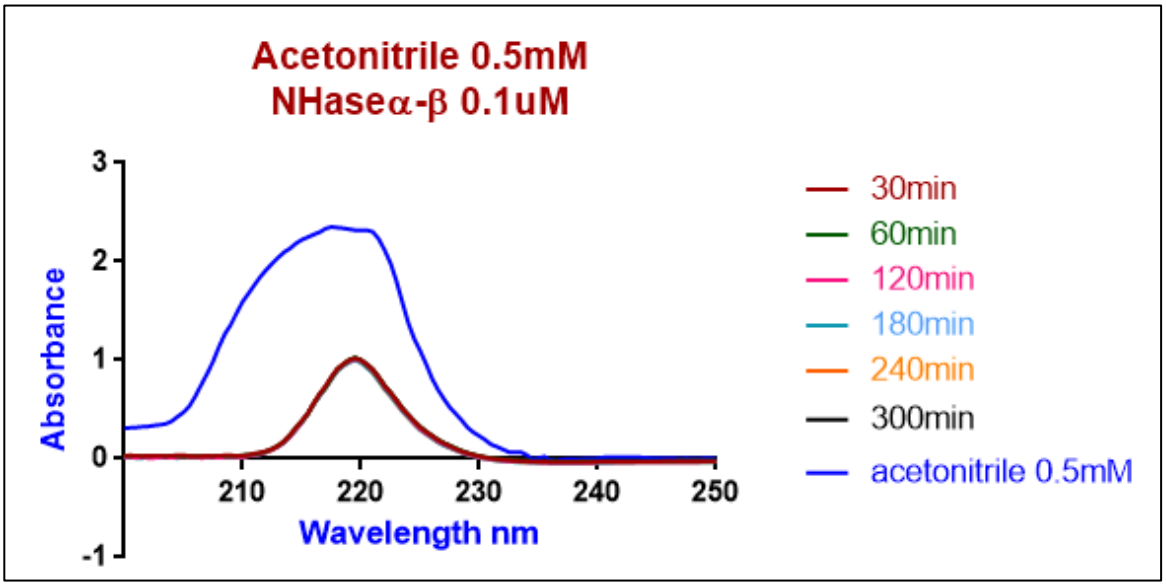

(e)

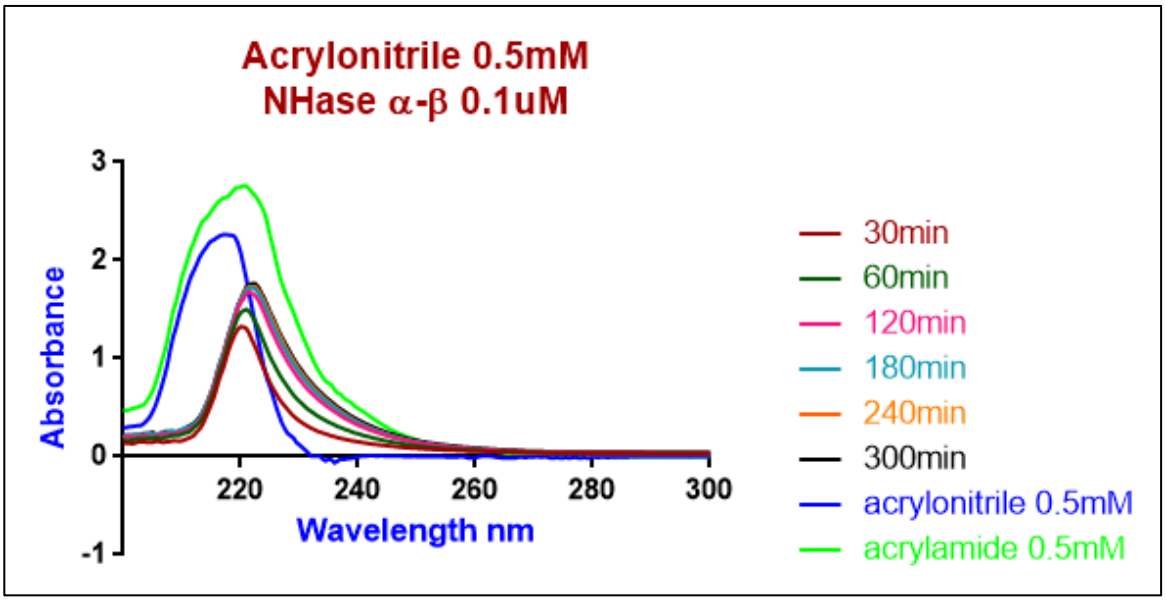

(f)

Figure 5.10: Nitrile substrates spectrum assay of NHaseα-β from *R. palustris*. Standard reaction mixture of 50mM Tris/HCl buffer pH7.5, 0.5 mM DTT, 40 mM butyric acid, 0.1 µM enzyme and reaction was started with 0.5 mM nitrile substrate (3-Indoleacetonitrile (a), 4-Cyanopyridine (b), Benzonitrile **(c)**, Mandelonitrile (d), Acetonitrile (e) and Acrylonitrile (f) spectrophotometry between 250-400 nm. The assay was conducted once for a single protein batch

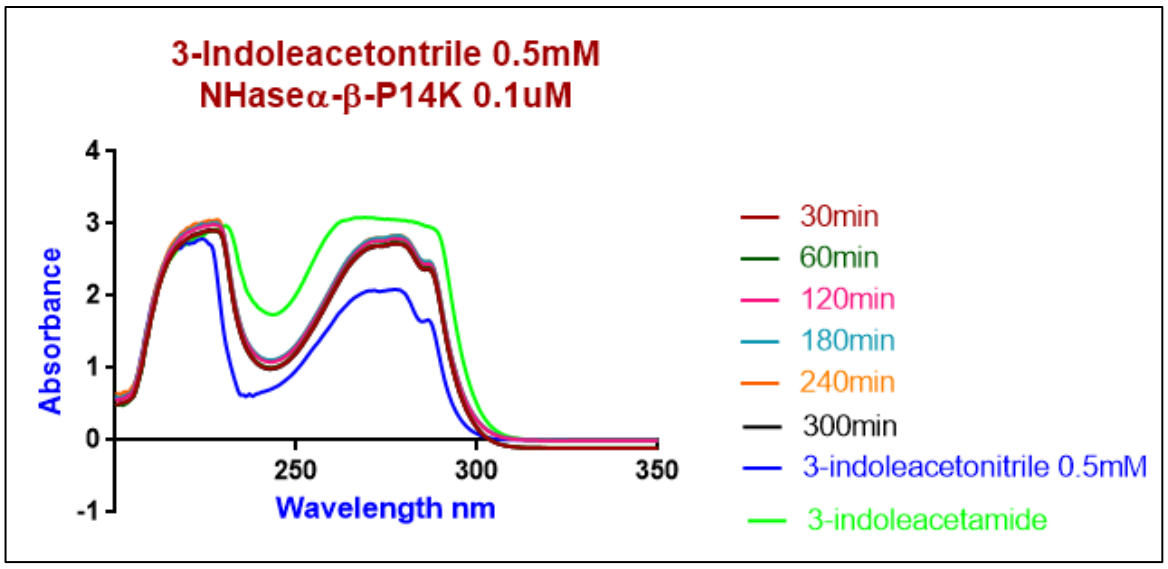
3-Indoleacetontrile 0.5mM
NHaseα-β-P14K 0.1uM
Absorbance
Wavelength nm
4
3
2
1
0
-1
250
300
350
30min
60min
120min
180min
240min
300min
3-indoleacetonitrile 0.5mM
3-indoleacetamide

(a)

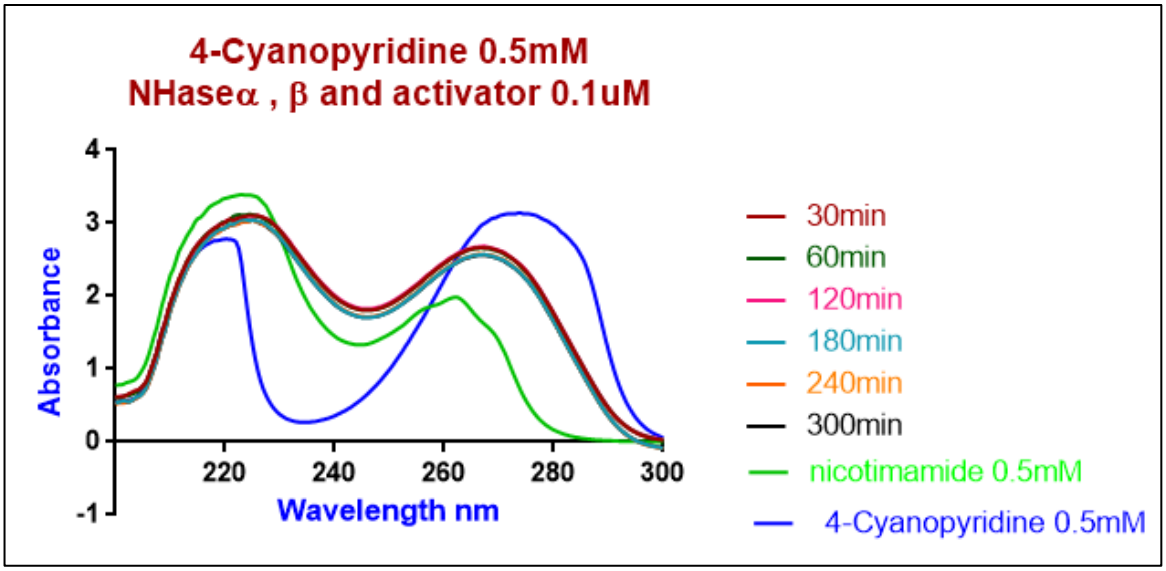
4-Cyanopyridine 0.5mM
NHaseα , β and activator 0.1uM
Absorbance
Wavelength nm
4
3
2
1
0
-1
220
240
260
280
300
30min
60min
120min
180min
240min
300min
nicotimamide 0.5mM
4-Cyanopyridine 0.5mM

(b)

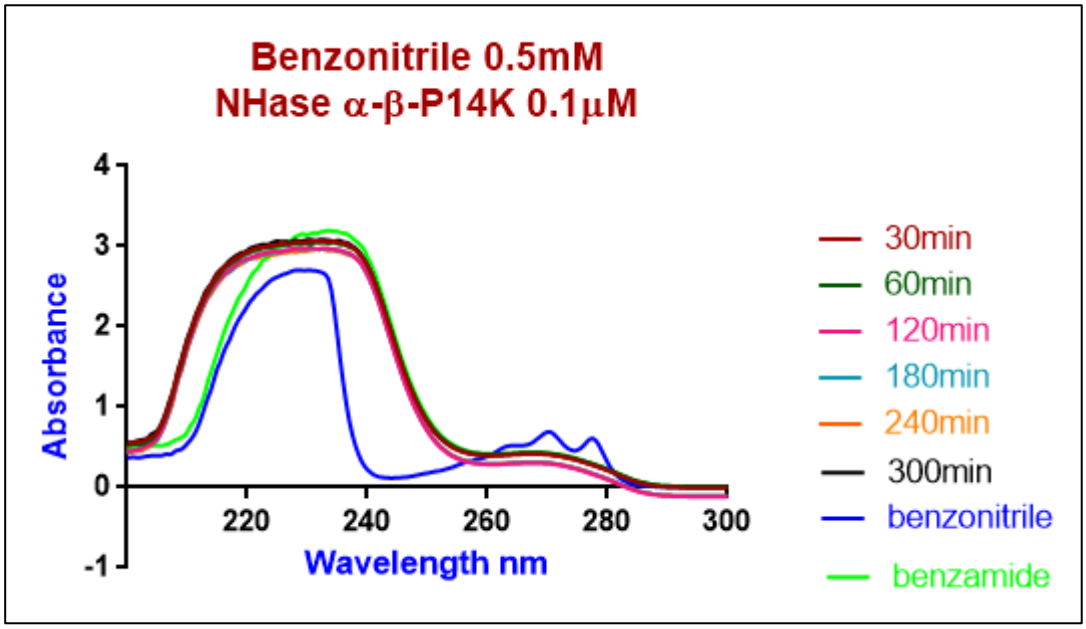
Benzonitrile 0.5mM
NHase α-β-P14K 0.1μM
Absorbance
Wavelength nm
30min
60min
120min
180min
240min
300min
benzonitrile
benzamide

(c)

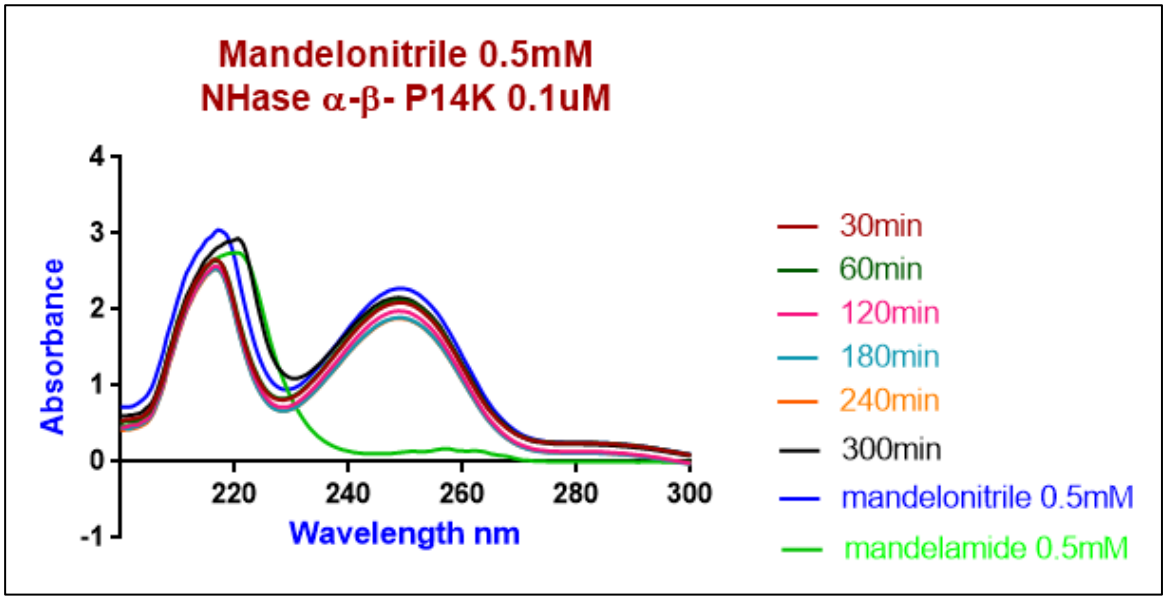
Mandelonitrile 0.5mM
NHase α-β- P14K 0.1uM
Absorbance
Wavelength nm
30min
60min
120min
180min
240min
300min
mandelonitrile 0.5mM
mandelamide 0.5mM

(d)

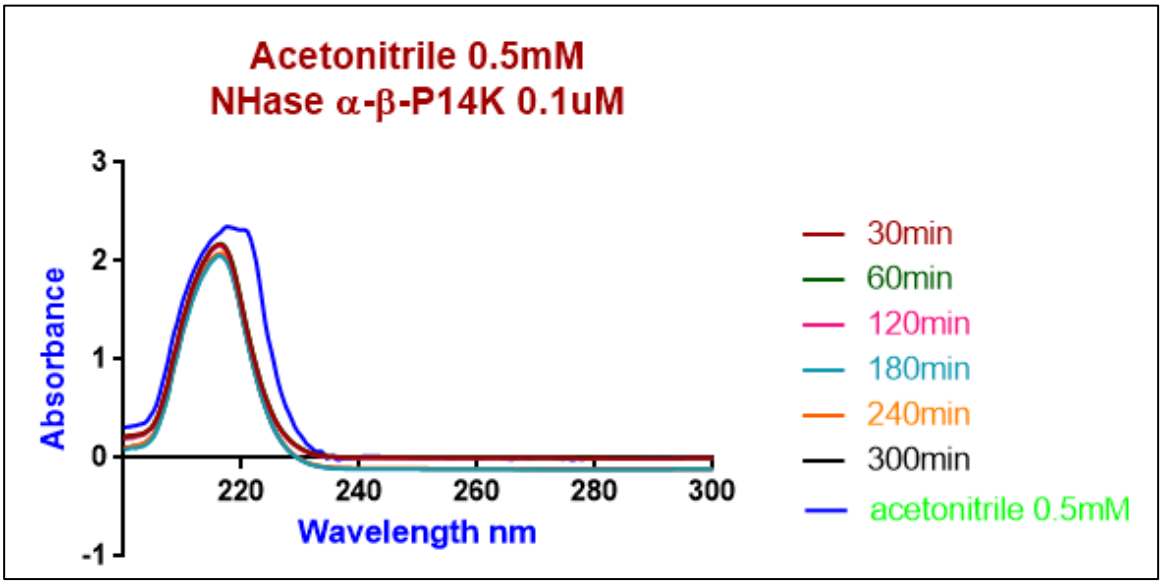

(e)

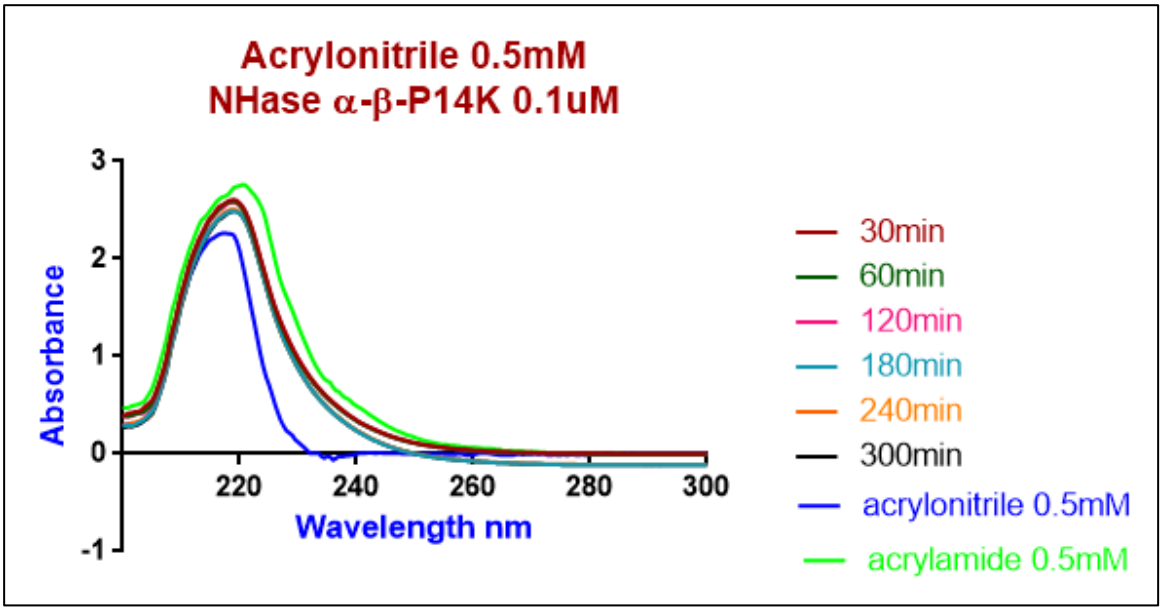

(f)

Figure 5.10: Nitrile substrates spectrum assay of NHaseα-β-P14K from *R. palustris*. Standard reaction mixture of 50mM Tris/HCl buffer pH7.5, 0.5 mM DTT, 40 mM butyric acid, 0.1 µM enzyme and reaction was started with 0.5 mM nitrile substrate (3-Indoleacetonitrile (a), 4-Cyanopyridine (b), Benzonitrile **(c)**, Mandelonitrile (d), Acetonitrile (e) and Acrylonitrile (f) spectrophotometry between 250-400 nm. The assay was conducted once for a single protein batch.

Table 5.4:The percentage of consumed nitriles and amides formation of spectrum analysis. The data shows the percentage of consumed nitrile in the reaction mixture of 50 mM Tris/HCl buffer pH7.5, 0.5 mM DTT, 40 mM butyric acid, 0.1 µM enzyme and reaction was started with 0.5 mM nitrile substrate spectrophotometry between 250-400 nm after 300 min in all substrate except benzonitrile after 120 min. Relative activity 100% was estimated as starting reaction mixtures without enzyme.

Nitriles	Nitrile consumed %	
	NHase α-β	NHase α-β-P14K
Mandelonitrile 257 nm	20 %	38 %
3-Indoleacetonitrile 270 nm	90 %	90 %
4-Cyanopyridine 262nm	66%	77 %
Benzonitrile 268 nm	60 %	100 %
Acrylonitrile 220 nm	58 %	90 %
Acetonitrile 220 nm	43%	37 %

5.3 Discussion:

The *R. palustris* genome codes for a 2 subunit nitrile hydratase α and β type protein, RPA2805 and RPA2806 and a putative nitrile hydratase activator RPA2807. NHase α-β from *R. palustris* has been previously identified and studied by (Black et al., 2010). The presence of an activator to enhance NHase activity in *R.palustris* was not addressed previously by Black et al. (2010) thus, putative nitrile hydratase activator sequence alignments using CLUSTAL W software were performed and the results showed that the percentage identity ranged from 25-36 % between the *R. palustris* NHase activator P14K and known nitrile hydratase activators from different bacteria such as *Bordetella petrii, Pseudomonas chlororaphis, Rhodococcus rhodochrous* and *Pseudomonas putida* (Table 5.1). RPA2807 is thus a good candidate to be the activator of the *R. palustris* Nhase and this was tested experimentally.

Two combinations of NHase genes *rpa2805-rpa2806* and *rpa2805-rpa2806-rpa2807* were successfully cloned into the pET21a(+) expression vector. The recombinant proteins from *R. palustris* were expressed in *E. coli* BL21 cells and purified by nickel affinity chromatography and the purified protein with the activator in this work was investigated to compare the substrate specificity of NHase α-β-P14K with the previous published work of (Black et al., 2010).

NHases consist of α- and β-subunits (Sun et al., 2016, Xia et al., 2016, Liu et al., 2014). The molecular weight of the α-subunit and β-subunit are usually less than 30 kDa, for exapmle those in *Bordetella petrii* DSM 12804 α-subunit and β-subunit 23.2 and 24.1 kDa respectively (Sun et al., 2016) and (α-subunit, 24.6 kDa and β-subunit, 26.5 kDa) in *Bacillus pallidus* RAPc8 (Cameron et al., 2005). The purified *R. palustris* NHase α-β enzyme showed two bands with molecular weights of approximately ~23.7 and~25

kDa confirming the presence of the α and β subunits. On the other hand, purified NHase α-β-P14K enzyme showed good expression of three distinct bands α, β and P14K at size ~23.7, ~24.2 and ~16.2 KDa respectively. Conversely, certain activators in *Bacillus pallidus* RAPc8 and *Pseudomonas putida* NRRL-18668 are hardly detectable in SDS-PAGE (Liu et al., 2013, Liu et al., 2014). Recently, the activator P14K from *Pseudomonas putida* was successfully expressed by fusing a strep tag on the N-terminal (Liu et al., 2014).

Co-NHase are different in gene organization and usually, the activator genes of Co-type NHase are 300–400 bp long and located downstream of the NHase genes (Cameron et al., 2005, Kataoka et al., 2006, Kim and Oriel, 2000). The NHase from *R. palustris* has the gene order <α-subunit><β-subunit><activator> and the coding sequences of the three genes overlap. This is typical for proteins where a 1:1:1 ratio of the subunits must be maintained. The NHase from *Pseudomonas putida* NRRL-18668 has the same gene order as *R. palustris* but it was difficult to detect the activator protein in SDS PAGE gels (Liu et al., 2013). On the other hand, in *Rhodococcus rhodochrous* J1 the gene order is < β-subunit><α-subunit><activator> (Zhou et al., 2008),while the gene order <α-subunit><activator>< β-subunit> found in *Rhodococcus jostii* RHA1 (Okamoto et al., 2010).

Both NHase α- β and NHase α-β-P14K were analyzed for metal content (Table 5.3) and the results showed the highest metal content was cobalt. The protein:cobalt ratio was found to be 1:0.5 and 1:1 in purified proteins NHase α- β and NHase α-β-P14K respectively. These results strongly suggested that the P14K activator from *R. palustris* promoted activity of nitrile hydratase α and β subunits by assisting the full incorporation of a cobalt ion into NHase α subunit. However, it was clear that the activator protein is

not absolutely essential for some cobalt incorporation to occur. In other bacteria, it has been stated that the P14K activator is essential for cobalt insertion into active site in the α-subunit. Thus, the P14K activator is crucial for the functional expression of NHase such as those containing cobalt in the active site as a cofactor from *Rhodococcus rhodochrous* J1 RHA1(Zhou et al., 2008) and *Pseudomonas putida* NRRL-18668 (Liu et al., 2014). However, there seem to be no studies where the activity of the 2 subunit versus 3 subunit enzyme has been directly compared.

A Spectrophotometric assay was used in this work to monitor the conversion of nitriles to amides by monitoring changes in the UV spectra of these compounds. It was found that the difference in spectral peaks between the nitrile and corresponding amide was sufficiently different to allow the progress of the reaction to be monitored. However, there were some issues due to the sensitivity of the spectrophotometric assay. We could only use around 0.5 mM substrate because of the high absorbance of these compounds in the UV region (i.e. high extinction coefficient), whereas with non-optical methods like HPLC, much higher starting substrate concentrations can be used (Kamble et al., 2013, Pérez et al., 2005, Black et al., 2010).

The results showed that all tested aromatic and aliphatic nitriles can be utilized by both NHase enzyme with or without activator and the summary results are shown in (Table 5. 4). Complete conversion ~100% of benzonitrile was utilized using NHase α-β-P14K and approximately half of this percentage was observed with NHase α-β after incubating the reaction mixtures for 2 hours, followed by 90% of 3-indoleacetonitrile was consumed by both enzymes. The lowest activity for both enzymes was detected with mandelonitrile .On the other hand , Black et al. (2010) showed that NHase α and β form

R. palustris can convert 99.9 % of nitriles containing a benzene or heterocyclic moiety by using Gas chromatography.

In conclusion, our results have shown that the presence of the activator protein seemingly had little influence on enzyme activity in terms of conversion of nitrile to amide, but it enhanced cobalt incorporation , However, further work is needed to confirm this and in particular it was difficult in this work to measure actual rates of amide formation. Ideally the rates of enzyme activity with different substrates with and without the activator protein need to be compared.

CHAPTER 6

CONCLUSIONS AND FUTURE WORK

6 Conclusions and future work

In the work described in this thesis, the proteins involved in nitroaromatic and aromatic nitrile compounds degradation pathways were identified and charactrerised in the photosynthetic bacterium *Rhodopseudomonas palustris*. In 2004 when the *R. palustris* strain CGA009 genome was sequenced, its annotated genes were shown to code for 6 possible nitroreductase enzymes, 4 nitrilases and 1 nitrile hydratase. These enzymes are involved in the breakdown of compounds containing a nitro group in nitroaromatic or containing -CN group in nitriles. In the present work, the genes were cloned and proteins were purified and analyzed biochemically to assess their activity *in vitro*. Only 2 out of the 6 nitroreductases could be studied in detail, and it was apparent that these had a very limited substrate specificity. Both RPA1711 and RPA4285 activity were analyzed biochemically and their activity was significant only with 2,4-DNT and 2,6 DNT with RPA1711 showing 2 times higher activity than RPA4285. These enzymes are thus unlikely to be of future use for biotransformations or detoxification, unless their substrate range can be enhanced, e.g. by site-directed mutagenesis to change the active site residues. This will require the crystal structures of these enzymes to be obtained. This is a future goal and is possible now that conditions for their over-production and purification have been developed in this study. The other nitroreductases should also be purified in future work to see if they have a broader substrate range than RPA1711 and RPA4285.

Aliphatic and aromatic nitriles are hydrolyzed by two different pathways. Nitriles are directly hydrolyzed to carboxylic acid and ammonia by nitrilases (Kobayashi and Shimizu, 1994). On the other hand, nitriles are utilized by nitrile hydratase to produce amides that would be then hydrolyzed to carboxylic acid by amidases (Komeda et al., 1996b; Kobayashi and Shimizu, 1998). The 4 different nitrilases RPA0599, RPA1563,

RPA2416 and RPA4166 were cloned and purified. Their activities investigated mainly by ammonia detection using 3 different methods. The GDH continuous assay was un-successful in this study, due to colour interference, concentration limitation and ammonia interference from the GDH stock. If these issues can be overcome then this would be an ideal assay as it the only one that offers a continuous measurement or rate. All of the other methods in the literature based on other ammonia assays or HPLC are discontinuous. The second method used here, the Berthelot method (phenol assay) was very difficult and impractical and such difficulty was reflected in the results as no variation between tested compound was recorded (Xue et al., 2016, Weatherburn, 1967). The last method used was the OPA method which was more sensitive and high enzymatic activity was recorded with the aromatic nitrile 4-cyanopyridine for RPA4166, RPA1563 and RPA0599. This method was easier and more sensitive because small variations were recorded between different nitrile compounds tested and both aliphatic and aromatic compounds were utilized by purified enzymes. Future work should focus on improving the available assays for these nitrilases, particularly in developing continuous coupled assays for example.

Finally, a nitrile hydratase with its activator was cloned and purified from *R. palustris* (NHase α-β-P14K) and the metal content was found to be higher than the purified enzyme without the activator. Such results indicated that cobalt integration is assisted by the activator and hence enhanced activity of nitrile hydratase. But on the other hand in-vitro analyses for enzyme kinetics suggest that the presence of the activator did not enhance enzyme kinetics and both NHase α-β-P14K and NHase α-β utilize aliphatic and aromatic nitriles. However, we used a spectrophotemetric assay here for convenience, but there were several problems with this in terms of spectral overlap and further work with better assays would be useful to fully explore the differences in the

activity and substrate range of the enzyme with and without the activator. Many nitrile degrading microorganisims possess either NHase/amidase or nitrilase activity even if the two systems are present in the microorganism only one enzyme system would be functional for specific nitrile compound (Fang et al., 2015). In future work HPLC could be used to analyze nitrilase activity in more detail and to understand the degradation pathway. We did not explore amidase activities in *R. palustris* and this is also worth studying in parallel with nitrile hydratase studies. In addition, the question of how nitriles are transported into the cell is completely unknown. Several of the nitrilases studied here are encoded in gene clusters with associated ABC transporters. Although not reported in this thesis, the periplasmic binding-proteins of three of these were cloned and purified but we failed to demonstrate the binding of any nitrile to any of these proteins.

The presence of nitro-aromatic and aromatic nitriles contaminants in nature are usually accompanied by the presence of other simpler substrates that could also be utilized alongside these compounds and hence enhance their degradation *in vivo* (Shin and Crawford, 1995). While *in vitro* the utilization of nitro-aromatic or aromatic nitriles was carried out in ways which may contribute to the low activity and low substrate range recorded. *Clostridium* sp showed the ability to degrade TNT but the degradation of TNT required a co-substrate which provides the reducing power to remove the nitro group in nature (Shin and Crawford, 1995). On the other hand, *Desulfovibrio sp.* utilizes TNT by using it as a nitrogen source while using pyruvate as a carbon and energy source (Preuß and Rieger, 1995). Similar findings were recorded in this study where nitriles were not utilized as a carbon source and only benzoate was utilized.

In conclusion, the work described in this thesis has highlighted the problems associated with expressing and assaying recombinant enzymes for substrates that are

difficult to study but has contributed to knowledge about the degradative abilities of *R. palustris* for nitro and nitrile compounds.

REFERENCES

References

AGARWAL, A., NIGAM, V. K. & VIDYARTHI, A. S. 2012. Nitrilases – an attractive nitrile degrading biocatalyst *International Journal of Pharma and Bio Sciences* 3**,** 232 - 246

ALEXIEVAB, Z., GERGINOVAB, M., ZLATEVAA, P., MANASIEVB, J., IVANOVAC, D. & DIMOVAA, N. 2008. Monitoring of aromatic pollutants biodegradation. *Biochemical Engineering Journal,* 40**,** 233–240.

AUSTIN, S., KONTUR, W. S., ULBRICH, A., OSHLAG, J. Z., ZHANG, W., HIGBEE, A., ZHANG, Y., COON, J. J., HODGE, D. B., DONOHUE, T. J. & NOGUERA, D. R. 2015. Metabolism of Multiple Aromatic Compounds in Corn Stover Hydrolysate by *Rhodopseudomonas palustris*. *Environmental Science & Technology,* 49**,** 8914-8922.

BANERJEE, A., SHARMA, R. & BANERJEE, U. C. 2002. The nitrile-degrading enzymes: current status and future prospects. *Appl Microbiol Biotechnol,* 60.

BANG, S. Y., KIM, J. H., LEE, P. Y., BAE, K. H., LEE, J. S., KIM, P. S., LEE DO, H., MYUNG, P. K., PARK, B. C. & PARK, S. G. 2012. Confirmation of Frm2 as a novel nitroreductase in *Saccharomyces cerevisiae*. *Biochem Biophys Res Commun,* 423**,** 638-41.

BAYER, S., BIRKEMEYER, C. & BALLSCHMITER, M. 2011. A nitrilase from a metagenomic library acts regioselectively on aliphatic dinitriles. *Appl Microbiol Biotechnol,* 89**,** 91-8.

BELLINZONI, M., BURONI, S., PASCA, M. R., GUGLIERAME, P., ARCESI, F., DE ROSSI, E. & RICCARDI, G. 2005. Glutamine amidotransferase activity of NAD+ synthetase from *Mycobacterium tuberculosis* depends on an amino-terminal nitrilase domain. *Research in Microbiology,* 156**,** 173-177.

BENNER, R., MACCUBBIN, A. E. & HODSON, R. E. 1984. Anaerobic biodegradation of the lignin and polysaccharide components of lignocellulose and synthetic lignin by sediment microflora. *Appl Environ Microbiol,* 47**,** 998-1004.

BHALLA, T. C., SHARMA, M. & BHATIA, R. K. 2012. Microbial degradation of Cyanides and Nitriles. *In:* SATYANARAYANA, T., JOHRI, B. N. & PRAKASH, A. (eds.) *Microorganisms in Environmental Management: Microbes and Environment.* Springer Netherlands.

BLACK, G. W., BROWN, N. L., PERRY, J. J., RANDALL, P. D., TURNBULL, G. & ZHANG, M. 2015. A high-throughput screening method for determining the substrate scope of nitrilases. *Chem Commun (Camb),* 51**,** 2660-2.

BLACK, G. W., GREGSON, T., MCPAKE, C. B., PERRY, J. J. & ZHANG, M. 2010. Biotransformation of nitriles using the solvent-tolerant nitrile hydratase from *Rhodopseudomonas palustris* CGA009. *Tetrahedron Letters,* 51**,** 1639-1641.

BLASCO, R. & CASTILLO, F. 1993. Characterization of a nitrophenol reductase from the phototrophic bacterium *Rhodobacter capsulatus* E1F1. *Applied and Environmental Microbiology,* 59**,** 1774-1778.

BORK, P. & KOONIN, E. V. 1994. A new family of carbon-nitrogen hydrolases. *Protein Sci,* 3**,** 1344-6.

BRADFORD, M. M. 1976. A rapid and sensitive method for the quantitation of microgram quantities of protein utilizing the principle of protein-dye binding. *Anal Biochem,* 72**,** 248-54.

BRYANT, D. W., MCCALLA, D. R., LEEKSMA, M. & LANEUVILLE, P. 1981. Type I nitroreductases of *Escherichia coli*. *Can J Microbiol,* 27**,** 81-6.

BUTLER, C. S. & MASON, J. R. 1997. Structure-function analysis of the bacterial aromatic ring-hydroxylating dioxygenases. *Adv Microb Physiol,* 38**,** 47-84.

CABALLERO, A., LAZARO, J. J., RAMOS, J. L. & ESTEVE-NUNEZ, A. 2005. PnrA, a new nitroreductase-family enzyme in the TNT-degrading strain *Pseudomonas putida* JLR11. *Environ Microbiol,* 7**,** 1211-9.

CAMERON, R. A., SAYED, M. & COWAN, D. A. 2005. Molecular analysis of the nitrile catabolism operon of the thermophile *Bacillus pallidus* RAPc8. *Biochim Biophys Acta,* 1725**,** 35-46.

CANALA-ECHVARRIA, F. A. 2010. *Degradation of polycyclic aromatic hydrocarbons by the whiterot fungus Anthracophyllum discolor Sp4 and nanoclayimmobilized manganese peroxidase.* Doctor of Sciences in Natural Resources, Universidad de La Frontera.

CARMONA, M., ZAMARRO, M. T., BLAZQUEZ, B., DURANTE-RODRIGUEZ, G., JUAREZ, J. F., VALDERRAMA, J. A., BARRAGAN, M. J., GARCIA, J. L. & DIAZ, E. 2009. Anaerobic catabolism of aromatic compounds: a genetic and genomic view. *Microbiol Mol Biol Rev,* 73**,** 71-133.

CHARAN, R. D., SCHLINGMANN, G., BERNAN, V. S., FENG, X. & CARTER, G. T. 2006. Dioxapyrrolomycin biosynthesis in *Streptomyces fumanus*. *J Nat Prod,* 69**,** 29-33.

CHAUHAN, S., WU, S., BLUMERMAN, S., FALLON, R. D., GAVAGAN, J. E., DICOSIMO, R. & PAYNE, M. S. 2003. Purification, cloning, sequencing and over-expression in *Escherichia coli* of a regioselective aliphatic nitrilase from Acidovorax facilis 72W. *Appl Microbiol Biotechnol,* 61.

CHO, Y.-S., LEE, B.-U. & OH, K.-H. 2008. Simultaneous degradation of nitroaromatic compounds TNT, RDX, atrazine, and simazine by *Pseudomonas putida* HK-6 in bench-scale bioreactors. *Journal of Chemical Technology & Biotechnology,* 83**,** 1211-1217.

DE OLIVEIRA, I. M., HENRIQUES, J. A. & BONATTO, D. 2007. In silico identification of a new group of specific bacterial and fungal nitroreductases-like proteins. *Biochem Biophys Res Commun,* 355**,** 919-25.

DE OLIVEIRA, I. M., ZANOTTO-FILHO, A., MOREIRA, J. C., BONATTO, D. & HENRIQUES, J. A. 2010a. The role of two putative nitroreductases, Frm2p and Hbn1p, in the oxidative stress response in *Saccharomyces cerevisiae*. *Yeast,* 27**,** 89-102.

DE OLIVEIRA, L. M., BONATTO, D. & HENRIQUES, J. A. 2010b. Nitroreductases: Enzymes with Environmental, Biotechnological and Clinical Importance *Current Research, Technology and Education*

Topics in Applied Microbiology and Microbial Biotechnology Spain: FORMATEX

DIAZ, E., FERRANDEZ, A., PRIETO, M. A. & GARCIA, J. L. 2001. Biodegradation of aromatic compounds by *Escherichia coli*. *Microbiol Mol Biol Rev,* 65**,** 523-69, table of contents.

DÍAZ, E., JIMÉNEZ, J. I. & NOGALES, J. 2013. Aerobic degradation of aromatic compounds. *Current Opinion in Biotechnology,* 24**,** 431-442.

DUTTON, P. L. & EVANS, W. C. 1969. The metabolism of aromatic compounds by *Rhodopseudomonas palustris.* A new, reductive, method of aromatic ring metabolism. *Biochem J,* 113**,** 525-36.

EHRLICH, J., GOTTLIEB, D., BURKHOLDER, P. R., ANDERSON, L. E. & PRIDHAM, T. G. 1948. *Streptomyces venezuelae*, N. Sp., the Source of Chloromycetin. *Journal of Bacteriology,* 56**,** 467-477.

EISLER, R. 1991. Cyanide Hazards to Fish, Wildlife, and Invertebrates: A Synoptic Review. *Contaminant Hazard Reviews.* Laurel, MD.

EMPTAGE, C. D., KNOX, R. J., DANSON, M. J. & HOUGH, D. W. 2009. Nitroreductase from *Bacillus licheniformis*: a stable enzyme for prodrug activation. *Biochem Pharmacol,* 77**,** 21-9.

FANG, S., AN, X., LIU, H., CHENG, Y., HOU, N., FENG, L., HUANG, X. & LI, C. 2015. Enzymatic degradation of aliphatic nitriles by *Rhodococcus rhodochrous* BX2, a versatile nitrile-degrading bacterium. *Bioresource Technology,* 185**,** 28-34.

FITZPATRICK, T. B., AMRHEIN, N. & MACHEROUX, P. 2003. Characterization of YqjM, an Old Yellow Enzyme Homolog from *Bacillus subtilis* Involved in the Oxidative Stress Response. *Journal of Biological Chemistry,* 278**,** 19891-19897.

FLETCHER, J. H., HAMILTON, J. C., HECHENBLEIKNER, I., HOEGBERG, E. I., SERTL, B. J. & CASSADAY, J. T. 1950. The Synthesis of Parathion and Some Closely Related Compounds. *Journal of the American Chemical Society,* 72**,** 2461-2464.

FUCHS, G. 2008. Anaerobic metabolism of aromatic compounds. *Ann N Y Acad Sci,* 1125**,** 82-99.

FUCHS, G., BOLL, M. & HEIDER, J. 2011. Microbial degradation of aromatic compounds - from one strategy to four. *Nat Rev Microbiol,* 9**,** 803-16.

GALL, D. L., RALPH, J., DONOHUE, T. J. & NOGUERA, D. R. 2013. Benzoyl coenzyme a pathway-mediated metabolism of meta-hydroxy-aromatic acids in *Rhodopseudomonas palustris. J Bacteriol,* 195**,** 4112-20.

GONG, J.-S., LU, Z.-M., LI, H., SHI, J.-S., ZHOU, Z.-M. & XU, Z.-H. 2012. Nitrilases in nitrile biocatalysis: recent progress and forthcoming research. *Microbial Cell Factories,* 11**,** 1-18.

GUILLEN, H., CURIEL, J. A., LANDETE, J. M., MUÑOZ, R. & HERRAIZ, T. 2009. Characterization of a nitroreductase with selective nitroreduction properties in the food- and intestinal-occurring lactic acid bacterium *Lactobacillus plantarum* WCFS1. *Agricultural and Food Chemistry,* 57(21)**,** 10457–10465.

GUZMAN, L. M., BELIN, D., CARSON, M. J. & BECKWITH, J. 1995. Tight regulation, modulation, and high-level expression by vectors containing the arabinose PBAD promoter. *J Bacteriol,* 177**,** 4121-30.

HANAHAN, D. 1983. Studies on transformation of *Escherichia coli* with plasmids. *J Mol Biol,* 166**,** 557-80.

HARRISON, F. H. & HARWOOD, C. S. 2005. The pimFABCDE operon from *Rhodopseudomonas palustris* mediates dicarboxylic acid degradation and participates in anaerobic benzoate degradation. *Microbiology,* 151**,** 727-36.

HARWOOD, C. S. & GIBSON, J. 1988. Anaerobic and aerobic metabolism of diverse aromatic compounds by the photosynthetic bacterium *Rhodopseudomonas palustris*. *Appl Environ Microbiol,* 54**,** 712-7.

HASHIMOTO, Y., NISHIYAMA, M., HORINOUCHI, S. & BEPPU, T. 1994. Nitrile hydratase gene from *Rhodococcus* sp. N-774 requirement for its downstream region for efficient expression. *Biosci Biotechnol Biochem,* 58**,** 1859-65.

HAYNES, C. A., KODER, R. L., MILLER, A. F. & RODGERS, D. W. 2002. Structures of nitroreductase in three states: effects of inhibitor binding and reduction. *J Biol Chem,* 277**,** 11513-20.

HEIDER, J. & FUCHS, G. 1997. Anaerobic metabolism of aromatic compounds. *Eur J Biochem,* 243**,** 577-96.

HEINEMANN, U., ENGELS, D., BURGER, S., KIZIAK, C., MATTES, R. & STOLZ, A. 2003. Cloning of a Nitrilase Gene from the Cyanobacterium *Synechocystis* sp. Strain PCC6803 and Heterologous Expression and Characterization of the Encoded Protein. *Applied and Environmental Microbiology,* 69**,** 4359-4366.

HONGWEI, Y., ZHANPENG, J. & SHAOQI, S. 2006. Aromatic compounds biodegradation under anaerobic conditions and their QSBR models. *Science of The Total Environment,* 358**,** 265–276.

HOWDEN, A. J., HARRISON, C. J. & PRESTON, G. M. 2009. A conserved mechanism for nitrile metabolism in bacteria and plants. *Plant J,* 57**,** 243-53.

JIM, C. 2000. *The names of aromatic compounds* [Online]. UK. Available: http://www.chemguide.co.uk/basicorg/conventions/names3.html [Accessed].

JU, K. S. & PARALES, R. E. 2010. Nitroaromatic Compounds, from Synthesis to Biodegradation. *Microbiology and Molecular Biology Reviews : MMBR,* 74**,** 250-272.

KABAIVANOVA, L., DIMITROV, P., BOYADZHIEVA, I., ENGIBAROV, S., DOBREVA, E. & EMANUILOVA, E. 2008. Nitrile degradation by free and immobilized cells of the thermophile *Bacillus* sp. UG-5B, isolated from polluted industrial waters. *World Journal of Microbiology and Biotechnology,* 24**,** 2383-2388.

KAMBLE, A. L., BANOTH, L., MEENA, V. S., SINGH, A., CHISTI, Y. & BANERJEE, U. C. 2013. Nitrile hydratase of *Rhodococcus erythropolis:* characterization of the enzyme and the use of whole cells for biotransformation of nitriles. *3 Biotech,* 3**,** 319-330.

KAPLAN, O., VEJVODA, V., PLÍHAL, O., POMPACH, P., KAVAN, D., BOJAROVÁ, P., BEZOUŠKA, K., MACKOVÁ, M., CANTARELLA, M., JIRKŮ, V., KŘEN, V. & MARTÍNKOVÁ, L. 2006. Purification and characterization of a nitrilase from *Aspergillus niger* K10. *Appl Microbiol Biotechnol,* 73.

KATAOKA, S., ARAKAWA, T., HORI, S., KATAYAMA, Y., HARA, Y., MATSUSHITA, Y., NAKAYAMA, H., YOHDA, M., NYUNOYA, H., DOHMAE, N., MAEDA, M. & ODAKA, M. 2006. Functional expression of thiocyanate hydrolase is promoted by its activator protein, P15K. *FEBS Letters,* 580**,** 4667-4672.

KAUL, P., BANERJEE, A. & BANERJEE, U. C. 2007. Oxidoreductases and other enzymes of diverse function. *In:* POLAINA, J. & MACCABE, A. P. (eds.) *Industrial enzymes : structure, function, and applications.* Dordrecht: Springer.

KIM, J.-S., TIWARI, M. K., MOON, H.-J., JEYA, M., RAMU, T., OH, D.-K., KIM, I.-W. & LEE, J.-K. 2009. Identification and characterization of a novel nitrilase from *Pseudomonas fluorescens* Pf-5. *Applied Microbiology and Biotechnology,* 83**,** 273-283.

KIM, S.-H. & ORIEL, P. 2000. Cloning and expression of the nitrile hydratase and amidase genes from *Bacillus* sp. BR449 into Escherichia coli. *Enzyme and Microbial Technology,* 27**,** 492-501.

KIVISAAR, M. 2011. Evolution of catabolic pathways and their regulatory systems in synthetic nitroaromatic compounds degrading bacteria. *Mol Microbiol,* 82**,** 265-8.

KIZIAK, C., CONRADT, D., STOLZ, A., MATTES, R. & KLEIN, J. 2005. Nitrilase from *Pseudomonas fluorescens* EBC191: cloning and heterologous expression of the gene and biochemical characterization of the recombinant enzyme. *Microbiology,* 151**,** 3639-48.

KOBAYASHI, M. & SHIMIZU, S. 1998. Metalloenzyme nitrile hydratase: structure, regulation, and application to biotechnology. *Nat Biotechnol,* 16**,** 733-6.

KOBAYASHI, M., YANAKA, N., NAGASAWA, T. & YAMADA, H. 1990. Monohydrolysis of an aliphatic dinitrile compound by nitrilase from r*hodococcus rhodochrous* k22. *Tetrahedron,* 46**,** 5587-5590.

KOBORI, T., SASAKI, H., LEE, W. C., ZENNO, S., SAIGO, K., MURPHY, M. E. & TANOKURA, M. 2001. Structure and site-directed mutagenesis of a flavoprotein from *Escherichia coli* that reduces nitrocompounds: alteration of pyridine nucleotide binding by a single amino acid substitution. *J Biol Chem,* 276**,** 2816-23.

KOCH, J., EISENREICH, W., BACHER, A. & FUCHS, G. 1993. Products of enzymatic reduction of benzoyl-CoA, a key reaction in anaerobic aromatic metabolism. *Eur J Biochem,* 211**,** 649-61.

LARIMER, F. W., CHAIN, P., HAUSER, L., LAMERDIN, J., MALFATTI, S., DO, L., LAND, M. L., PELLETIER, D. A., BEATTY, J. T., LANG, A. S., TABITA, F. R., GIBSON, J. L., HANSON, T. E., BOBST, C., TORRES, J. L., PERES, C., HARRISON, F. H., GIBSON, J. & HARWOOD, C. S. 2004. Complete genome sequence of the metabolically versatile photosynthetic bacterium *Rhodopseudomonas palustris*. *Nat Biotech,* 22**,** 55-61.

LAYH, N., STOLZ, A., BÖHME, J., EFFENBERGER, F. & KNACKMUSS, H.-J. 1994. Enantioselective hydrolysis of racemic naproxen nitrile and naproxen amide to S-naproxen by new bacterial isolates. *Journal of Biotechnology,* 33**,** 175-182.

LIANG, B., CHENG, H.-Y., KONG, D.-Y., GAO, S.-H., SUN, F., CUI, D., KONG, F.-Y., ZHOU, A.-J., LIU, W.-Z., REN, N.-Q., WU, W.-M., WANG, A.-J. & LEE, D.-J. 2013. Accelerated Reduction of Chlorinated Nitroaromatic Antibiotic Chloramphenicol by Biocathode. *Environmental Science & Technology,* 47**,** 5353-5361.

LITTLE , R. F. 2015. *Directed Evolution and Discovery of Nitroreductase Enzymes for Targeted Cell Ablation.* Master Victoria University of Wellington

LIU, J., YU, H. & SHEN, Z. 2008. Insights into thermal stability of thermophilic nitrile hydratases by molecular dynamics simulation. *J Mol Graph Model,* 27**,** 529-35.

LIU, Y., CUI, W., FANG, Y., YU, Y., CUI, Y. & XIA, Y. 2013. Strategy for successful expression of the *Pseudomonas putida* nitrile hydratase activator P14K in Escherichia coli. *BMC Biotechnol,* 13.

LIU, Y., CUI, W., LIU, Z., CUI, Y., XIA, Y. & KOBAYASHI, M. 2014. Effect of flexibility and positive charge of the C-terminal domain on the activator P14K function for nitrile hydratase in *Pseudomonas putida*. *FEMS Microbiol Lett,* 352.

LIU, Y., CUI, W., XIA, Y., CUI, Y., KOBAYASHI, M. & ZHOU, Z. 2012. Self-subunit swapping occurs in another gene type of cobalt nitrile hydratase. *PLoS One,* 7.

LU, J., ZHENG, Y., YAMAGISHI, H., ODAKA, M., TSUJIMURA, M., MAEDA, M. & ENDO, I. 2003. Motif CXCC in nitrile hydratase activator is critical for NHase biogenesis in vivo. *FEBS Lett,* 553.

MANINA, G., BELLINZONI, M., PASCA, M. R., NERES, J., MILANO, A., RIBEIRO, A. L., BURONI, S., SKOVIEROVA, H., DIANISKOVA, P., MIKUSOVA, K., MARAK, J., MAKAROV, V., GIGANTI, D., HAOUZ, A., LUCARELLI, A. P., DEGIACOMI, G., PIAZZA, A., CHIARELLI, L. R., DE ROSSI, E., SALINA, E., COLE, S. T., ALZARI, P. M. & RICCARDI, G. 2010. Biological and structural characterization of the *Mycobacterium smegmatis* nitroreductase NfnB, and its role in benzothiazinone resistance. *Mol Microbiol,* 77**,** 1172-85.

MARVIN-SIKKEMA, F. D. & DE BONT, J. A. M. 1994. Degradation of nitroaromatic compounds by microorganisms. *Applied Microbiology and Biotechnology,* 42**,** 499-507.

MASCRÉ NEL, A. J. 2009. *dentification of novel cold-adapted nitrilase superfamily enzymes Andrew James Mascré Nel* Doctor of philosophy University of the Western Cape.

MATAM, S. K. 2013. *Studies on the biotransformation of acrylonitrile to acrylic acid using Rhodococcus Ruber Aksh-84.* PhD, Acharya Nagarjuna University

MISAL, S. A., HUMNE, V. T., LOKHANDE, P. D. & GAWAI, K. R. 2015. Biotransformation of Nitro Aromatic Compounds by Flavin-Free NADHAzoreductase. *Journal of Bioremediation & Biodegradation,* 06.

NAGASAWA, T., NANBA, H., RYUNO, K., TAKEUCHI, K. & YAMADA, H. 1987. Nitrile hydratase of *Pseudomonas chlororaphis* B23. Purification and characterization. *Eur J Biochem,* 162**,** 691-8.

NIGAM, V. K., KHANDELWAL, A. K., GOTHWAL, R. K., MOHAN, M. K., CHOUDHURY, B., VIDYARTHI, A. S. & GHOSH, P. 2009. Nitrilase-catalysed conversion of acrylonitrile by free and immobilized cells of *Streptomyces* sp. *J Biosci,* 34**,** 21-6.

O'REILLY, C. & TURNER, P. D. 2003. The nitrilase family of CN hydrolysing enzymes - a comparative study. *Journal of Applied Microbiology,* 95**,** 1161-1174.

OKAMOTO, S., VAN PETEGEM, F., PATRAUCHAN, M. A. & ELTIS, L. D. 2010. AnhE, a metallochaperone involved in the maturation of a cobalt-dependent nitrile hydratase. *J Biol Chem,* 285.

OSATO, T., UEDA, M., FUKUYAMA, S., YAGISHITA, K., OKAMI, Y. & UMEZAWA, H. 1955. Production of tertiomycin (a new antibiotic substance), azomycin and eurocidin by *S. eurocidicus. J Antibiot (Tokyo),* 8**,** 105-9.

PACE, H. C. & BRENNER, C. 2001. The nitrilase superfamily: classification, structure and function. *Genome Biology,* 2**,** reviews0001.1-reviews0001.9.

PARK, J. T. 2014 *Enzymatic reduction of nitro compounds to amines with nitroreductases.* Doctor of Philosophy Georgia Institute of Technology

PARKINSON, G. N., SKELLY, J. V. & NEIDLE, S. 2000. Crystal structure of FMN-dependent nitroreductase from *Escherichia coli* B: a prodrug-activating enzyme. *J Med Chem,* 43**,** 3624-31.

PATTERSON, S. & WYLLIE, S. 2014. Nitro drugs for the treatment of trypanosomatid diseases: past, present, and future prospects. *Trends in Parasitology,* 30**,** 289-298.

PELLETIER, D. A. & HARWOOD, C. S. 2000. 2-Hydroxycyclohexanecarboxyl Coenzyme A Dehydrogenase, an Enzyme Characteristic of the Anaerobic Benzoate Degradation Pathway Used by *Rhodopseudomonas palustris. Journal of Bacteriology,* 182**,** 2753-2760.

PENG, X., MASAI, E., KATAYAMA, Y. & FUKUDA, M. 1999. Characterization of the meta-cleavage compound hydrolase gene involved in degradation of the lignin-related biphenyl structure by *Sphingomonas paucimobilis* SYK-6. *Appl Environ Microbiol,* 65**,** 2789-93.

PÉREZ, H. I., MANJARREZ, N., LUNA, H., SOLÍS, A. & RAMÍREZ, C. 2005. Nitrile hydratase activity of *Nocardia corallina* B-276. *Journal of the Brazilian Chemical Society,* 16**,** 1150-1153.

PETERSON, F. J., MASON, R. P., HOVSEPIAN, J. & HOLTZMAN, J. L. 1979. Oxygen-sensitive and -insensitive nitroreduction by *Escherichia coli* and rat hepatic microsomes. *J Biol Chem,* 254**,** 4009-14.

PFENNIG, N., EIMHJELLEN, K. E. & LIAAEN JENSEN, S. 1965. A new isolate of the *Rhodospirillum fulvum group* and its photosynthetic pigments. *Arch Mikrobiol,* 51**,** 258-66.

PIERSMA, S. R., NOJIRI, M., TSUJIMURA, M., NOGUCHI, T., ODAKA, M., YOHDA, M., INOUE, Y. & ENDO, I. 2000. Arginine 56 mutation in the beta subunit of nitrile hydratase: importance of hydrogen bonding to the non-heme iron center. *J Inorg Biochem,* 80**,** 283-8.

PRECIGOU, S., GOULAS, P. & DURAN, R. 2001. Rapid and specific identification of nitrile hydratase (NHase)-encoding genes in soil samples by polymerase chain reaction. *FEMS Microbiology Letters,* 204**,** 155-161.

PREUß, A. & RIEGER, P.-G. 1995. Anaerobic Transformation of 2,4,6-Trinitrotoluene and Other Nitroaromatic Compounds. *In:* SPAIN, J. C. (ed.) *Biodegradation of Nitroaromatic Compounds.* Boston, MA: Springer US.

RACE, P. R., LOVERING, A. L., GREEN, R. M., OSSOR, A., WHITE, S. A., SEARLE, P. F., WRIGHTON, C. J. & HYDE, E. I. 2005. Structural and mechanistic studies of *Escherichia coli* nitroreductase with the antibiotic nitrofurazone. Reversed binding orientations in different redox states of the enzyme. *J Biol Chem,* 280**,** 13256-64.

RAMTEKE, P. W., MAURICE, N. G., JOSEPH, B. & WADHER, B. J. 2013. Nitrile-converting enzymes: An eco-friendly tool for industrial biocatalysis. *Biotechnology and Applied Biochemistry,* 60**,** 459-481.

RAO, M. A., SCELZA, R., SCOTTI, R. & GIANFREDA, L. 2010. ROLE OF ENZYMES IN THE REMEDIATION OF POLLUTED ENVIRONMENTS. *Journal of soil science and plant nutrition,* 10**,** 333-353.

ROBINSON, W. G. & HOOK, R. H. 1964. Ricinine nitrilase: I. Reaction product and substrate specificity. *J Biol Chem,* 239.

ROLDAN, M. D., PEREZ-REINADO, E., CASTILLO, F. & MORENO-VIVIAN, C. 2008. Reduction of polynitroaromatic compounds: the bacterial nitroreductases. *FEMS Microbiol Rev,* 32**,** 474-500.

ROSANO, G. L. & CECCARELLI, E. A. 2014. Recombinant protein expression in *Escherichia coli*: advances and challenges. *Frontiers in Microbiology,* 5**,** 172.

RUSTLER, S., CHMURA, A., SHELDON, R. A. & STOLZ, A. 2008. Characterisation of the substrate specificity of the nitrile hydrolyzing system of the acidotolerant black yeast *Exophiala oligosperma* R1. *Stud Mycol,* 61**,** 165-74.

RZEZNICKA, K., SCHÄTZLE, S., BÖTTCHER, D., KLEIN, J. & BORNSCHEUER, U. T. 2010. Cloning and functional expression of a nitrile hydratase (NHase) from *Rhodococcus equi* TG328-2 in Escherichia coli, its purification and biochemical characterisation. *Applied Microbiology and Biotechnology,* 85**,** 1417-1425.

SALMON, R. C., CLIFF, M. J., RAFFERTY, J. B. & KELLY, D. J. 2013. The CouPSTU and TarPQM Transporters in *Rhodopseudomonas palustris:* Redundant, Promiscuous Uptake Systems for Lignin-Derived Aromatic Substrates. *PLOS ONE,* 8**,** e59844.

SAMBROOK, J., FRITSCH, E. F. & MANIATIS, T. 1989. *Molecular Cloning: A laboratory manual.,* Cold Spring Harbour NY, Cold Spring Harbour Laboratory Press.

SEINER, D. R., HEGDE, S. S. & BLANCHARD, J. S. 2010. Kinetics and Inhibition of Nicotinamidase from Mycobacterium tuberculosis. *Biochemistry,* 49**,** 9613-9619.

SEMPLE, K. T., CAIN, R. B. & SCHMIDT, S. 1999. Biodegradation of aromatic compounds by microalgae. *FEMS Microbiology Letters,* 170**,** 291-300.

SEO, J. S., KEUM, Y. S. & LI, Q. X. 2009. Bacterial degradation of aromatic compounds. *Int J Environ Res Public Health,* 6**,** 278-309.

SHARMA, N. N., SHARMA, M. & BHALLA, T. C. 2012. Nocardia globerula NHB-2 nitrilase catalysed biotransformation of 4-cyanopyridine to isonicotinic acid. *AMB Express,* 2**,** 25-25.

SHIN, C. Y. & CRAWFORD, D. L. 1995. *Biodegradation of trinitrotoluene (TNT) by a strain of Clostridium bifermentans*, Battelle Press, Columbus, OH (United States).

SINGH, D., MISHRA, K. & RAMANTHAN, G. 2015. Bioremediation of Nitroaromatic Compounds. *In:* SAMER, M. (ed.) *Wastewater Treatment Engineering.* Rijeka: InTech.

SINGH, R., SHARMA, R., TEWARI, N. & RAWAT, D. S. 2006. Nitrilase and its application as a 'green' catalyst. *Chem Biodivers,* 3**,** 1279-87.

SONBOL, S. A., FERREIRA, A. J. & SIAM, R. 2016. Red Sea Atlantis II brine pool nitrilase with unique thermostability profile and heavy metal tolerance. *BMC Biotechnol,* 16**,** 14.

SONG, H. N., JEONG, D. G., BANG, S. Y., PAEK, S. H., PARK, B. C., PARK, S. G. & WOO, E. J. 2015. Crystal structure of the fungal nitroreductase Frm2 from *Saccharomyces cerevisiae*. *Protein Science : A Publication of the Protein Society,* 24**,** 1158-1163.

SONG, Y. 2009. Characterization of Aromatic Hydrocarbon Degrading Bacteria. *Kor. J. Microbiol. Biotechnol* 37**,** 333–339.

SPAIN, J. C. 1995. Biodegradation of nitroaromatic compounds. *Annu Rev Microbiol,* 49**,** 523-55.

SUGIMOTO, K., SENDA, T., AOSHIMA, H., MASAI, E., FUKUDA, M. & MITSUI, Y. 1999. Crystal structure of an aromatic ring opening dioxygenase LigAB, a protocatechuate 4,5-dioxygenase, under aerobic conditions. *Structure,* 7**,** 953-65.

SUN, W., ZHU, L., CHEN, X., CHEN, P., YANG, L., DING, W., ZHOU, Z. & LIU, Y. 2016. Successful expression of the *Bordetella petrii* nitrile hydratase activator P14K and the unnecessary role of Ser115. *BMC Biotechnology,* 16**,** 21.

TAKÁČOVÁ, A., , S., M., , S., M. & , M., P 2015. Degradation of btex by microalgae *Parachlorella kessleri*. *Petroleum & Coal,* 52**,** 101-107.

THUKU, R. N. 2006 *The structure of the nitrilase from Rhodococcus rhodochrous j1: Homology modeling and threedimensional reconstruction.* M.Sc. minithesis,, University of the Western cape.

THUKU, R. N., WEBER, B. W., VARSANI, A. & SEWELL, B. T. 2007. Post-translational cleavage of recombinantly expressed nitrilase from *Rhodococcus rhodochrous* J1 yields a stable, active helical form. *Febs j,* 274**,** 2099-108.

VERGNE-VAXELAIRE, C., BORDIER, F., FOSSEY, A., BESNARD-GONNET, M., DEBARD, A., MARIAGE, A., PELLOUIN, V., PERRET, A., PETIT, J.-L., STAM, M., SALANOUBAT, M., WEISSENBACH, J., DE BERARDINIS, V. & ZAPARUCHA, A. 2013. Nitrilase Activity Screening on Structurally Diverse Substrates: Providing Biocatalytic Tools for Organic Synthesis. *Advanced Synthesis & Catalysis,* 355**,** 1763-1779.

WALDRON, K. J., RUTHERFORD, J. C., FORD, D. & ROBINSON, N. J. 2009. Metalloproteins and metal sensing. *Nature,* 460**,** 823-830.

WAMPLER, D. A. & ENSIGN, S. A. 2005. Photoheterotrophic Metabolism of Acrylamide by a Newly Isolated Strain of *Rhodopseudomonas palustris. Applied and Environmental Microbiology,* 71**,** 5850-5857.

WEATHERBURN, M. W. 1967. Phenol-Hypochlorite Reaction for Determination of Ammonia. *Analytical Chemistry,* 39**,** 971.

WHITEWAY, J., KOZIARZ, P., VEALL, J., SANDHU, N., KUMAR, P., HOECHER, B. & LAMBERT, I. B. 1998. Oxygen-insensitive nitroreductases: analysis of the roles of nfsA and nfsB in development of resistance to 5-nitrofuran derivatives in *Escherichia coli*. *J Bacteriol,* 180**,** 5529-39.

WILLIAMSON, D. S., DENT, K. C., WEBER, B. W., VARSANI, A., FREDERICK, J., THUKU, R. N., CAMERON, R. A., VAN HEERDEN, J. H., COWAN, D. A. & SEWELL, B. T. 2010. Structural and biochemical characterization of a nitrilase from the thermophilic bacterium, *Geobacillus pallidus* RAPc8. *Appl Microbiol Biotechnol,* 88**,** 143-53.

WINKLER, M., GLIEDER, A. & KLEMPIER, N. 2006. Enzyme stabilizer DTT catalyzes nitrilase analogue hydrolysis of nitriles. *Chem Commun (Camb)***,** 1298-300.

WONG, W.-T., TSENG, C.-H., HSU, S.-H., LUR, H.-S., MO, C.-W., HUANG, C.-N., HSU, S.-C., LEE, K.-T. & LIU, C.-T. 2014. Promoting Effects of a Single *Rhodopseudomonas palustris* Inoculant on Plant Growth by Brassica rapa chinensis under Low Fertilizer Input. *Microbes and Environments,* 29**,** 303-313.

XIA, Y., CUI, W., LIU, Z., ZHOU, L., CUI, Y., KOBAYASHI, M. & ZHOU, Z. 2016. Construction of a subunit-fusion nitrile hydratase and discovery of an innovative metal ion transfer pattern. *Scientific Reports,* 6**,** 19183.

XIE, Z., FENG, J., GARCIA, E., BERNETT, M., YAZBECK, D. & TAO, J. 2006. Cloning and optimization of a nitrilase for the synthesis of (3S)-3-cyano-5-methyl hexanoic acid. *Journal of Molecular Catalysis B: Enzymatic,* 41**,** 75-80.

XUE, Y. P., YANG, Y. K., LV, S. Z., LIU, Z. Q. & ZHENG, Y. G. 2016. High-throughput screening methods for nitrilases. *Appl Microbiol Biotechnol,* 100**,** 3421-32.

YAMADA, H. & KOBAYASHI, M. 1996. Nitrile hydratase and its application to industrial production of acrylamide. *Biosci Biotechnol Biochem,* 60.

YANG, J., XIE, B., BAI, J. & YANG, Q. 2012. Purification and characterization of a nitroreductase from the soil bacterium *Streptomyces mirabilis*. *Process Biochemistry,* 47**,** 720-724.

YANG, Y., LIN, J. & WEI, D. 2016. Heterologous Overexpression and Biochemical Characterization of a Nitroreductase from *Gluconobacter oxydans* 621H. *Mol Biotechnol,* 58**,** 428-40.

ZHANG, C. & ANDERSON, A. J. 2012. Multiplicity of genes for aromatic ring-hydroxylating dioxygenases in *Mycobacterium* isolate KMS and their regulation. *Biodegradation,* 23**,** 585-596.

ZHOU, Z., HASHIMOTO, Y., SHIRAKI, K. & KOBAYASHI, M. 2008. Discovery of posttranslational maturation by self-subunit swapping. *Proc Natl Acad Sci U S A,* 105**,** 14849-54.

ZHOU, Z. M., HASHIMOTO, Y., CUI, T. W., WASHIZAWA, Y., MINO, H. & KOBAYASHI, M. 2010. Unique Biogenesis of High-Molecular Mass Multimeric Metalloenzyme Nitrile Hydratase: Intermediates and a Proposed Mechanism for Self-Subunit Swapping Maturation. *Biochemistry,* 49.

ZHOU, Z. M., HASHIMOTO, Y. & KOBAYASHI, M. 2009. Self-subunit swapping chaperone needed for the maturation of multimeric metalloenzyme nitrile hydratase by a subunit exchange mechanism also carries out the oxidation of the metal ligand cysteine residues and insertion of cobalt. *J Biol Chem,* 284.

ZHU, D., MUKHERJEE, C., YANG, Y., RIOS, B. E., GALLAGHER, D. T., SMITH, N. N., BIEHL, E. R. & HUA, L. 2008. A new nitrilase from *Bradyrhizobium japonicum* USDA 110: Gene cloning, biochemical characterization and substrate specificity. *Journal of Biotechnology,* 133**,** 327-333.